BRNO UNIVERSITY OF TECHNOLOGY

VYSOKÉ UČENÍ TECHNICKÉ V BRNĚ

FACULTY OF MECHANICAL ENGINEERING

FAKULTA STROJNÍHO INŽENÝRSTVÍ

INSTITUTE OF AEROSPACE ENGINEERING

LETECKÝ ÚSTAV

FLEXIBLE STRUCTURE DEVELOPMENT FOR EFFICIENT HEAT TRANSFER

VÝVOJ STRUKTURY PRO EFEKTIVNÍ PŘENOS TEPLA

MASTER'S THESIS

DIPLOMOVÁ PRÁCE

AUTHOR   Bc. Jakub Černoch

AUTOR PRÁCE

SUPERVISOR   Ing. Jakub Mašek

VEDOUCÍ PRÁCE

BRNO 2020

Specification Master's Thesis

Department:	Institute of Aerospace Engineering
Student:	**Bc. Jakub Černoch**
Study programme:	Mechanical Engineering
Study branch:	Aircraft Design
Supervisor:	**Ing. Jakub Mašek**
Academic year:	2019/20

Pursuant to Act no. 111/1998 concerning universities and the BUT study and examination rules, you have been assigned the following topic by the institute director Master's Thesis:

Flexible structure development for efficient heat transfer

Concise characteristic of the task:

The flexible structures are used in many technical disciplines. Moreover, they can also be used in very special cases, such as a heat management. As part of the development of space heat switch, such structure finds its application for heat conduction. However, how to ensure sufficient thermal conductivity, variable height and durability in parallel with a minimum weight requirement?

Goals Master's Thesis:

– Acquaint with the problematics of heat switch flexible structure and identify its conventional design improvement potential based on literature review
– Study of a joint between flexible structure and the interface plates to maximize conductivity
– Conceptual designs and their critical assessment in accordance to requirements
– Assessment of manufacturability and technology availability, trade–off between concepts

Recommended bibliography:

PAI, P. Frank. Highly flexible structures: modeling, computation, and experimentation. Reston: American Institute of Aeronautics and Astronautics, 2007, 742 s. ISBN 978-1-56347-917-5.

Deadline for submission Master's Thesis is given by the Schedule of the Academic year 2019/20

In Brno,

L. S.

....
doc. Ing. Jaroslav Juračka, Ph.D.   doc. Ing. Jaroslav Katolický, Ph.D.
Director of the Institute   FME dean

Abstrakt

Diplomová práce se zabývá teoretickými výpočty a návrhem struktury pro přenos tepla, která je součástí Miniaturizovaného tepelného spínače podle zadaných požadavků Evropské Kosmické Agentury.

Základními parametry jsou nízká hmotnost a vysoká tepelná vodivost. Práce navazuje na spínač navržený firmou Arescosmo, který nesplňoval požadované limity zejména v oblasti hmotnosti a tepelné vodivosti.

Pomocí teoretických výpočtů hmotnosti a tepelné vodivosti bylo ověřeno 49 variant ve třech základních konceptech – Mechanická struktura, flexibilní struktura složená z drátků a foliová struktura.

Z hlediska tepelné vodivosti jako nejlepší struktury vycházejí ty, které jsou založené na použití ochranných kovových opletů. Z dostupných zdrojů byly rovněž navrženy technologie, které by bylo možné využít pro výrobu těchto struktur.

Pro splnění požadavků, bude v další fázi projektu nutné vyrobit experimentální vzorky na kterých budou teoretické výpočty a vybrané technologie ověřeny.

Summary

The master's thesis deals with theoretical calculations and design of a structure for heat transfer, which is part of a Miniaturized Heat Switch according to the specified requirements of the European Space Agency.

The basic parameters are low weight and high thermal conductivity. The work follows the switch designed by Arescosmo, which did not meet the requirements, especially in the area of weight and thermal conductivity.

Using theoretical calculations of weight and thermal conductivity, 49 variants were verified in 3 basic concepts – Mechanical contact structure, flexible structure composed of wires and foil structure.

In terms of thermal conductivity, the best structures are those based on the use of metal stocking and sleeving braids. Manufacturing technologies have also been proposed from available sources that could be used to produce these structures.

To meet the requirements, in the next phase of the project it will be necessary to produce experimental samples on which the theoretical calculations and selected technologies will be verified.

Klíčová slova

Miniaturizovaný tepelný spínač, tepelná vodivost, Vesmír, ESA, měděné oplety, hliníkové oplety, hliníkové folie, měděné folie, uhlíkové materiály, grafen, měděné pletené pásky

Key words

Miniaturized heat switch, Thermal conductivity, Space, ESA, copper shielding braids, aluminium shielding braids, aluminium foil, copper foil, carbon materials, graphene, copper textile braid

Rozšířený abstrakt

Od dob prvních letů do vesmíru se stále častěji lidé dívají na Vesmír jako na místo plné příležitostí a dobrodružství. Agentury pro výzkum vesmíru ať už americká NASA nebo evropská ESA se stále snaží rozšiřovat naše znalosti o vesmíru a dalších planetách či vesmírných objektech. V posledních letech se na Vesmír rovněž zaměřují různé společnosti, které mají zájem o využití vesmírného prostoru ke komerčním účelům. Z tohoto důvodu se v dnešní době uplatňují malé satelity a sondy, které vyžadují miniaturizované zařízení pro svůj provoz. Tato zařízení musí náležitě plnit svou funkci a být co nejmenší a co nejlehčí. Vesmírné agentury se rovněž snaží o miniaturizaci některých zařízení z důvodu snížení nákladů na start.

Projekt miniaturizovaného tepelného spínače (MHS) je zaměřen na vývoj malého tepelného spínače pro tepelné řízení kosmické lodi. Klíčovými parametry jsou například plně autonomní funkce bez jakékoli spotřeby energie, malé rozměry, nízká hmotnost a zvýšená tepelná vodivost. Celý tento projekt spadá pod řízení Evropské vesmírné agentury (ESA), která si rovněž stanovila požadavky, které musí spínač splňovat. Tato diplomová práce je zaměřena na vývoj teplo-vodivé struktury, která bude součástí tohoto spínače.

V prvních kapitolách práce jsou rozebrány požadavky na spínač stanovené ESA, které jsou pro tuto práci důležité tedy požadované hodnoty tepelné vodivosti, rozsahy teplot spínání apod. Zároveň je zde rozebrán popis současného designu spínače a popis principu jeho fungování. Základním principem funkce spínače je, že po zahřátí se parafín umístěný v nitru spínače začne rozpouštět, tím začne vyvíjet tlak na vnitřní strukturu a posune „contact plate" vůči horní části spínače, čímž zapojí teplo-vodivou cestu. Po ochlazení parafín opět ztuhne, tlak se uvolní a teplo-vodivá cesta se rozepne.

V další části práce jsou detailně rozebrány problémy aktuálního řešení teplo-vodivé struktury, chyby v původním návrhu a je zde zmíněno, že změřená tepelná vodivost současného spínače je 0,235 $W \cdot K^{-1}$, přičemž původní výpočty ukazovaly na vodivost 0,91 $W \cdot K^{-1}$.

V dalších kapitolách jsou rozebrány rozměry, kterých se musí jednotlivé navrhované struktury držet, tedy maximální rozměry spínače a rovněž jsou zde také zjednodušeně popsány jednotlivé koncepty.

Následující kapitoly obsahují informace o materiálech a výrobních technologiích, které je možné využít v jednotlivých konceptech a jsou zde zmíněné hlavní přednosti a nevýhody materiálů a jednotlivých technologií.

Postup výpočtu jednotlivých konceptů je založený na základním výpočtu tepelné vodivosti pomocí rovnice pro tepelný odpor a v případě struktur využívající mechanického kontaktu jednotlivých částí je do výpočtu zahrnut ještě Yovanovitchův model pro výpočet tepelného kontaktu. Z těchto údajů je následně spočítána tepelná vodivost jednotlivých struktur. Tyto struktury jsou roztříděny do tří základních kapitol podle základních znaků. Jsou to kapitoly o pletených strukturách, mechanických kontaktních strukturách a foliových strukturách.

Kapitola o pletených strukturách se zabývá výpočtem těchto struktur, rovněž je v této kapitole detailněji popsán důvod proč výpočet tepelné vodivosti původního spínače navrženého firmou Arescocmo vycházel tak optimistický. Z těchto důvodů jsou v této kapitole uvedeny výpočty jiných pletených struktur z nichž nejvýhodnější variantou se jeví

právě měděné ochranné oplety. V rámci této kapitoly byly také prošetřovány uhlíková vlákna.

Dalším rozebíraným konceptem jsou struktury založené na mechanickém kontaktu, spodní a horní části struktury. Tyto struktury se dále dělí na další tři typy, které jsou nazvány „T-shape structure", „Cylindrical contact structure" a „Helix structure". Každá z těchto struktur se liší, jak už názvy naznačují typem kontaktních ploch. Nejvýhodnější strukturou z této kapitoly se jeví tzv. „double T-shape", která využívá dvě roviny kontaktu ploch ve tvaru T.

Posledním konceptem je kapitola věnující se foliovým strukturám, které využívají tenké proužky měděných nebo hliníkových folií, případně grafenu. Tyto fólie se následně prohýbají při spínání a rozepínání spínače.

Dle výpočtů vypadá nejpříznivěji struktura opletů, vyrobených z mědi a hliníku, z nichž jsou nejlepší struktury založené na měděných drátech, protože mají tepelnou vodivost zhruba 2 W·K^{-1}, což je vyšší, než požadovaných 1,5 W·K^{-1}, hmotnost 35 gramů a vyžaduje pro realizaci kontaktu zhruba 180 mm^2. Hmotnost těchto opletů je také vyšší než požadovaná hodnota, ale po kombinaci různých typů těchto opletů je možné snížit hmotnost a zároveň tepelnou vodivost. Další výhodou je, že tyto struktury nepotřebují pro svůj pohyb další prostor a tento prostor je zhruba stejný jako plocha potřebná pro jejich napojení na části spínače. Bylo rozhodnuto upřednostnit měděné oplety, protože hliníkové oplety vyžadují více prostoru pro kontakt. Problém této struktury může být ve výrobě, protože původně použitá metoda pájení není příliš vhodná, jak ukázala předchozí konstrukce CTB. Jedinou možností je svařování elektronovým paprskem. Tato technologie je velmi drahá a mohou existovat problémy s jejím ověřením.

Projekt miniaturizovaného tepelného spínače by měl být řešen do konce roku 2021, právě teď je dokončena teoretická část tepelně vodivé konstrukce s návrhem nejvýhodnější struktury. V příštích měsících bude nutné potvrdit teoretické výsledky praktickými zkouškami všech tří struktur (mechanická kontaktní struktura, pletená struktura, fóliová struktura) a ověřit svařovací technologii. Po výběru nejlepší struktury podle praktických zkoušek a metody konečných prvků v případě mechanických kontaktních struktur, bude možné definitivně rozhodnout o finální podobě této teplo vodivé struktury.

Bibliography

ČERNOCH, Jakub. *Vývoj struktury pro efektivní přenos tepla* [online]. Brno, 2020 [cit. 2020-06-26]. Dostupné z: https://www.vutbr.cz/studenti/zav-prace/detail/125297. Diplomová práce. Vysoké učení technické v Brně, Fakulta strojního inženýrství, Letecký ústav. Vedoucí práce Jakub Mašek.

Declaration of authenticity

I declare that I have elaborated my master thesis on the theme of "Flexible structure development for efficient heat transfer" independently with the use of literature and other sources of information, which are all quoted in the thesis and detailed in the list of literature at the end of the thesis.

In Brno on 26. June 2020 ....

Jakub Černoch

Acknowledgement

Content

1 Introduction

Since the first space flights, people have increasingly looked at the Universe as a place full of opportunities and adventures. Space research agencies, whether US NASA or European ESA, are constantly working to expand our knowledge of space and other planets or space objects. In recent years, various companies are interested in using space for commercial purposes. For this reason many small satellites and probes are used today, which require miniaturized equipment for their operation. These devices must perform their function properly and be as small and as light as possible. Space agencies are also working on how to miniaturize devices to reduce launch costs.

The Miniaturised Heat Switch (MHS) project is aimed at developing a small, heat switch for thermal management of spacecraft. The key parameters are for example fully autonomous function without any energy consumption, small dimensions and increased thermal conductivity. These parameters are described in more detail in Chapter 2. The initial contractor for this project was the Aerosekur Company, subsequently Arescosmo, which executed a preliminary heat switch design that did not meet key specifications. This preliminary design is called Breadboard (BB). Because the project was terminated prematurely by the first contractor it was subsequently transferred to the Brno University of Technology (BUT), which is now the main contractor.

The MHS is primarily designed for the Martian environment and for this type of environment it should be tested. The MHS can probably be used in the outer Solar system because of the requirements on radiation resistance.

Many changes were required in the design of the MHS due to the problems with low thermal conductivity, extensive deformation and other issues.

This master's thesis focuses on increasing the thermal conductivity of the MHS heat conductive structure. This should be done by using a different design for this structure or by replacing the material used.

It also aims at lowering the weight parameters of MHS, since the current design of MHS is very heavy

Different approaches of heat conductive structures are mentioned in this master's thesis too. The first heat conductive structures are based on the actual design of MHS, which uses flexible textile braids (TB). The second concept of the heat conductive structure is based on mechanical contact of two structures and the last concept uses foils flexibility.

There are also mentioned procedures for calculating thermal conductivity and weight of individual structures and procedures for detecting shortcomings in the heat conductivity of the original concept.

The following chapters also deal with the analysis of production technologies that could be used in the production of the proposed MHS heat conductive structures.

2 Miniaturised heat Switch (MHS)

The Miniaturised Heat Switch is a mechanical stand-alone device, which is intended to be located between the inner part of the probe (Hot Interface) and the radiator (Cold Interface). It should toggle the thermal path between the ON and OFF positions. The European Space Agency (ESA) set out the conditions that should be met by this device. Those conditions are mentioned in Attachment_A. The main conditions that are essential for this master's thesis are mentioned in Table 2.1.

Table 2.1 Miniaturised Heat Switch main requirements [1]

Specification reference	Description
FPR1	The Heat Switch shall have a peak conductance value greater than 1 W·K^{-1}.
FPR2	The Heat Switch shall have an ON/OFF ratio greater than 100.
FPR4	The variable conductivity of the Heat Switch shall be between 15°C to 25°C of the hot interface.
FPR5	The Heat Switch shall be designed to transport 1 W to 10 W in closed/ON mode with a maximum delta temperature of 10 K.
PRR1	The Heat Switch shall have a mass lower than 60 grams.
DR4	The requirements on material section, material design allowable and characterisation shall be in conformance with ECSS-E-ST-32C Rev.1

2.1 The actual design

The actual design of the Heat Switch under the name of Breadboard (BB) was created by Arescosmo. This design consists of 3 main components. The first part of the Heat Switch is the Actuator, which raises the heat conductive structure so that it comes into contact. The second part of the MHS is the copper braid structure (conductive cover, contact plate and base braid textile in the Picture 2.1). This part of the Heat Switch creates a heat conductive path when the Heat Switch is in the ON position and enables disconnection of the Heat Conductive path. The third part of the Heat Switch is the structure consisting of the Hot plate (Base plate), Cold plate and insulators. This structure contains the actuator component and the conductive cover.

The function of the Heat Switch consists of switching from the OFF position to the ON position, during which the Heat conductive path is connected, and subsequently back to the OFF position. This is carried out by the actuator, which is filled with paraffin. When the base plate (hot plate) temperature rises, the paraffin begins to dissolve. When the paraffin is dissolved it has a greater volume than when it is in its solid state. This change in volume begins to exert internal pressure, which then shifts the actuator and the return springs begin to shrink. This results in movement of the contact plate on the upper part of the actuator, which then connects with the cold plate, thereby connecting the heat conductive path. The heat is then able to travel through the entire switch and conductive cover to the radiator. When the base plate (hot plate) cools down, the paraffin begins to solidify which results in reduced inner pressure. The return springs then start to expand and this moves the contact plate in the opposite direction, which disconnects the heat conductive path. The switch is now in the OFF position again.
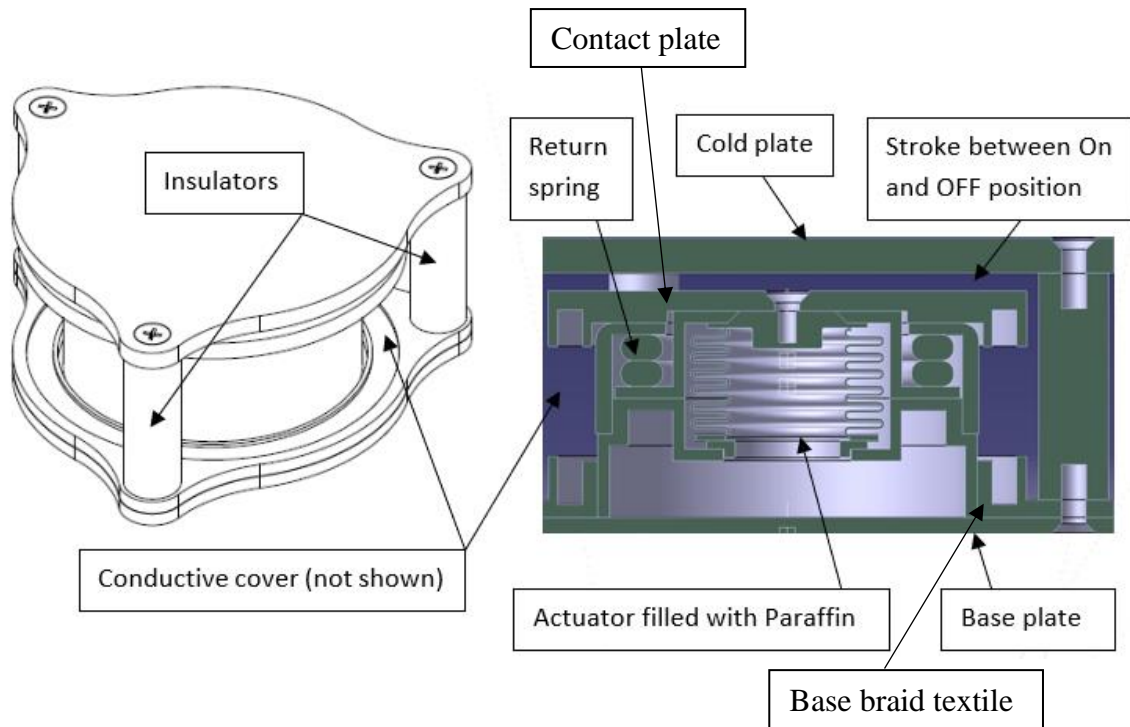
Picture 2.1 Miniaturised Heat Switch Cut through switch [2]

The textile braid (TB), which is the most important part for this thesis, is manufactured from Copper Braid strip. This strip is cut to the desired length. The next step is cutting the edges along the strip, because free wire ends are required that can be connected to the contact plate and the base braid textile. The result of cutting is also that basic number of wires, for example 191, that are in the transversal cross-section area (can be seen in Picture 2.5) and across the whole strip, is separated into more individual wires along the longitudinal cross-section.

Picture 2.2 Textile braid [3]

In the next step the edges of the strip are welded to the contact plate and the base braid textile. The ends of the TB are also welded together, but not through the entire cross-section area. A small area of free space must be left because the TB must be elastic. This small space could be seen in Picture 2.3. The welding was the most problematic part of the manufacturing process, as can be seen in Chapter 4. Arescosmo tried many approaches to join the thermal strip with these parts, for example soldering in an oven. The final approach that was applied was laser welding, but it is probable that it was just soldering and the solder was melted by laser.

Picture 2.3 Small free space in CTB [4]

Picture 2.4 CTB test samples [3]
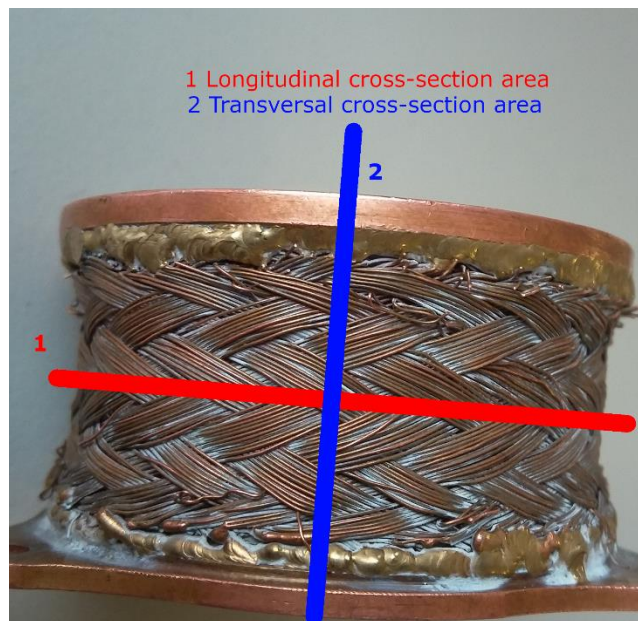
Picture 2.5 Indication of cross-sections of braided strip

3 Thermal computations

This chapter focuses on the basic methodology used for the thermal computations used in all conceptual designs for thermal conductive structures.

Heat transfer is realized by three possible processes. These are conduction, convection and radiation [5].

Only thermal conduction was used for thermal computations in this master's thesis, along with a model for heat transfer through thermal contact. Thermal convection and radiation are not used for computations, because heat transfer through these processes was evaluated as negligible.

3.1 Thermal Conduction

Heat transfer through thermal conduction could be characterized as transfer of energy from a point where there is more energy to a point where there is less energy. Heat is transferred by atoms. Heat is transferred towards the point with the lower temperature [5].

The key equation of all thermal computations is based on Fourier's law. This is the equation for thermal resistivity and thermal conductivity is a reciprocal value for this equation [5].

$$R = \frac{\delta}{\lambda \cdot S} \tag{1}$$

In this equation R is thermal resistivity, δ is the thickness of the heat transfer structure (the length of heat conductive path), S is cross-section area of the heat transfer structure and λ is the coefficient of thermal conductivity.

This equation is analogical to Ohm's law [5]. This fact allows computation of the thermal structures as an electrical circuit with resistors, using the same resistivity equations for parallel and serial connection [6].
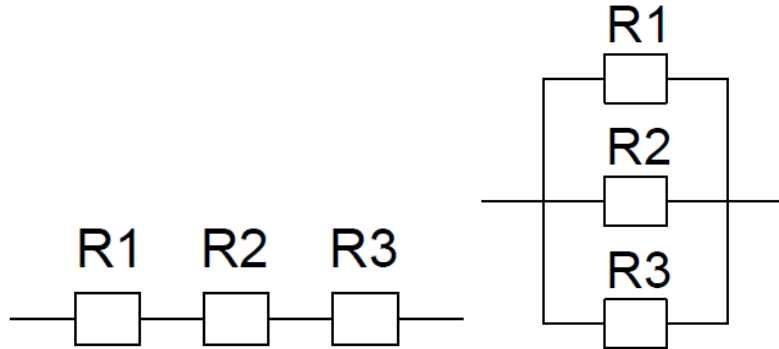
Picture 3.1 Resistors scheme connection in series (left), connection in parallel (right) [6]

Picture 3.1 shows connection of resistors in series and parallel connection, which could be analogical to the separated parts of the Heat switch.

The equation for connection of resistors in series is Equation (2) [6].

$$R = R_1 + R_2 + R_3 \tag{2}$$

The equation for connection in parallel is Equation (3) [6].

$$\frac{1}{R} = \frac{1}{R_1} + \frac{1}{R_2} + \frac{1}{R_3} \tag{3}$$

Because the change in temperature in the MHS during its operation is negligible, it does not affect the thermal conductivity coefficient, which can be considered constant.

3.2 Thermal contact

Because some types of Heat conductive structures are designed as mechanical contact structures, some computations for heat transfer through thermal contact must be found.

Yovanovich's model was used as the basis for thermal contact computations. This model takes into account contact pressure, atmospheric gaps between contact surfaces, microhardness Hc, Root Mean squared (RMS) roughness and other parameters of the used materials [7].

.
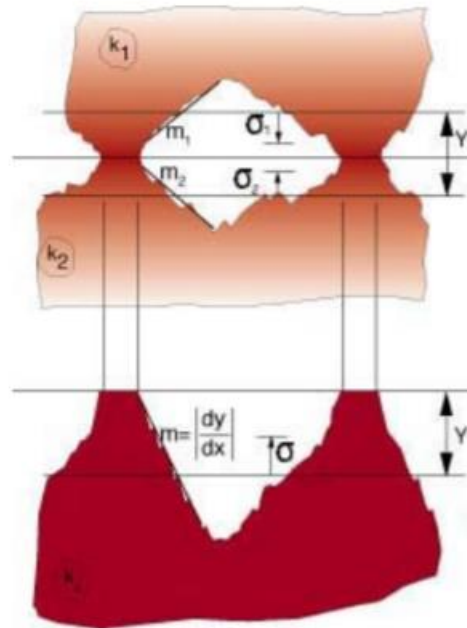
Picture 3.2 Gaps between surfaces [7]

As can be seen in Picture 3.2 the surface is not plane but uneven. Heat is transferred between the two surfaces through the projections. As can be seen in the Picture, there are also gaps filled with air, or in a vacuum these gaps would be filled with vacuum. Yovanovich's model also uses the parameters of these gaps [7].

This model is used even though our input parameters do not meet the conditions under which it should be used. But in relation to the results of a bachelor thesis by Timko Marek Mateášik, this is the best model for application. On the basis of the aforementioned bachelor's thesis we use the value that is calculated according to this model and then divided by six for calculation of the value, because the value actually measured during experiments is 6 times less than that predicted by the computation model [8].

4 Identification of Bread Board (BB) problems

The BB design does not meet many of the specifications. The main issues connected to thermal conductivity, identified by BUT during testing of the BB, are described in the Table 4.1.

Table 4.1 Table of specifications and actualy measured parameters [1]

Specification reference	Description	BB measured parameters
FPR1	The Heat Switch shall have a peak conductance value greater than $1 W \cdot K^{-1}$.	Average conductance is $0{,}235\ W \cdot K^{-1}$
FPR2	The Heat Switch shall have an ON/OFF ratio greater than 100.	The actual ON/OFF ratio is 23,5
FPR5	The Heat Switch shall be designed to transport 1W to 10W in closed/ON mode with a maximum delta temperature of 10K.	Average conductance is $0{,}235\ W \cdot K^{-1}$
PRR1	The Heat Switch shall have a mass lower than 60 grams.	The actual weight of Heat Switch is 173,1 grams

4.1 Problems with low thermal conductivity

Thermal conductivity is connected to specifications FPR1, FPR2 and FPR5. FPR1 is a key requirement designed by ESA and should be met to successfully complete the project. This requirement is also associated with the requirements of FPR5, which specifies the maximum heat conductivity of the MHS. The requirement of FPR2 specifies the conductivity of the ON/OFF ratio, which is significantly lower than was computed, but even the computed ratio was lower than the required 100.

The BB was designed to a heat conductivity of $0{,}91\ W \cdot K^{-1}$ and the ON/OFF ratio was computed at 75,8, but as seen in the table 4.2, the result was significantly less. This was due to many problems with the copper textile braid (CTB) and the Heat Switch itself, which will be specified below.

Table 4.2 Old thermal computations results [3]

Parameter	Value
BB Thermal conductivity	$0{,}91\ W \cdot K^{-1}$
Assumed TB Thermal Conductivity	$1{,}09\ W \cdot K^{-1}$
ON/OFF ratio	75,8
Heat conductive path through TB	17 mm

4.1.1 Insufficient welding quality

The first suspects were the welds between the TB and the Contact Plate and the base braid textile of the Heat Switch. As could be seen in the Picture 4.1, the wires of the TB are not connected to the base braid textile with filler metal in all places and they protrude laterally. This finding led to the decision that a Computed Tomography (CT) of this part of the Heat Switch was necessary and can be seen in Picture 4.2.

Picture 4.1 CTB with marked welds and free wires

These CT scans were performed in CEITEC. These scans shows that contact in the welded joints is insufficient. As can be seen in the Picture 4.2, the connecting metal did not fill the space between the individual wires and only connected the outer parts of the braid structure to the contact plate and the base braid textile.
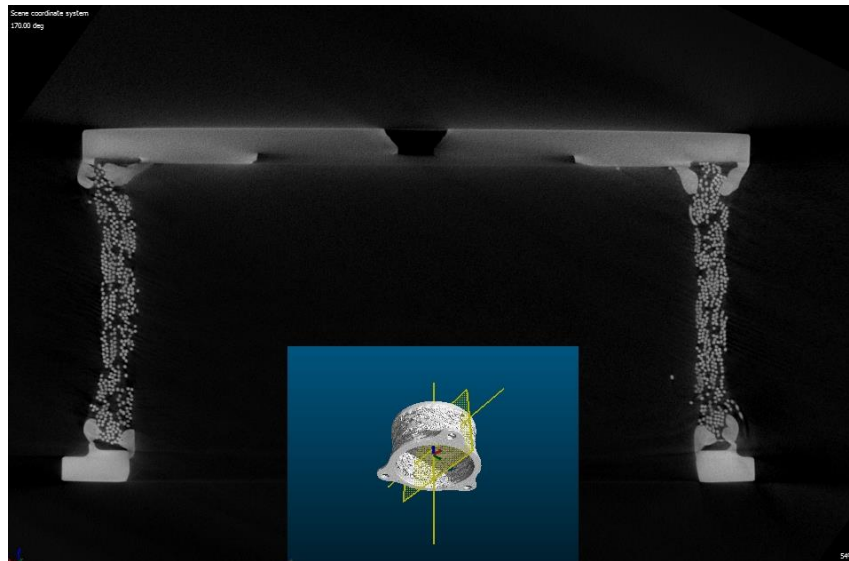
Picture 4.2 Side view CT scan of CTB [9]

This CT scans were also useful for recognition of other potential problem with this CTB structure concept.

4.1.2 Optimistic estimates of the conductivity of Copper textile Braid (CTB)

The computed conductivity of CTB with the welded contact plate and base braid textile was roughly $1{,}09$ W·K^{-1}. The Arescosmo Company used two braids of the same type to create the structure. This braid type is specified in the Table 4.3. Some parameters are known from the manufacturer, but the composition was calculated. Parameters connected to the Table 4.3 can be seen in Picture 4.3, which gives a schematic depiction of the braided strip.

Table 4.3 Textile braid parameters [10]

Parameter	Value
Thickness	1,2 mm
Height	10 mm
Length	120 mm
Full cross-section area	12 mm^2
Nominal cross-section area	6 mm^2
Wire diameter	0,2 mm
Composition	Strands: 12 Wires in strand: 16
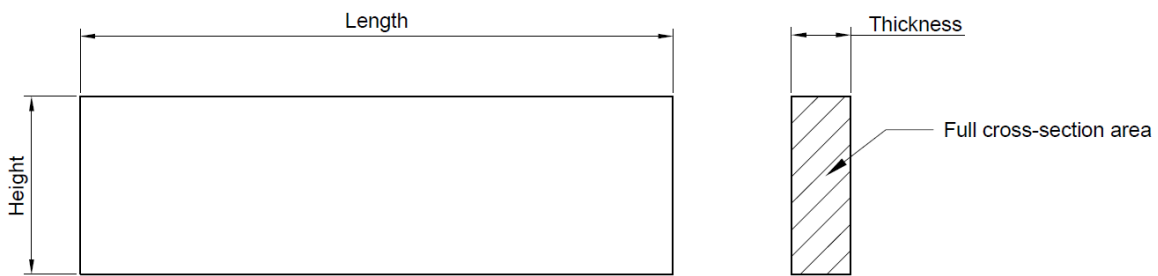
Picture 4.3 Flat braid strip parameters

When searching for BB design errors it was found that the thermal conductivity of the TB was calculated quite optimistically. As can be seen in the Table 4.3, the area that is occupied by copper wires (Nominal area) is only half of the full area of the textile braid in the transversal cross-section area. The computation of the initial TB estimated that the nominal area in the longitudinal cross-section area (area in direction of braiding) is one quarter of the whole area occupied by braid.
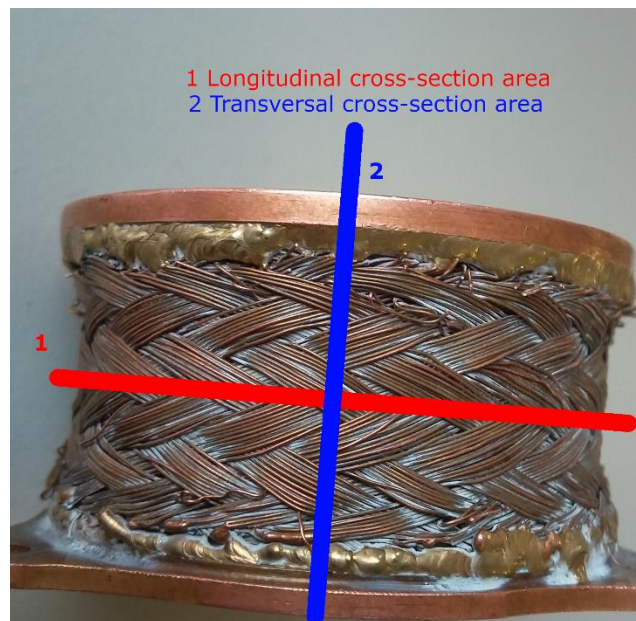
Picture 4.4 Indication of cross-sections of braided strip

After a CT scan, which can be seen in Picture 4.5, was performed the wires in the longitudinal direction of the copper braid were counted and it was found that the nominal area in the longitudinal cross-section area is smaller than was estimated.
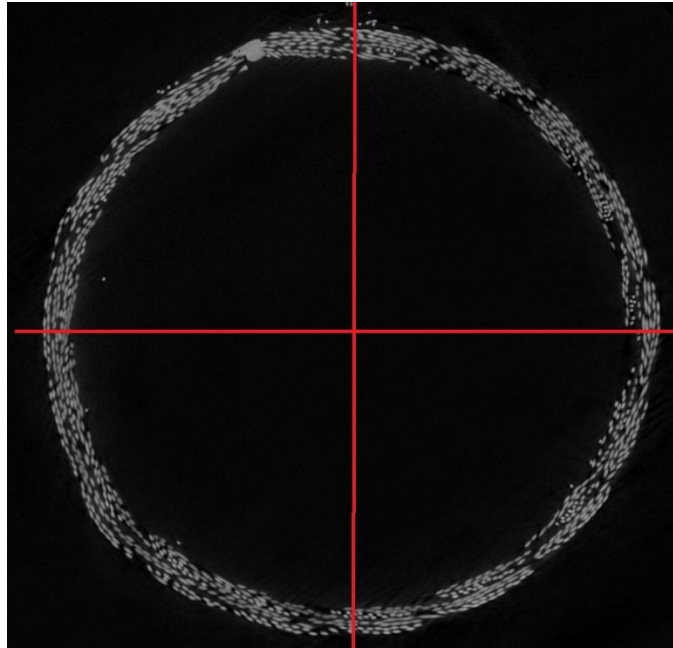
Picture 4.5 Upper view CT scan of CTB [9]

There was also a problem with the first computation of the BB, which only calculated the length of the thermal conductive path as the height of the TB in ON position, which is 17 mm. But it was found that heat is probably more likely to be transmitted along the wires than across the points where the wires are in contact with each other. So it was decided to measure the length of the wires in the TB and the thermal conductivity of the TB was subsequently. The result was less than a half the previous estimate and the next probable reason why the thermal conductivity of the Heat Switch itself was so small. The measured and calculated parameters are clearly listed in the Table 4.4.

Table 4.4 New computation results

Parameter	Value
BB Thermal conductivity (Measured)	0,235 W·K^{-1}
Computed TB Thermal conductivity	0,365 W·K^{-1}
ON/OFF ratio (Measured)	23,5
Wire length (Heat conductive path through TB)	39 mm
Number of wires in longitudinal cross-section	1200

4.2 Problem with excessive weight

The weight of the Heat switch is another important parameter specified in PRR1. Because this project is intended to be used in space projects, where every gram counts, the weight must be reduced as much as possible.

The main problem in relation to the weight of the actual design could be the use of copper, which is a highly conductive but also heavy material. This could be solved by use of lighter materials.

It is probable that reduction of the weight of the whole heat switch to 60 grams, which is the ESA requirement, will not be possible. But it is important to focus on maximizing reduction of weight while maintaining high thermal conductivity. The actual weight of the BB is given in the Table 4.5, which also gives the weight of the thermal conductive path of the BB. The table contains just some of the parts of the BB that are of importance to this thesis, it does not list all the parts of the BB.

Table 4.5 Actual weight parameters of BB

Parameter	Value
BB Weight	**173,1 g**
Heat conductive path (Contact plate, textile braid, base braid textile) CTB	**55,1 g**
Contact plate	23,6 g
Braid textile	22,1 g
Base braid textile	9,4 g
Base Plate	50,8 g

5 Conceptual re-design

This master's thesis is primarily aimed at conceptually redesigning the heat conductive structure, the problems in relation to which were defined in chapter 2. This redesign should be carried out in conformance with the design requirements that were specified in Attachment A and in conformance with ECSS documents. This chapter serves as a guideline to chapters devoted to specific elements of the design.

5.1 Design requirements

The key requirements are the small weight of the heat conductive structure and a thermal conductivity of 1,5 $W \cdot K^{-1}$.

The thermal conductivity mentioned here is higher than that stipulated in the requirements given in Attachment A. This value was determined because the thermal conductivity of the whole BB was calculated and it was decided that for a thermal conductivity of 1 $W \cdot K^{-1}$ required by the whole MHS, the heat conductive structure should have a thermal conductivity of 1,5 $W \cdot K^{-1}$. This is because the thermal conductivity is reduced significantly by other parts of the MHS. This is also somewhat of a reserve value, because unknown effects, which could lower thermal conductivity, must be taken into account.

The weight should also be reduced if possible, but as mentioned in chapter 4, the high weight is an issue that applies to the whole MHS. Even if this is taken into account, it is important to make all proposals as light as possible. The computational models are therefore designed in such a way that subsequent optimization is possible in subsequent design phases.

The other design parameter is stroke of the MHS. The stroke is parameter of the Gap between contact plate and cold plate. It is the parameter by how much the structure must move in order for contact to occur. In the actual design the Stroke of the BB is 1,7 mm.

The last important requirement is also specified in Attachment A. This is the fatigue requirement. Although these concepts are just initial conceptual designs, it is important to consider the fatigue behaviour of these designs and try to design them with respect to the planned lifetime and number of cycles.

Meeting all these requirements on such a small device is a great challenge.

5.2 Design Space definition

The MHS itself is very small device, so there is not much space for the heat conductive structure. The basic dimensions for the design itself are described in the Picture 5.1. The pictures give a side view of the BB and a top view of the base plate, without other parts of the Heat Switch.
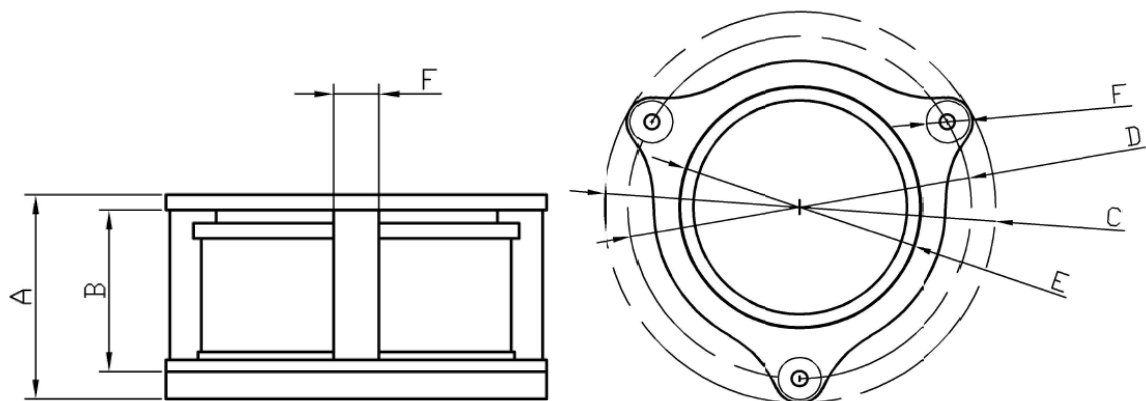
Picture 5.1 BB dimensions side view (left), top view (right)

In the picture:

- **A**: Is the height of the BB. (26,4 mm)
- **B**: Is the maximum height (height needed for thermal contact) of the Heat Conductive Structure. (20,9 mm)
- **C**: Is the maximum outer diameter of the BB. (⌀56 mm)
- **D**: This circle demonstrates the centre line of the elastomer insulators position. (⌀49 mm)
- **E**: This is the point of connection of the BB switch actuator, to the Base Plate. (⌀34,6 mm). The base braid textile has the smallest diameter 1 mm larger (⌀35,6 mm)
- **F**: This dimension is the elastomer insulator that connect the cold plate and the Base plate. (⌀6 mm)

The design area for the Heat Conductive structure in the BB switch was a circle from dimension "E" defined in the Picture 5.1 to ⌀40mm. This was found to be too small and the concept in this master's thesis operates with dimensions ranging from "E" to "C". But this has a disadvantage because of the elastomer insulators (marked "F") and the concepts are modified accordingly to allow the elastomer insulators to remain.

5.3 Design for Space Requirements – Engineering ECSS Standards

Because the MHS project is a European Space Agency (ESA) project, compliance with the requirements of ECSS standards is necessary. The European Cooperation for Space Standardization (ECSS) is an establishment designed to create standards that are useful for design of space related devices [11].

The standards that were realized as useful for this master's thesis are mentioned in the Table 5.1

Table 5.1 Important standards

Document number	Document name
ECSS-E-ST-32C	Structural General Requirements
ECSS-E-ST-32-03C	Structural finite element models
ECSS-E-ST-32-10C_Rev.2-Corr.1	Structural factors of safety for spaceflight hardware
ECSS-Q-70-71A_Rev.1	Data for selection of space materials and processes
ECSS-Q-ST-70C_Rev.2	Materials mechanical parts and processes
ECSS-E-HB-32-20	Structural materials handbook

5.4 Conceptual Designs

This chapter only briefly mentions basic concepts that will be described in subsequent chapters in detail. These concepts are divided into 3 different approaches. They are the basic types of concept that were found to be useful and computed in this master's thesis in more detail.

5.4.1 Wires/Straps (Braided structures)

This is the actual design of the Heat Conductive Structure as mentioned in Chapter 2. Redesign of this concept is described in detail in Chapter 9.

It was finally considered that useful straps for this concept could be manufactured from:

- Copper wires
- Aluminium wires
- Carbon fibres

5.4.2 Mechanical contact structures

This type of concept is based on mechanical contact between the surfaces of the lower part connected to the base plate and the upper part connected to the actuator. When switched the upper part makes contact with the cold plate. These concepts are described in Chapter 10 in detail. Some of them were rejected.

- T-shape
  - The contact surfaces are T-shaped, described in Chapter 10.5. in detail.
  - This concept is also connected to the double T-shape structures described in the same chapter.
- Cylindrical
  - The contact surfaces are located at the ends of cylinders that are connected to the base plate and contact plate. This concept is described in Chapter 10.4 in detail.
- Helix
  - The contact surfaces are helix-shaped, described in Chapter 10.6 in detail.
- L-shape
  - This contact structure concept is similar to the T-shaped structure, but each rib pair is not in contact with the others.
  - This concept was rejected because was found that pairs of ribs alone may have deformation problems.
- L-shape surrounding the perimeter
  - This type of concept is based on L-shapes surfaces that fit together and are distributed around the perimeter of the MHS.
  - This type of structure was rejected because it would be difficult to manufacture and would still be impossible to disassemble.

5.4.3 Foils

This is the last concept that could be useful for the MHS project. It is based on thermal strips manufactured from thin foil, which can bend. This thin foil could be connected with the base plate and the contact plate. When the actuator moves the contact plate up, the bend in the foil structure would be reduced and it would stretch [12]. This concept is described in Chapter 11 in detail.

These foils could be made from the following materials:
- Copper or Aluminium
- Graphite
- Graphene

5.5 Materials

As indicated by Chapter 4 the materials used in the MHS project must have high thermal conductivity and should be as light as possible. These materials should also have high fatigue resistance. The materials are described in Chapter 7 in detail.

6 ECSS requirements

In this chapter are mentioned the requirements and recommendations for space design that are connected to ECSS standards and ECSS handbooks and are useful for MHS project. The ECSS standards are divided into 4 branches which are Space project management branch, Space product assurance branch, Space engineering branch and Space sustainability branch [13]. For this master's thesis are especially important Space engineering branch and Space product assurance branch. The next chapters refers to these branches.

The ECSS standards also refer to ISO standards for example in case if some tests of materials and mechanical parts should be done.

6.1 Design

The standards and handbooks for Space engineering contains information, requirements and recommendations for design.

Here are mentioned some of them which were considered as important:

- Local yielding may occur for metal structures if it does not cause instability or fatigue failure [14].
- Thermal expansion must be taken into account in all stages of manufacturing, storage and during operation live of the part [14].
- Factors of Safety (FOS) are the values of the load that can be applied to a given component and standard aimed on them is ECSS-E-ST-32-10C [15].
  - o The main Factors of Safety are split to ultimate design factors of safety (FOSU) for design limit load and yield design factors of safety (FOSY) for design yield load [15].
  - o The FOS values are then different for every materials or type of vehicle [15].
  - o Values of FOSY differ from 1,1 to 1,25 [15].
  - o Values of FOSU differ from 1,25 for metallic materials in satellites to 3 for ceramic and glass materials in man-rated vehicles [15].
  - o The specific FOS values applicable to the thermally conductive structure of the MHS project are mentioned in the Table 6.1.

Table 6.1 Selected Factors of Safety [15]

Structure type	Vehicle	Requirements			
		FOSY	FOSU	FOSY verification by analysis only	FOSU verification by analysis only
Metallic parts	Satellite	1,1	1,25	1,25	2,0
Joints and inserts - Failure	Satellite	1,1	1,25	1,25	2,0
Joints and inserts -Gapping/Sliding (Other)		1,1		2,0	

- There is necessary to provide venting for enclosed-volumes, because when the air is escaping from them during rocket launch it can cause damage to payload [14].
- Other interesting problem covered by standards is stress-corrosion cracking which can occur on some materials in specific conditions. This problems are covered by standard ECSS-Q-ST-70-36 and stress-corrosion cracking tests are described in standard ECSS-Q-ST-70-37 [14].

- The standard also describes that is necessary to determine the structure weight and try to keep it as low as possible [14].
- The structures must be manufactured in conformance to geometrical interface requirements and the interchangeability must be observed between structures with same identification number [14].

6.2 Space product assurance

The Space product assurance is an important part of the space project. Because there is necessary to check that all standards have been met and the product have the best quality that is in the space project probably more important, than in other aviation cases. This master's thesis is aimed in the initial development part of the project, so quality assurance control is not in the main goals, but it is necessary to know the basic information.

The Space product assurance aims on these basic topics:

- Materials
- Manufacturing processes, used technologies and transport of the product
- Design and analyses
- Personnel training
- Documentation and traceability
- Certification

The space project operates with significantly smaller factors of safety [15] in some cases. This also requires higher quality assurance control.

The key parts of the Quality control is documentation according to the standards. For this purpose standards defines three main lists. It is Declared Materials List (DML), Declared Mechanical Parts List (DMPL) and Declared Processes List (DPL). These lists contain information about used processes, materials and mechanical parts, detailed information are located in standard ECSS-Q-ST-70C-Rev.2 [16].

The traceability is also defined in Product Assurance standards and it is key part also for this master's thesis. Because of the traceability are every concept from Chapter 10, named according to the nomenclature submitted [16].

The Space Product Assurance standards also defines how the tests of materials, mechanical parts and processes should be done. For example is here mentioned the standard ECSS-Q-ST-70-04C which defines how Thermal Cycling tests of the materials, mechanical parts etc. must be done [16] [17].

These information shows that the Space Project is really expensive and in the terms of saving time and money it is necessary to use "Space proven" materials and processes. This means materials and processes that were successfully used in some earlier Space project and do not require repetition of all the demanding tests described in the standards and could be verified by the costumer by similarities [14] [16].

6.3 Finite Elements Analysis (FEA)

Finite Elements Analysis (FEA) is also defined by standard. This standard defines for example that mesh convergence should be checked and documented or categorization of models etc. The standard aimed on FEA is ECSS-E-ST-32-03C. In general this standard contains requirements for models and methods to check the analysis accuracy [18].

6.3.1 Coordinate system

The coordination system is also described by standard. Basic coordinate system is Cartesian coordinate system.

In the case of mechanical contact structures the coordinate system origin is located in the center of the base plate as could be seen in Picture 6.1.
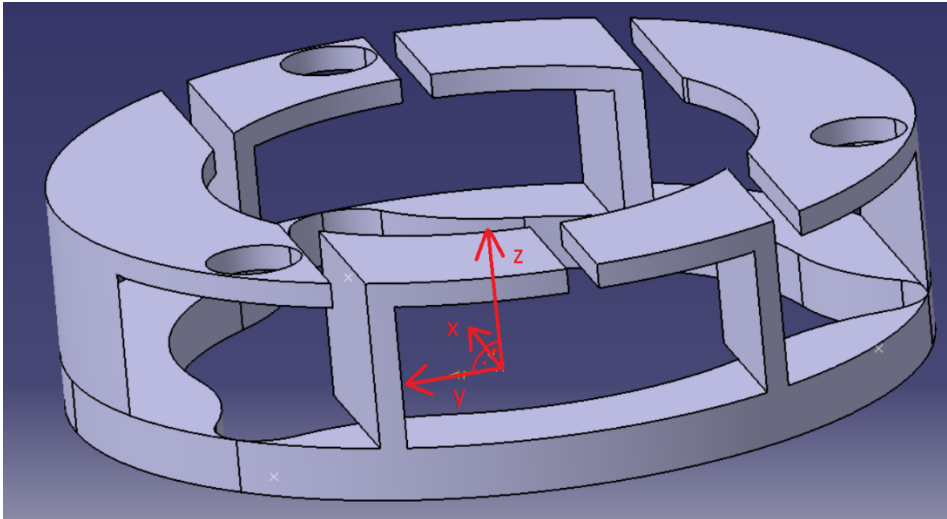
Picture 6.1 Coordinate system

7 Materials

Selection of materials is a crucial part of this project. Thermal conductivity and weight depends mainly on the material. The range of materials that could be used in this project is quite limited by current options.

The key property of the selected materials is thermal conductivity. Conventional materials with high thermal conductivity are silver, copper, aluminium and gold. Gold and silver are very expensive and have a high density, so structures made from these materials will be very heavy [19]. It follows that the only useful materials are copper and aluminium.

Other useful materials could be carbon-based materials. For example carbon fibre or graphene. These materials could also be very expensive, but have significantly higher thermal conductivity than conventional materials and low density. Structures designed using these materials could be very light with high thermal conductivity. Although these materials are used in space research we do not have any experience with them and we need to carry out more research.

The basic material parameters that are used in the computations are sourced from ECSS standards. Namely it is standard ECSS-Q-70-71A rev.1 [20]. This standard is older and was replaced by newer version which does not contain material characteristics.

7.1 Copper

Copper is metal with high density and thermal conductivity [19]. Its maximum thermal conductivity could be around 380 $W \cdot m^{-1} \cdot K^{-1}$ [19]. The density of this metal is 8 900 $kg \cdot m^{-3}$ [19].

As indicated by previous information, copper is very good for thermal conductivity and for applications that require thermal conductive structures of a low volume.

Copper was used mainly in the heat conductive structure design by Arescosmo. Parameters used in calculations by AresCosmo are mentioned in the Table 7.1. The material used in MHS project is copper (OFHC) which means oxygen free high conductive. In the Table 7.1 are also located parameters of other copper material type, it is Electrolytic Tough Pitch, (ETP).

Table 7.1 Copper materials parameters

Material	Density [$kg \cdot m^{-3}$]	Thermal conductivity [$W \cdot m^{-1} \cdot K^{-1}$]	Ultimate tensile strength [MPa]	Proof stress (0,2%) [MPa]	Microhardness Hc [MPa]
Copper OFHC	8900 [20]	394 [20]	220 – 450 [20]	45 – 320 [20]	882 [3]
Cu ETP (R290)	8900 [21]	390 [21]	290 – 360 [21]	≥ 250 [21]	-

7.2 Aluminium

Aluminium is metal with low density and good thermal conductivity [19]. Its maximum thermal conductivity could be around 237 $W \cdot m^{-1} \cdot K^{-1}$ [19]. The density of this material is 2 700 $kg \cdot m^{-3}$ [19].

Aluminium is a very light material with good conductivity, but according to computations a higher volume of material is needed for the same conductivity as parts made from copper. The aluminium alloy 7075 was used by Arescosmo for some parts of MHS and the parameters for calculation are mentioned in the Table 7.2.

Table 7.2 Aluminium materials parameters

Material	Density [kg·m⁻³]	Thermal conductivity [W·m⁻¹·K⁻¹]	Ultimate tensile strength [MPa]	Yield strength [MPa]	Microhardness Hc [MPa]
Aluminium (7075-T73)	2810 [3]	155 [3]	505 [22]	435 [3]	705 [3]
Al 99,5%	2700 [23]	235 [23]	75 – 146 [20]	55 – 133 [20]	-

7.3 Carbon Materials

The carbon materials were not initially considered useful for heat conduction in this project, because it was probably very difficult to connect them effectively with other parts of the MHS. The carbon materials cannot be easily connected to other materials without the use of adhesives, which may have poor thermal and electrical conductivity properties.

The most likely way to connect carbon materials to MHS parts is C-solder. This is a group of tin-based, lead-free, low-temperature soldering alloys. These soldering alloys could be used to connect various materials, for example carbon or ceramic materials to copper, or aluminium. C-solder allows thermal and electrical conductive contact between materials. This type of solder is relatively new [24]. The basic information about C-solder are mentioned in the Table 7.3. It is currently unknown whether this solder was used in space project, which means that the development costs could be higher than other verified technologies.

Table 7.3 C-solder parameters [24]

Melting point	Temperature range for soldering of carbon	Density	Thermal conductivity
232 °C	235 – 450 °C	7400 kg·m⁻³	yes

7.3.1 Highly conductive carbon fibres (graphite fibres)

In some cases the thermal conductivity of carbon fibres is significantly higher than that of conventional metal materials while maintaining low density, which means low weight [25].

Exceptional thermal properties could be observed in the case of high modulus pitch-based fibres, which could achieve a thermal conductivity of around 747 W·m⁻¹·K⁻¹ and some fibres may even achieve a higher conductivity value [25]. Carbon fibre covered with carbon nanotubes (CNT), could achieve a significantly higher thermal conductivity, reaching a value of around 967,1 W·m⁻¹·K⁻¹ [25]. Basic parameters of these fibres are mentioned in the Table 7.4.

The thermal conductivity of carbon fibres can be increased by heat treatment. According to experiments thermal conductivity can be significantly higher when compared to fibres that have not undergone heat treatment [26].

These parameters could be very useful for purposes of Heat conductive structure for miniaturised heat switch.

The biggest problem in relation to graphite fibre for thermal conductivity purposes is the fibre's potential to fracture and fray during manipulation or during launch etc. This results in foreign object debris (FOD) [27]. This debris would act as contamination in some cases. To prevent this problem the fibre would have to be covered by a sheath of aluminized Mylar or a conforming dry-on coating, which may cause additional design problems [27].

Another problem to take into account is the stiffness of graphite fibre. The graphite fibres that are used in thermal strips would have to be manufactured in a shape that is similar

to the shape of assembly. If this is not adhered to, the fibre may begin to fracture resulting in FOD in the device [27].

Testing of K13C2U carbon fibre manufactured by Mitsubishi shows that the thermal conductivity of these carbon fibres is not affected by vibrations during the launch of the Ariane 5 rocket [28]. These tests also show that K13C2U fibres are not harmed by slight bending, this information may be useful for the MHS project [28]. Parameters of these fibres are mentioned in the Table 7.4.

Table 7.4 Carbon fibre parameters

Fibre name	Density [kg·m⁻³]	Thermal Conductivity [W·m⁻¹·K⁻¹]	Tensile modulus [GPa]	Tensile strength [MPa]
T-1000GB PAN-based [25]	1800	12,6	291	5690
K13D pitch-based [25]	2200	747	940	3210
K13D pitch-based (CNTs - grafted) [25]	2200	967,1	989	4090
K13C2U [29]	2200	620	900	3800
K13D2U [29]	2200	800	935	3700

7.3.2 Graphene foil

Graphene materials for heat conduction are relatively new in space technologies, first thermal straps with graphene, were qualified by NASA in 2018. Since then they have been used in Space projects [30].

The graphene is used because in comparison with aluminium or copper foils it have higher thermal conductivity and lower weight [30].

According to the available information graphene should withstand 100 000 of cycles which is one of the requirements from ESA [31].

The probable disadvantage could be production of FOD which was mentioned in this chapter, but this problem can be solved by mylar foil sleeve [30].

The parameters of graphene are mentioned in the Table 7.5.

Table 7.5 Graphene parameters [31]

Thermal conductivity [W·m⁻¹·K⁻¹]	Product thicknesses [m]	Bending cycles without conductivity affect
1 700	$1·10^{-6} – 1·10^{-4}$	100 000

8 Technologies

There are not many potentially useful technologies for the MHS project, which could be used to manufacture a thermal conductive structure. It depends on the type of structure that will be used.

8.1 Laser Welding

Laser Welding technology was used in the MHS project by Arescosmo in the previous design of the Thermal conductive structure for connecting the textile braid (TB) with the contact plate and base braid textile.

This technology uses lasers to weld material parts together. Laser welding allows extremely small parts to be welded with high precision [32].

A number of types of laser can be used for laser welding, but the most frequently used lasers are probably Fibre Lasers, Nd: YAG Pulsed Lasers and Continuous Wave Lasers [32].

8.1.1 Fibre Lasers

This type of laser can weld very small parts used in electronics or the automotive and aerospace industry [32].

8.1.2 Nd: YAG Pulsed Lasers

This type of laser uses pulses to create spot weld or deep spot welds [32]. The advantage of pulsed laser is that it creates pulses of higher power than the average power of the laser itself. This results in more energy delivered to the weld when compared to Continuous Wave Laser. This means that reflective materials could be welded for example. These materials require more power for welding. Pulse Lasers also create a smaller heat affected area than Continuous Wave Lasers [33].

8.1.3 Continuous Wave Laser

These lasers emit a constant beam. They are suitable for high speed welding and deep penetration welding [32]. They are also suitable for welding high carbon stainless steel. Many materials require 200 W of energy to connect them and this method also offers the option of joining different materials with different properties. Materials like copper and aluminium require lasers with increased energy from 600 W to 800 W. These lasers are a type of Fibre Laser [33].

8.1.4 Capabilities of Laser Welding

The main advantage of Laser Welding is accuracy. This technology is very precise and can be used for small parts. It can also be used for very complicated joins. This technology also uses a small amount of heat that penetrates the material, so distortion is less than with conventional welding techniques and the thermally affected area is also smaller. This technology allows manufacturers to make high strength welds and there is also no need for a filler material [32]. Process gas consumption is also low. The other advantage of laser welding is the option of remote welding. The laser beam is targeted at the welding site by a set of mirrors. The targeted point is changed by changing the positions of the mirrors. This allows welding of large areas [34].

Welding copper materials is more complicated than welding other materials, because copper has greater thermal conductivity and also poor absorption of a laser beam at a standard wavelength of 1 µm which can be seen in the Figure 8.1. Copper can only absorb 5 % of the energy of a laser beam with this wavelength. This means that a laser with

enormous power is required to weld this material. But if a laser with a higher wavelength, of 500 nm for example, is used, copper can absorb 30 – 40 % of the laser beam energy [35].
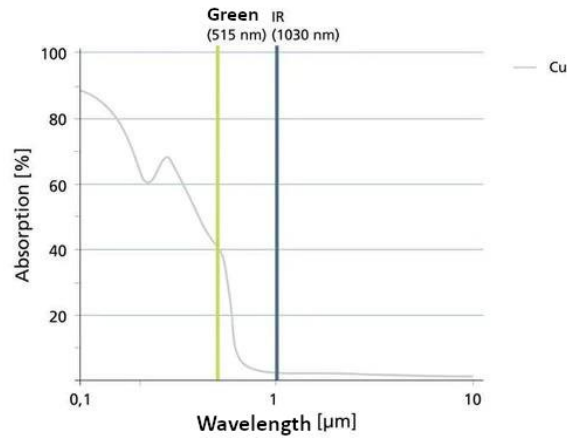

Figure 8.1 Copper absorption of laser beam [35]

The Trumpf Company manufactures a laser-welding device that uses a green laser beam, with a power of around 4 kW. This is the Trudisk 421 with a laser beam wavelength of 515 nm. This type of laser-welding device is intended for welding copper and other reflective materials [35].

8.2 Electron Beam Welding

This type of welding technique uses an electron beam in a vacuum chamber. Using a keyhole technique it is capable of welding materials of a thickness ranging from 0,01 mm to 250 mm in steel and up to 500 mm in aluminium. This technology even could be used to weld dissimilar metals. The vacuum range in the chamber is between 0,0001 Pa and 0,1 Pa. The diameter of the electron beam ranges between 0,1 – 0,8 mm [36].
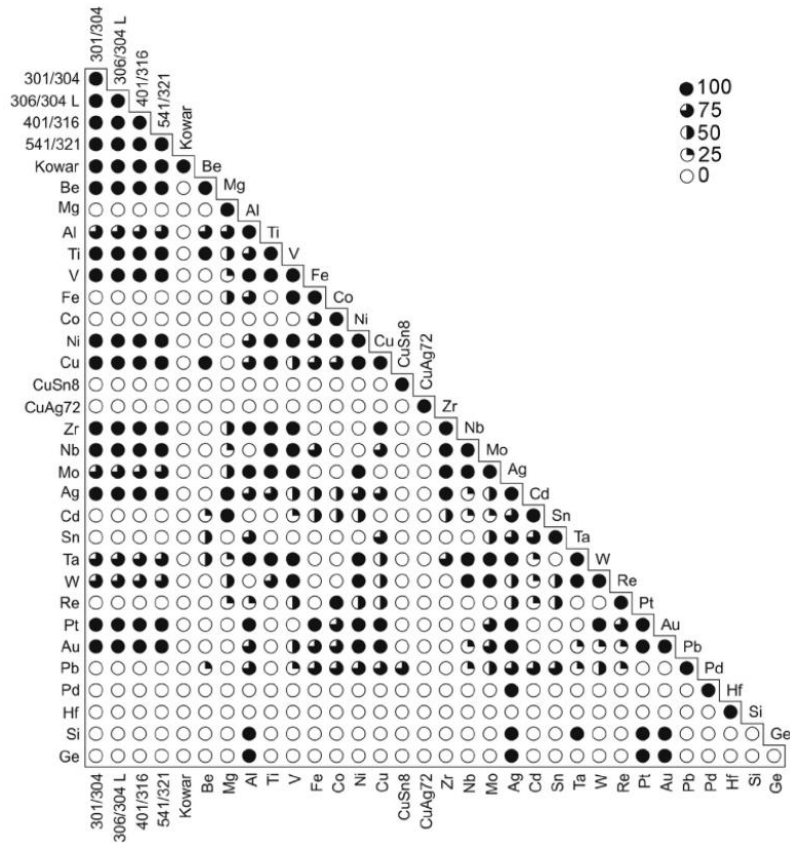
Pic. 8.1 Electron beam welding materials weldability [36]

Picture 8.1 gives a graphic depiction of the weldability of different metal combinations by electron beam welding. The quality of welds is expressed in numbers [36].

- 100 – All alloy combinations are weldable by Electron Beam.
- 75 – Electron Beam welding is possible.
- 50 – It may be possible to weld these materials.
- 25 – It is probable that these materials cannot be welded.
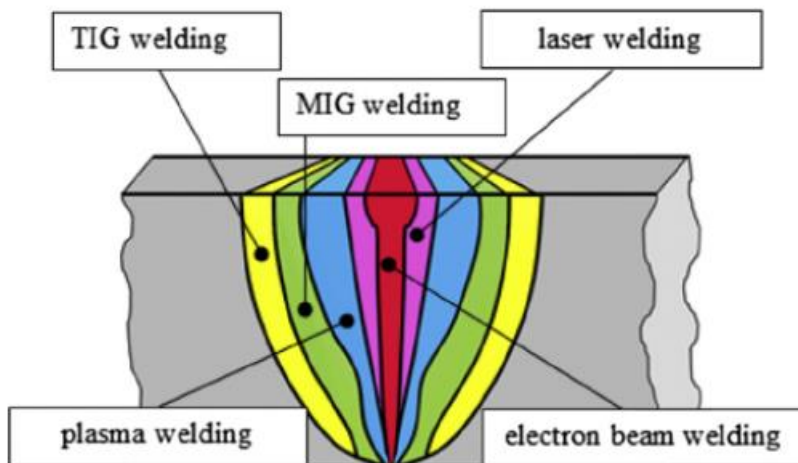- 0 – These materials cannot be welded by Electron Beam.

Pic. 8.2 Butt weld dimensions comparison [36]

8.2.1 Capabilities of Electron Beam Welding

The main advantage of Electron Beam Welding is use of a high power density of about 10^7 W·cm^{-2} at the focus of the beam. The welding energy is transferred by heat conduction across the surface of the welded part itself. There is no need for filler metal and the high

welding speed results in narrow welds with small heat affected zones, as can be seen in the Picture 8.2. A variable working distance is important for welding. This allows welding of a wide range of differently shaped workpieces [36].

Electron beam welding is carried out in a vacuum chamber so there is no need for processing gases. Another advantage is the reproducibility of weld quality and other welding parameters. Materials of thicknesses of less than 0,5 mm to 300 mm can be welded using an electron beam of a power ranging from 1 kW to 300 kW [36].

Electron Beam Welding can be used to weld a huge range of materials as can be seen in the Picture 8.1 [36].

One of the biggest problems in relation to Electron Beam Welding is the vacuum chamber. Because the workpiece may be bigger than the vacuum chamber of the welding device. If this situation occurs there is no way to weld this workpiece. The chamber and welded parts must also be clean and under high vacuum. Any impurities could mean problems with weld quality. There is also another problem connected to the dimensions and shape of the workpiece. The electron gun must "see" the area that is being welded, which means that the area and the gun must be in straight line [36].

Another problem related to Electron Beam Welding could be the magnetism of some materials. The electron beam could be deflected if the workpiece has even a slight magnetic field [36].

Because Electron Beam Welding is a very precise method, the welded surfaces should be manufactured within very precise tolerance ranges. The gap between surfaces must be less than 0,1mm. More than 0,1 mm cannot be tolerated [36].

8.3 Machining

Machining can be defined as the general term for the process of controlled removal of chips from a basic material. Many of these methods have lower set-up costs than forming, moulding and casting for example [37].

The most common machining technologies are turning, drilling and milling. The Table 8.1 gives a list of individual technologies with basic information about their accuracy and the surface condition after the fine machining that is used as the last part of the machining process [38] [39].

Table 8.1 Precision parameters after fine machining [38] [39]

Machining method	Name of Technology	Dimensions precision IT		Surface roughness Ra [µm]	
		mean	range	mean	Range
Outer rotary surfaces	*Turning* Roughing Finishing Softly CC[1] Softly DIA[2]	13 10 8 6	11 - 14 9 - 11 7 - 9 5 - 7	25 3,2 0,8 0,4	12,5 - 50 1,6 - 12,5 0,4 - 1,6 0,2 - 0,8
Inner rotary surfaces	*Turning* Roughing Finishing	12 10	11-13 9-12	25 3,2	12,5 - 50 1,5 - 12,5
	Drilling with a drill bit Without lead With lead	13 12	12 - 14 10 - 13	6,3 3,2	6,3 - 25 3,2 - 25
	Boring Roughing Finishing Softly CC Softly DIA	12 10 6 5	11 - 14 9 - 11 5 - 8 4 - 7	25 3,2 0,8 0,4	12,5 - 50 1,6 - 6,3 0,4 - 1,6 0,2 - 0,8
	Broaching Roughing Finishing	8 7	7 - 8 5 - 7	1,6 0,4	0,8 - 3,2 0,1 - 0,8
Plane surfaces	*Milling* Roughing end mill Finishing end mill Roughing with fly cutter Finishing with fly cutter Softly CC	12 10 11 9 6	10 - 13 9 - 11 10 - 13 8 - 9 5 - 7	25 3,2 25 3,2 0,8	12,5 - 50 1,6 - 6,3 12,5 - 50 0,8 - 6,3 0,4 - 0,6

---

[1] Cemented Carbide
[2] Diamond

9 Braided Structure

The braid structure consists of wires that are braided together [40]. It was one of the first concepts considered by the Arescosmo Company and was used in the final design of the heat switch.

Unfortunately, this concept was overrated by Arescosmo and the measured thermal conductivity was significantly smaller than the calculated value, as can be seen in the Chapter 4.

Braid structures can provide good flexibility in connection with good thermal conductance and can be designed from metals like copper and aluminium, and also from carbon fibres.

Welding is a technology that can be used for braided structure manufacturing, or soldering with C-solder can be used in the case of carbon fibres. Because copper materials are harder to weld by laser the option of electron beam welding can be used.

Braided structure concepts can be divided into two types based on flexibility. The first type is Flat braid – Heat transfer in the transversal direction: the sleeving braid concept and the stocking braid concept, where flexibility is ensured by movement of the wires (contraction of the structure), which can be seen in the Picture 9.1. The second type is the Flat braid concept – Heat transfer in the longitudinal direction. In this type of concept flexibility is ensured by the bending the entire braid, as can be seen in the Picture 9.2.
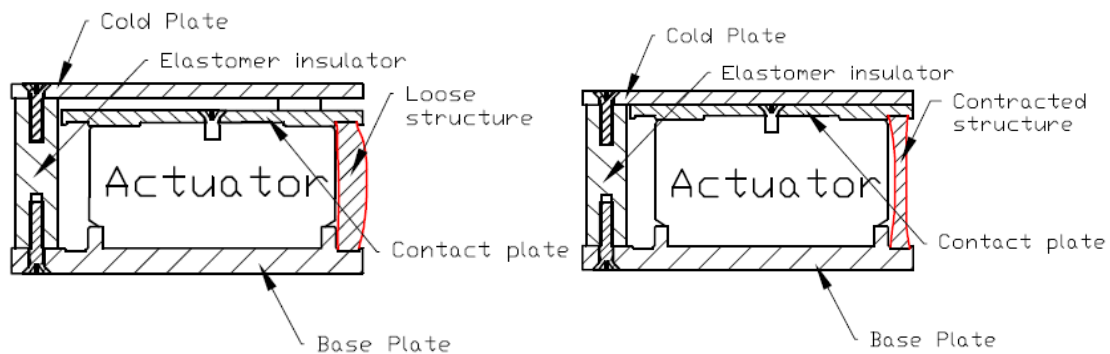
Picture 9.1 Structure loose in the OFF position (left) and contraction in the ON position (right)
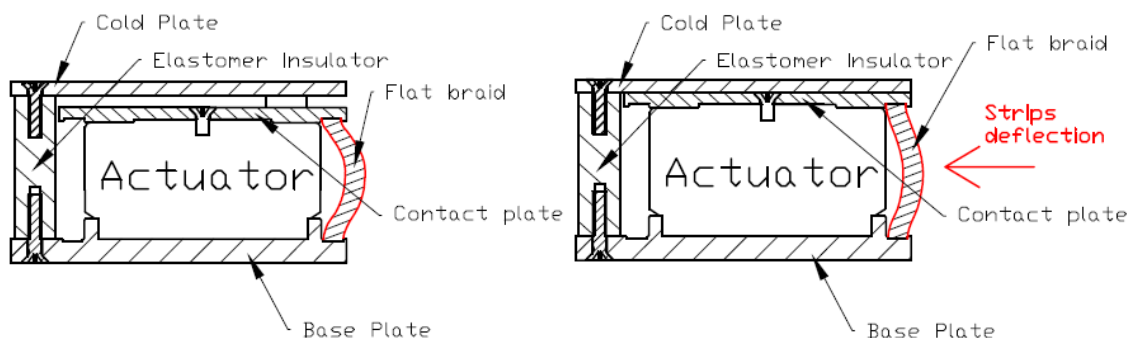
Picture 9.2 Structure bending in the OFF position (left) and the ON position (right)

First of all it must be explained that each calculation outlined in the following procedures was primarily intended to identify approximate basic parameters, which could subsequently be used as a starting point for detailed design, and further refined by more sophisticated methods.

9.1   Flat braid – Heat transfer in the transversal direction

Flat braid is a structure used for grounding lightning conductors, or for some connections of high voltage devices such as transformers for example [41]. Flat braids, but more often round braids, are used in thermal strap designs for heat conduction in the space industry or the cryogenic industry [42].

The braided strip is cut to the required length according to the Picture 9.3. In the next step the edges of the longitudinal cross-section are cut and the strip is then connected to the contact plate and the base braid textile as mentioned in Chapter 2.1. Heat transfer is then realised in the transversal direction through the braided strip (longitudinal cross-section area).
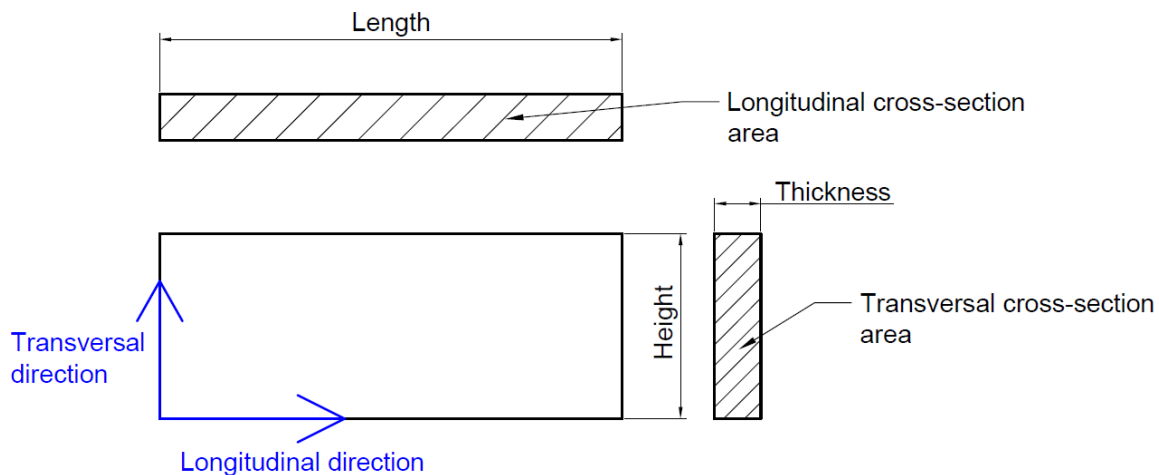
Picture 9.3 Flat braid coordination system

This type of structure was chosen by the Arescosmo Company for its flexibility and conductivity, as demonstrated by their calculations and tests. They tested multiple types of flat braid structures, but only one provided sufficient flexibility required by the heat switch. After testing heat switch potential in a Heat Switch test chamber, this structure was considered insufficient from the aspect of heat transfer and would require redesigning.

The flat braid has more flexibility in relation to heat transfer in the transversal direction (longitudinal cross-section area), than in the longitudinal direction (transversal cross-section area). But, in comparison to heat transfer in the longitudinal direction, the nominal area (area fully occupied by wires) is significantly smaller than the nominal area in the longitudinal direction, which means that heat conductivity is also significantly smaller. This fact was observed in CT scans mentioned in Chapter 4. After this problem was realised, it was necessary to find a method for computing the number of copper wires in the longitudinal cross-section, which is how large the nominal area is in the longitudinal cross-section.

The number of wires is computed using two different approaches:
- First calculation method (by constant)
- Second calculation method (by number of wires in the transversal nominal area)

9.1.1   First calculation method (by Constant)

When work on the braided strip concept was started, it was realised that the nominal area (area occupied by wires) in the transversal direction is approximately half of the full area occupied by the strip. This finding has been verified in MS excel by basic computation. This finding was verified on braided strips made by several companies. Table 9.1 gives some examples. The transversal geometric area was computed as a rectangle. Other

parameters were specified by the manufacturer. Difference from half" indicates how much the nominal area differs from half of the geometric area.

Table 9.1 Examples of flat braid strips

Manufacturer	Height [mm]	Thickness [mm]	transversal nominal area [mm²]	transversal geometric area [mm²]	Difference from half [mm²]
Hesselmann [10]	20	2	20	40	0
Hesselmann [10]	20	2,5	25	50	0
Hesselmann [10]	28	5,4	75	151	0,6
copper braid products [41]	14	1,5	10	21	0,5
copper braid products [41]	25	2	25	50	0
Tranect [40]	16	2	16	32	0
Tranect [40]	16	3	25	48	-1

After verifying that this correlation to the transversal direction actually exists, it was decided to find a correlation to the longitudinal direction.

The number of wires in the CT scan was initially counted. The result was roughly 1200 wires that are in contact with the lower braid structure.
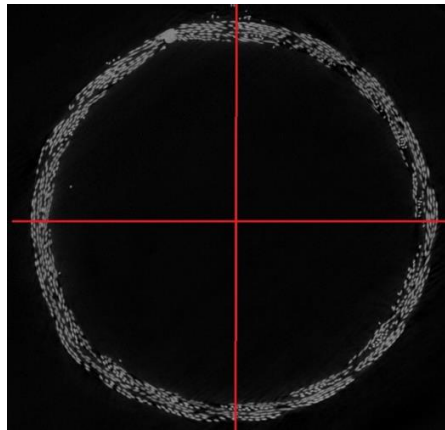
Picture 9.4 Upper view CT scan of CTB [9]

Table 9.2 Parameters of one strip used on BB [10]

Height a [mm]	Thickness e [mm]	Length l [mm]
10	1,2	120

The next step was to calculate the area occupied by the braided strip, which can be seen in Picture 9.4 in the longitudinal direction, and used data from Table 9.2. The area was computed as the area of the annulus. The result was that the area occupied by one strip is 144 mm².

In the next step the area occupied by the wires was calculated and then the number of wires was divided by 2 because two strips were used in the BB design. The area was computed as the circular area of one wire and then multiplied by the number of wires counted. The result of the nominal area (the area occupied by wires) in the longitudinal direction is 18,8495 mm² for one strip.

After all these computations, it was realised that the nominal area for heat transfer in the transversal direction is about 0,131 times the area occupied by the braided strip itself. This relationship applies only to the braid type used by Arescosmo for the final BB design, because when the braid is more densely woven the relation number may be greater.

When these numbers were realised, it was possible to approximately compute the parameters of other braided strips that could potentially be used. This allows at least approximation of the thermal conductivity of each type of braided strip using an equation (1). The results of some braided strips are given in Table 9.9.

Table 9.3 Final parameters

Parameters	Values
Number of wires (two strips)	1200
Number of wires (one strip)	600
Geometrical area in longitude (two strips)	288 mm^2
Geometrical area in longitude (one strip)	144 mm^2
Area occupied by wires (two strips)	37,699 mm^2
Area occupied by wires (one strip)	18,8495 mm^2
Constant	0,131

9.1.2 Second calculation method (by number of wires in the transversal cross-section)

The second calculation method uses the nominal area of the braided strip in the transversal cross-section area as specified by the manufacturer, the diameter of the wires in the braided strip and the computed angle between wire and longitudinal direction. The main parameters are highlighted in Picture 9.5. Letter a is the height of the braided strip as given in Picture 9.5. Value c is the length of the longest wire in the transversal cross-section, α is the angle between the longest wire and the longitudinal direction and b is the length of the longest wire in the longitudinal direction.
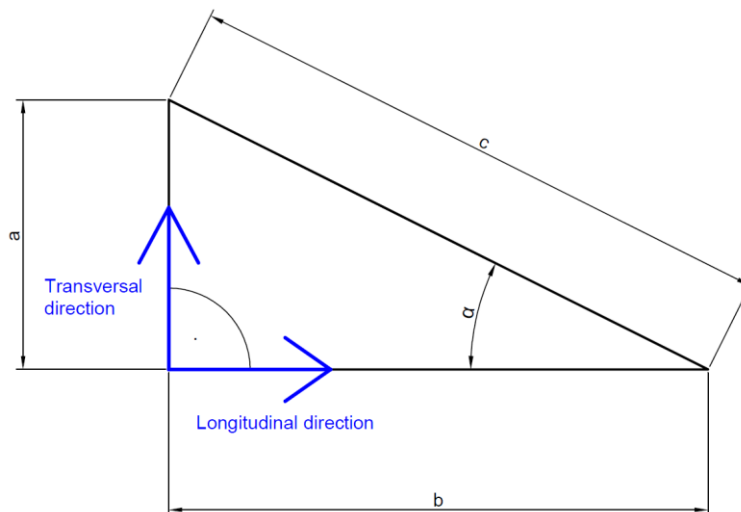
Picture 9.5 Wire geometry

How many wires there are in the transversal cross-section nominal area of the braided strip was initially calculated. This computation was based on Equation (4) where n_t is the number of wires in the transversal cross-section, S_t is the transversal nominal area and d is the diameter of the wires. The results were rounded up to whole numbers.

$$n_t = \frac{S_t \cdot 4}{\pi \cdot d^2} \tag{4}$$

In the next step, it was necessary to determine the angle between the wires and the longitudinal direction. This was computed using basic data from measurement of the BB switch. The average length of the wires was measured. This length (c) was 40 mm, and the approximate height of the original braided strip a was used. After this, the angle between the wire and the longitudinal direction (α) was calculated using equation (5). The angle was approximately 14,48 °.

$$\alpha = \sin^{-1} \frac{a}{c} \tag{5}$$

In this step it was finally possible to determine how many individual wires there were in the longitudinal direction. The calculation was based on the rule of three and the Pythagoras theorem. If the number of wires in the transversal cross-section area, the angle between the wires and the longitudinal direction are known, and the length of the longest wire was also known, it was possible to easily compute how many wires there are in the longitudinal direction. The first equation was derived from direct proportion.

$$n_l = \frac{n_t \cdot l_m}{b} \tag{6}$$

Where n_l is the number of wires in the longitudinal cross-section, n_t is the number of wires in the transversal cross-section, l_m is median length and b is the length of the longest wire projecting in the longitudinal direction, see Picture 9.5
Value b is calculated using Equation (7).

$$b = \sqrt{c^2 - a^2} \tag{7}$$

Where c is the length of the longest wire from the transversal cross-section and a is the height of the braided strip.
In the case of strips of a height greater than 10 mm, this value is recalculated as it should have 10 mm as well as other parameters, such as the nominal area, but, as can be seen in Table 9.7, the resulting number of wires is similar to the version that is not cut.
The length of the longest wire (c) is computed on the basis of Equation (8)

$$c = \frac{a}{\sin \alpha} \tag{8}$$

Where α is the angle between the wires and the longitudinal direction.
The whole equation is then applied in MS Excel as follows:

$$n_l = \frac{n_t \cdot l_m}{\sqrt{\left(\frac{a}{\sin \alpha}\right)^2 - a^2}} \tag{9}$$

The median length of the strip was used in calculations as the value (l_m). The median length was computed on the basis of the dimensions of the actual design described in Chapter 2.The computed value is the circumference of the median circle in the actual design of the braided strip, which is ⌀37,9 mm in diameter. The computed value is 119 mm. The dimensions are given in Picture 9.6.

Part of BB in the Picture 9.6 is the part called the Base braid textile, which has the same outer dimensions as the base plate. The median value is used because braided strips of many various thicknesses were used in the computations.
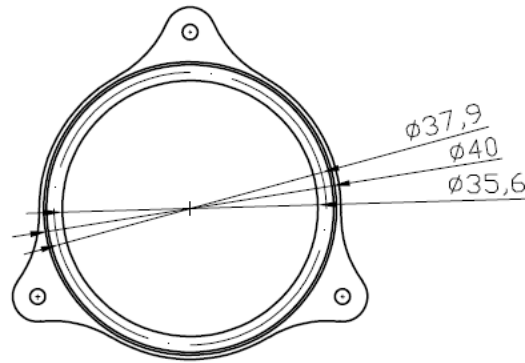
Picture 9.6 Base braid textile

After computation of the number of wires in longitude, it is finally possible to compute the nominal area in longitude (S_l) using the number of wires (n_l) and their diameter (d), using Equation (10).

$$S_l = n_l \cdot \frac{\pi \cdot d^2}{4}$$
(10)

Table 9.4 Final parameters of the strip

Parameters	Values
Length of a longest wire c	40 m
Angle between longitudinal direction and longest wire α	14,48 °
Height of the strip a	10 mm^2

9.1.3 Methodology

The final part is computation of weight and thermal conductivity.

Thermal resistivity (R) is computed using equation (1), which is then used to compute the thermal conductivity of one strip (C).

The weight of each strip is computed using Equation (12), where ρ is the density of the wire material and V is volume, which is computed using Equation (11), where δ is the length of the wires and S_l is the nominal area of the longitudinal cross-section.

$$V = S_l \cdot \delta$$
(11)

$$m = \rho \cdot V$$
(12)

The final steps are computation of the parameters of the structure that has the required thermal conductivity of the textile braid (TB) mentioned in Chapter 5.1, which is at least 1.5 W·K^{-1}. These parameters are: required length, which is the total length of the flat braid strip, which is wound around the actuator, the total weight of this flat braid and the area needed to attach the flat braid to the base plate.

The required length (L) is computed using Equation (13), where C is the thermal conductivity of one strip of median length (l_m) and the value 1,5 represents the required value of TB thermal conductivity.

$$L = \frac{1,5}{C} \cdot l_m \tag{13}$$

The final weight of the TB (M) is computed using Equation (14), which was derived using the rule of three. In this equation m is the weight of a strip of Median Length (l_m) and L is the required length of the strip.

$$M = \frac{m}{l_m} \cdot L \tag{14}$$

The required area of the TB (S_{TB}) is calculated as a rectangle of the required length (L) and the thickness of the particular strip (e).

These final computations were only carried out for the nominal area calculated on the basis of the number of wires in the longitudinal cross-section.

9.1.4 Computation results

Table 9.6 gives the values for the selected braided strips that are usable for the MHS project. Some of the strips have similar dimensions, but the difference may be in the diameter of the used wire.

The braided strips are numbered for example: [3;1].

- The first number refers to the strip number.
- The second number refers to the material from which is the strip manufactured.

The number of the materials and their specifications are given in Table 9.5. The braided strip actually used in the BB design is marked [1;1], for comparison.

Braided strips with materials numbered 2 and 3 are included because the manufacturer of these strips did not specify what type of aluminium material was used in their manufacture [43]. Calculations were therefore based on two different aluminium materials for the same braided strip in order to provide a range of values.

The selected strips are representatives intended to compare the effects of different wire diameters, different materials and different dimensions.

Table 9.5 Strip materials

Material number	Material type	Thermal conductivity λ [W·m^{-1}·K^{-1}]	Density ρ [kg·m^{-3}]
1	Cu ETP [21]	390	8900
2	Alu 7075-T73 [3]	155	2810
3	Al 99,5% [23]	235	2700

Table 9.6 Strip manufacturer's parameters

Designation [strip number; material number]	Manufacturer	Nominal area – transversal cross-section S_t [mm²]	Height approx. a [mm]	Braid Thickness e Approx. [mm]	Wire diameter d [mm]
1;1	Hesselmann [10]	6	10	1,2	0,2
2;1	Hesselmann [10]	6	10	1,2	0,15
3;1	Hesselmann [10]	6	10	1,2	0,1
4;1	Hilltop [43]	6	12	1	0,15
5;2	Hilltop [43]	6	12	1	0,2
6;2	Hilltop [43]	6	12	1	0,15
7;3	Hilltop [43]	6	12	1	0,2

Table number 9.7 gives the results of wire computations for the selected braided strips. These results are connected to the computation method described in Chapter 9.1.2.

Table 9.7 Computed number of wires in the strips

Designation [strip number; material number]	Median length l_m [mm]	Number of wires in the transversal cross-section n_t	Number of wires in the longitudinal cross-section n_l	Number of wires in the transversal cross-section (cut) n_t	Number of wires in the longitudinal cross-section (cut) n_l
1;1	119	191	588	191	588
2;1	119	340	1046	340	1046
3;1	119	764	2349	764	2349
4;1	119	340	871	283	870
5;2	119	191	490	160	492
6;2	119	340	871	283	870
7;3	119	191	490	160	492

Table number 9.8 gives the final results for thermal conductivity for the selected braided strips. These results are also given for a median length of strip of 119 mm.

The length of the individual wires was required for calculations of thermal conductivity. The wire length was used in all computations as a constant value, because the constant height of the braided strip was needed. The length was not changed in other braids computations because was used values of only one available reference strip.
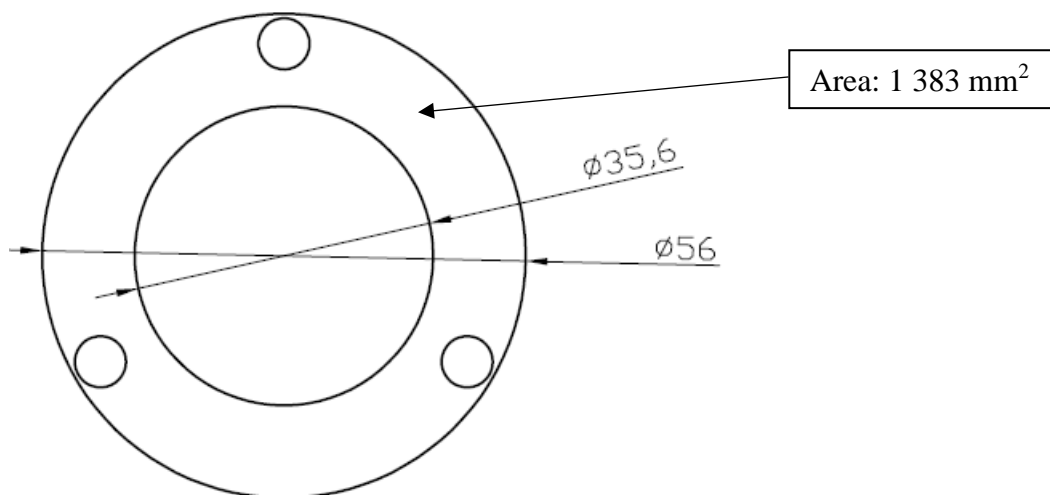
Table 9.8 Computed parameters of the strips in the longitudinal cross-section

Designation [strip number; material number]	Wire length δ [mm]	Nominal area – longitudinal cross-section S_n [mm²]		Weight m [g]		Thermal conductivity C [W·K⁻¹]	
		Constant	Wire computation	Constant	Wire computation	Constant	Wire computation
1;1	40	18,70	18,47	6,66	6,57	0,182	0,180
2;1	40	18,70	18,48	6,66	6,58	0,182	0,180
3;1	40	18,70	18,45	6,66	6,57	0,182	0,180
4;1	40	15,56	15,37	1,75	1,73	0,092	0,090
5;2	40	15,56	15,46	1,75	1,74	0,092	0,091
6;2	40	15,56	15,37	1,68	1,66	0,060	0,060
7;3	40	15,56	15,46	1,68	1,67	0,060	0,060

The final Table 9.9 contains the final dimensions of this concept after the condition set out in Chapter 5.1 is applied, whereas the structure itself must have a total thermal conductivity of 1,5 W·K⁻¹. These parameters can be easily compared to the limit parameters given in Picture 9.7.

Table 9.9 Final parameters of the TB

Designation [strip number; material number]	Strip length required for conductivity of 1,5W·K⁻¹ L [m]	Weight for 1,5W·K⁻¹ M [g]	Total area required for TB S_{TB} [mm²]
1;1	0,99	55,45	1 190
2;1	0,99	55,42	1 189
3;1	0,99	55,52	1 192
4;1	3,00	44,11	2 998
5;2	2,98	43,87	2 982
6;2	1,98	27,95	1 977
7;3	1,97	27,81	1 967

Picture 9.7 Representative useable area

9.1.5 Comparison between requirements and results

After comparing how large an area the TB needs and how large an area the current design of the switch provides, it appears that aluminium flat braids do not meet requirements, as they require a larger area.

The results show that the copper flat braid itself will be too heavy to be used on MHS and will also require a large area for connection to the base plate. Furthermore, if the TB is as large as required, it is likely to place a great amount of resistance against the movement of the actuator.

Another finding based on these results is that, in the absence of the specific detailed parameters of flat braid weaving, many results are quite similar, including the most important ones that relate to the complete TB. There is also no relationship between the nominal area and the diameter of the wires and flat braid dimensions.

9.2 Flat braid – Heat transfer in the longitudinal direction

This type of Heat conductive structure also uses a flat braided strip like the first, mentioned in Chapter 9.1. However, the difference is that in this type of concept the heat is transferred in longitudinal direction (transversal cross-section area), as can be seen in Picture 9.8. The basic concept is that the strips will be connected to the base braid textile and contact plate side by side. The strip will be slightly longer than the distance between the base braid textile and contact plate in the ON position and so it will be slightly bent. When the actuator moves and the contact is in the ON position, the strips' deflection is reduced, as can be seen in Picture 9.9. As mentioned in Chapter 9.1, the nominal area of the transversal cross-section is roughly half of the geometrical cross-section area. This means that results could be better than heat transfer in the transversal direction.
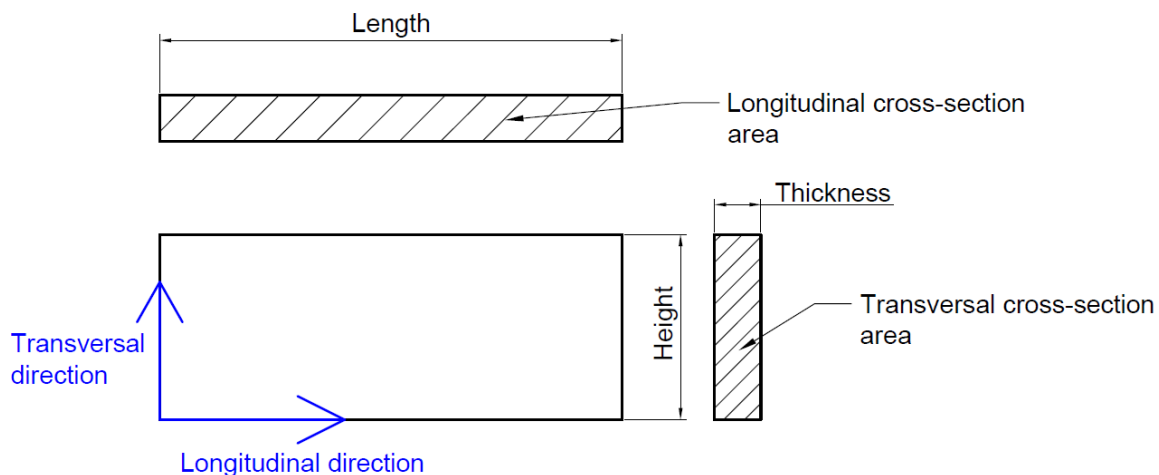
Picture 9.8 Flat braid coordination system
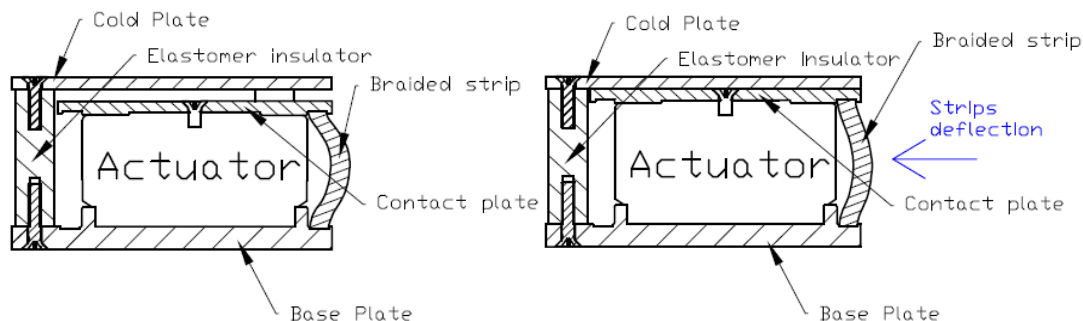
Picture 9.9 Schematic section of the MHS in OFF position (left) and ON position (right)

As can be seen in Picture 9.9, the problem with this concept is the elastomer insulators around the perimeter. There is not enough space for the bent braid strip between the elastomer insulator and the actuator, so the strips can only be placed in the area between these elastomer insulators or the dimensions of the entire MHS must be changed. There is also the possibility that the whole strip could bend and be inserted in this small space.

9.2.1 Methodology

The methodology of computation in this concept was similar to the methodology of computation for heat transfer in the transversal direction as specified in Chapter 9.1, but much easier because the nominal area of the transversal cross-section is given by the manufacturer.

The thermal conductivity of 1 strip of a specific length was initially calculated. Computations were based on equation (1), which is then used to compute thermal conductivity (C).

The length of each wire for the required strip length was estimated as 40 mm. This is the same value as in Chapter 9.1, but can be assumed that the length in the actually application could be smaller, so that the thermal conductivity would be higher and weight would be also reduced.

Volume (V) is computed using equation (15), where S_t is the transversal nominal area and δ is the length of the wires.

$$V = S_t \cdot \delta \tag{15}$$

Equation (12) is then used to calculate the weight of each strip.

The number of single strips (n_{TB}) required for a thermal conductivity of the TB of at least 1,5 W·K^{-1} is computed using equation (16), where C is the thermal conductivity of one strip. The result was rounded up.

$$n_{TB} = \frac{1,5}{C} \tag{16}$$

The weight of the TB (M) is then computed on the basis of the weight of one strip (m) and the number of strips (n_{TB}).

$$M = m \cdot n_{TB} \tag{17}$$

The total cross-section area (S_{TB}) required for the TB is computed using equation (18), where a is the height of one strip and e is the thickness of one strip.

$$S_{TB} = a \cdot e \cdot n_{TB} \tag{18}$$

The strips are connected to the base braid textile and contact plate side by side so welds are required.

9.2.2 Computation results

Table 9.11 gives the basic parameters published by the manufacturers of the braided strips, which were considered useful for this purpose. The braided strips are numbered and the numbers in the following tables refer to the numbers in this table.

The braided strips are numbered for example: [3;1].
- The first number refers to the strip number.
- The second number refers to the material from which is the strip manufactured.

The numbers of the materials and their specifications are given in table 9.10. The braided strip actually used in the BB design is designated [1;1], for comparison.

The braided strips with materials numbered 2 and 3 are included because manufacturer of these strips did not specify what type of aluminium material was used in their

manufacture [43]. Calculations were therefore based on two different aluminium materials for the same braided strip in order to provide a range of values.

Table 9.10 Table of strip materials

Material number	Material type	Thermal conductivity λ [W·m^{-1}·K^{-1}]	Density ρ [kg·m^{-3}]
1	Cu ETP [21]	390	8900
2	Alu 7075-T73 [3]	155	2810
3	Al 99,5% [23]	235	2700

Table 9.11 Strip manufacturer's parameters

Designation [strip number; material number]	Manufacturer	Nominal area – transversal cross-section S_t [mm^2]	Height approx. a [mm]	Braid Thickness Approx. e [mm]	Wire diameter d [mm]
1;1	Hesselmann [10]	6	10	1,2	0,2
2;1	Hesselmann [10]	6	10	1,2	0,1
3;1	Hesselmann [10]	10	15	1,3	0,1
4;1	Copper braid products [41]	0,75	2,5	0,5	0,1
5;2	Hilltop [43]	10	15	1,5	0,15
6;2	Hilltop [43]	6	12	1	0,15
7;3	Hilltop [43]	10	15	1,5	0,15
8;3	Hilltop [43]	6	12	1	0,2

Table 9.12 Computed parameters of the strips and the final parameters of the TB

Designation [strip number; material number]	Wire length δ [mm]	Thermal Conductivity of 1 strip C [W·K^{-1}]	Weight of 1 strip m [g]	Strips required for conductivity 1,5 W·K^{-1} n_{TB}	Weight for 1,5 W·K^{-1} M [g]	Total area required for TB S_{TB} [mm^2]
1;1	40	0,0585	2,14	26	55,54	312
2;1	40	0,0585	2,14	26	55,54	312
3;1	40	0,0975	3,56	16	56,96	312
4;1	40	0,0073	0,27	206	55,02	258
5;2	40	0,0388	1,12	39	43,84	878
6;2	40	0,0233	0,67	65	43,84	780
7;3	40	0,0588	1,08	26	28,08	585
8;3	40	0,0353	0,65	43	27,86	516

Picture 9.10 shows the representative useable area with dimensions for this type of concept. The representative area is smaller than the area for the previous design given in Chapter 9.1 for the reasons mentioned above.

Area: 1 284 mm^2
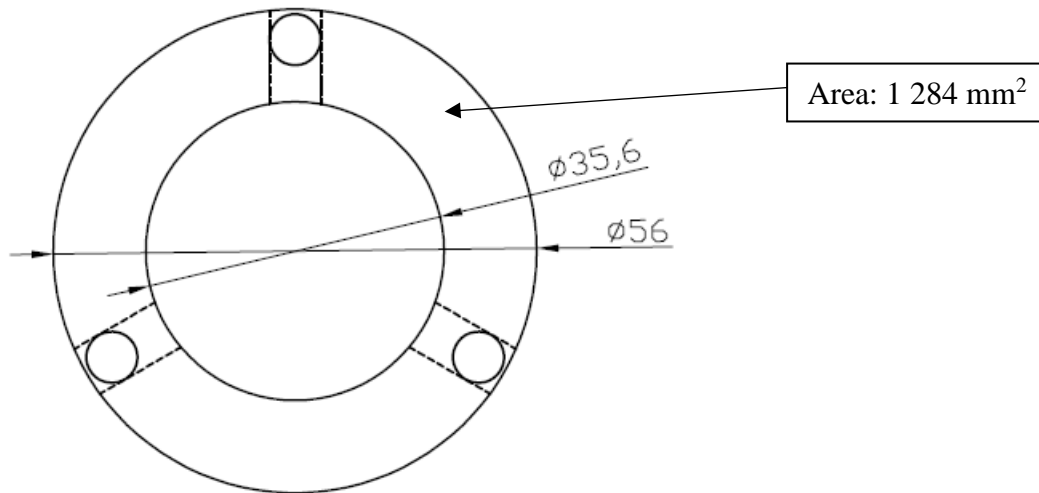
Picture 9.10 Representative useable area

9.2.3 Comparison between requirements and results

After comparison of the selected flat braids it seems that both selected aluminium materials and copper ETP meet dimensional requirements, as the area required for the TB is smaller than the available area.

Due to the use of a wire length of 40 mm, the weight of the copper strips is quite high, but this is not the case for aluminium materials, which are only slightly heavier than the currently used TB and are likely to be lighter than the current TB if the wire length is reduced, and will also be more conductive using this concept. The required area will also be smaller if shorter wires are used in the computations.

The wire length depends on the weaving of the strip and on the length of the strip itself that is required for its movement.

Another finding is that a TB composed of strips of different nominal areas has similar weight parameters or the required area. This is probably due to the efficiency of space utilization, thus the relationship between the nominal cross-sectional area and the cross-sectional area.

The wire diameters do not affect the results of the calculations, but it is possible that they will affect the flexibility of the structure.

The last finding is the fact that in terms of reduction of the required area, it could be more efficient to use a larger number of smaller strips.

9.3 Sleeving braid

Sleeving braid is type of braided structure used for covering cables to give them electro magnetic compatibility (EMC) protection and radio frequency (RF) protection [44]. This cover can also be used for mechanical hosepipe and cable protection [45].

Picture 9.11 Sleeving braid [44]

Sleeving braid is type of braid that can be stretched. As can be seen in Picture 9.1 it is manufactured from wires, which are distributed around the perimeter, so that cables or pipes can be placed inside. This also allows for expansion or contraction of this braid [44].

The concept using sleeving braid is designed with regard to thermal conductivity and flexibility. This concept is intended to cut the desired length of the sleeving braid which will then be expanded to required diameter and placed between contact plate and base braid textile. The edges will be connected to the contact plate and base braid textile, probably by welding.

The function of the Sleeving braid TB is outlined in Picture 9.12. The Sleeving braid is placed between the Base plate and the Contact plate. When the actuator moves up to the ON position the sleeving braid contracts and when the actuator moves down the sleeving braid expands.
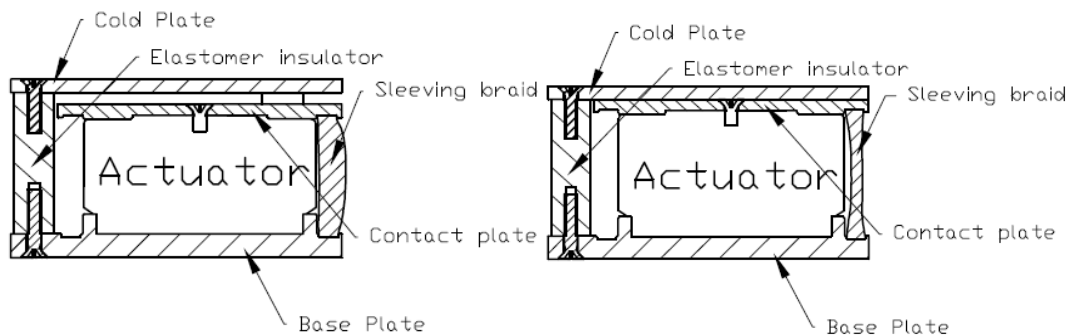
Picture 9.12 Schematic section of MHS in the OFF position (left) and the ON position (right)

9.3.1 Methodology

The methodology is quite similar to the previous concepts of textile braid. The nominal area initially had to be established, but this value is specified by the manufacturer. It was also necessary to establish the minimum diameter of each sleeving braid. The minimum diameter is given by the dimensions of the actuator and the value is given in Picture 9.6. Sleeving braids with a value less than the minimum diameter were not evaluated.

Computation of the thermal conductivity (C) of one braid was again based on equation number (1), where the nominal area of the transversal cross-section (S_t), the length of the wires (δ) and the thermal conductivity of the material (λ), were used.

The length of each wire in one sleeving braid purchased from the manufacturer was measured. This braid was expanded to the required diameter of 42 mm and then the length of the wires was measured at the required length of the sleeving braid, which is 25 mm. The length was approximately estimated to be necessary for the proper functioning of the

entire concept. The measurements can be seen in Picture 9.13 and the measurements are given in Table 9.13. The required length of 25 mm is between the two pieces of black tape.

The diameter of 42 mm is used because it can be assumed to be an average value. With the greater shrinkage (smaller diameter) of the sleeving braid, the individual wires will be shorter and with the greater expansion (higher diameter) they will be longer.

Table 9.13 Measured sleeving braid parameters

Parameter	Value	
Diameter of the braid d_{sl}	⌀42 mm	
Required length of the braid L	25 mm	
Wire length δ	[1;1]	[2;1]
	32 mm	27 mm

The wire length in other sleeving braids was approximately estimated at 34 mm.
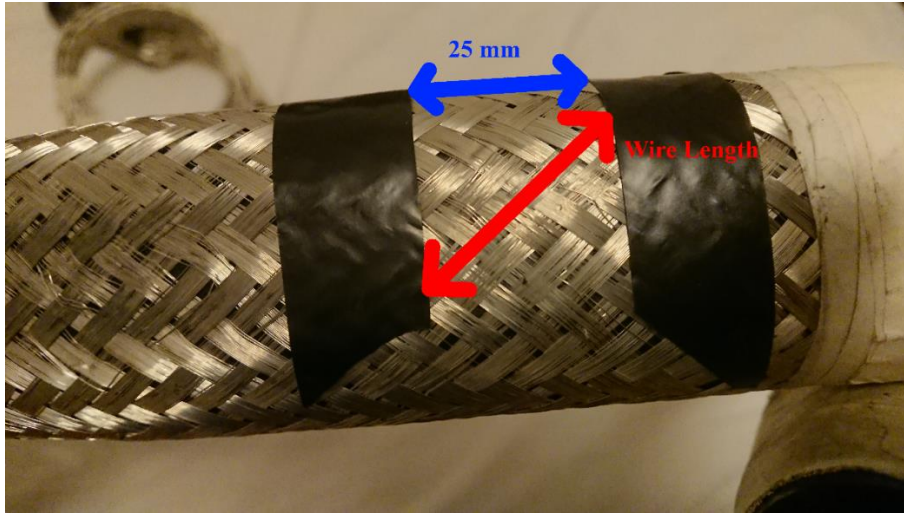
Picture 9.13 Sleeving braid parameters

Volume (V) is computed on the basis of equation (15), where S_t is the transversal nominal area and δ is the length of wires.

Equation (12) is used to calculate the weight of each braid.

The final parameter of the TB is number of single braids (n_{TB}) used and the total area required for connection of the TB (S_{TB}) to the base braid textile.

The number of single braids (n_{TB}) required for a thermal conductivity of the TB of at least 1.5 W·K^{-1} is computed using Equation (16), where C is the thermal conductivity of one braid. The result was rounded up, because it is impossible to use just part of a sleeving braid.

The total area required for the TB (S_{TB}) cannot be calculated exactly, because the arrangement of the wires changes as the braids expand and contract. Therefore, this value was calculated only approximately using equation (19), where n_t is computed using equation (4).

The approximation itself takes the number of wires from the transversal nominal area and then computes the area as the area of a rectangle filled by all these wires according to the Picture 9.14.

$$S_{TB} = n_t \cdot d^2 \cdot n_{TB}$$

(19)
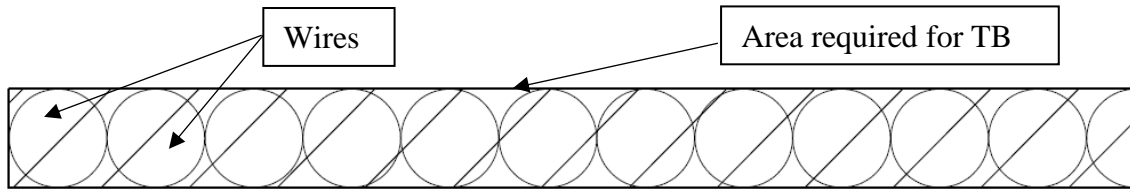
Picture 9.14 Computation of approximate area required for the TB

9.3.2 Computation results

Table 9.15 gives the basic parameters published by the manufacturer of the sleeving braids considered useful as representatives. The sleeving braids are numbered and the numbers in the following tables refer to the numbers in this table.

The sleeving braids are numbered for example: [3;1].

- The first number refers to the strip number.
- The second number refers to the material from which is the strip manufactured.

The numbers of the materials and their specifications are given in Table 9.14.

The measured sleeving braids are designated [1;1] and [2;1]. The one designated [1;1] is made of tinned copper ETP.

Table 9.14 Table of sleeving braid materials

Material number	Material type	Thermal conductivity λ [W·m^{-1}·K^{-1}]	Density ρ [kg·m^{-3}]
1	Cu ETP [21]	390	8900
2	Alu 7075-T73 [3]	155	2810
3	Al 99,5% [23]	235	2700

Table 9.15 Sleeving braid manufacturer's parameters

Designation [strip number; material number]	Manufacturer	Nominal area – transversal cross-section S_t [mm^2]	Min. braid diameter [mm]	Max. braid diameter [mm]	Wire diameter d [mm]
1;1	Copper braid products [44]	40	35	60	0,2
2;1	Leoni [46]	48,3	–	80	0,4
3;1	Revelet [47]	23,8	–	50	0,3
4;3	Leoni [46]	23,8	–	50	0,3
5;3	Leoni [46]	30,5	–	60	0,3

Table 9.16 Computed parameters of the sleeving braids and the final parameters of the TB

Designation [strip number – material number]	Wire length δ [mm]	Thermal Conductivity of 1 strip C [W·K^{-1}]	Weight of 1 strip m [g]	Braids required for conductivity 1,5 W·K^{-1} n_{TB}	Weight for 1,5 W·K^{-1} M [g]	Total area required for TB S_{TB} [mm^2]
1;1	32	0,488	11,39	4	45,57	204
2;1	27	0,698	11,61	3	34,82	185
3;1	34	0,273	7,20	6	43,21	182
4;3	34	0,165	2,19	10	21,85	303
5;3	34	0,211	2,80	8	22,40	311

Because the sleeving braids could not be cut like the flat braids used in Chapter 9.1, the thermal conductivity of all the braid is necessary for a thermal conductivity of exactly 1,5 W·K^{-1}. Due to this fact, the thermal conductivity of a given sleeving braid is often higher than is required and this also results in an increase in weight. Figure 9.1 gives all sleeving braids that were calculated and those marked in yellow have been selected in the Table 9.15 and Table 9.16.
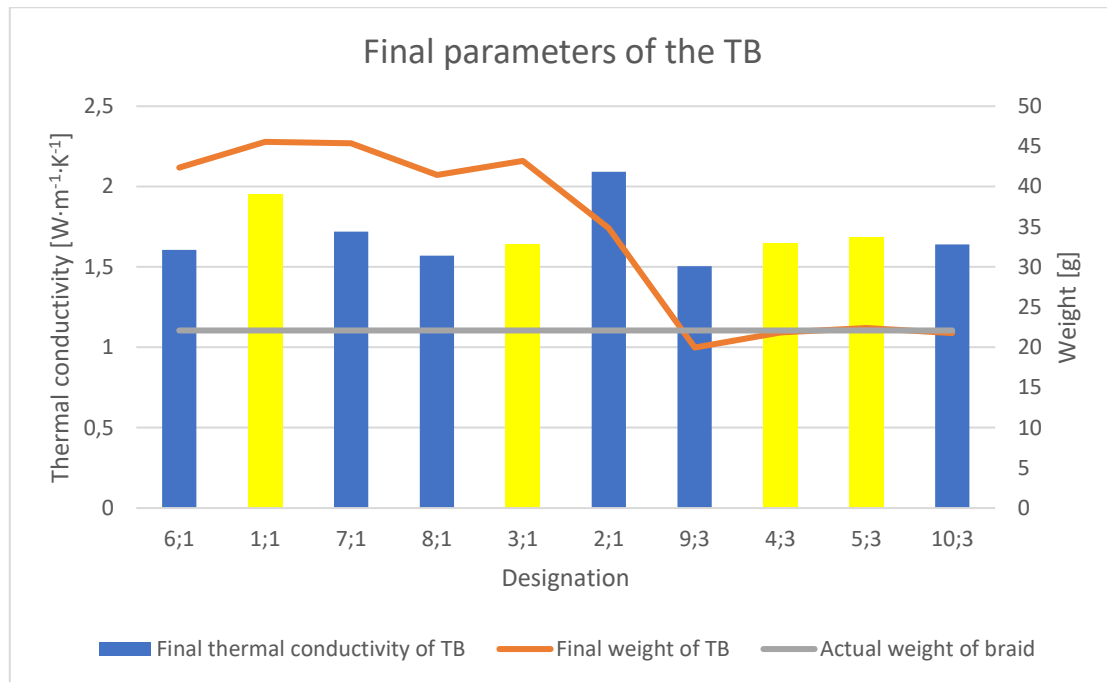
Figure 9.1 Final parameters of the TB

Picture 9.15 gives data for the maximum, representative usable area for this type of concept. Because the sleeving braids cannot be cut, this area is limited by the elastomer insulators.
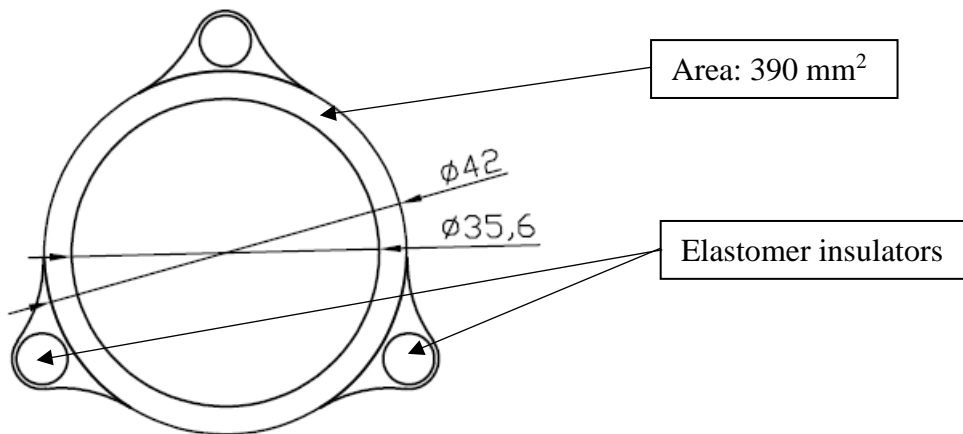
Picture 9.15 Representative usable area

9.3.3 Comparison between requirements and results

Following comparison of the selected sleeving braids it seems that both selected materials, aluminium and copper ETP, meet dimensional requirements, as the area required for the TB is less than the available area.

As shown in Figure 9.1, the TB made of aluminium wires is approximately two times lighter than that made of copper wires, but the area required for the TB is only 1,5 times greater for approximately the same thermal conductivity. It is probable that sleeving braids made from aluminium would be more useful than those made of copper, but it is also possible that the flexibility of the structure will be reduced by a greater number of braids.

According to the calculation method, thermal conductivity and weight are parameters related to the nominal area of the braid and the length of wires. Other braid parameters may be connected to the flexibility or possibility of placement in the MHS design space for example.

Two or more types of braid can be combined in order to achieve the precise thermal conductivity value and simultaneously the lowest weight, for the best performance of this structure.

9.4 Stocking braid

Stocking braid is also a type of braided structure similar to sleeving braid, but this type of braid provides more flexibility than sleeving braid. Usage of this type of braid is similar to sleeving braid but as it is more flexible it can be used for covering joints etc. [44].

Picture 9.16 Stocking braid [44]

The concept using stocking braid is similar to the sleeving braid concept, as can be seen in Picture 9.17, but the difference may be in the greater flexibility of stocking braid. This flexibility can provide greater mobility in relation to the contact plate.
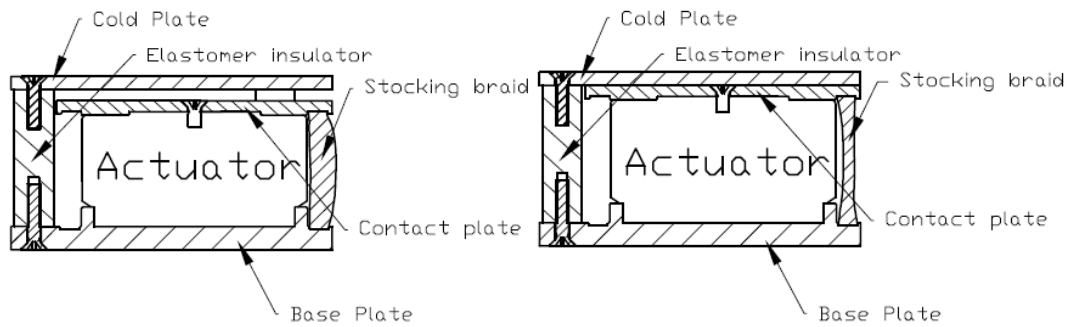
Picture 9.17 Schematic section of MHS in the OFF position (left) and the ON position (right)

9.4.1 Methodology

The methodology is the same as in the previous concept, which used sleeving braid and is described in Chapter 9.3.

Measurement of the wire length also performed in the same way according to the Picture 9.18.
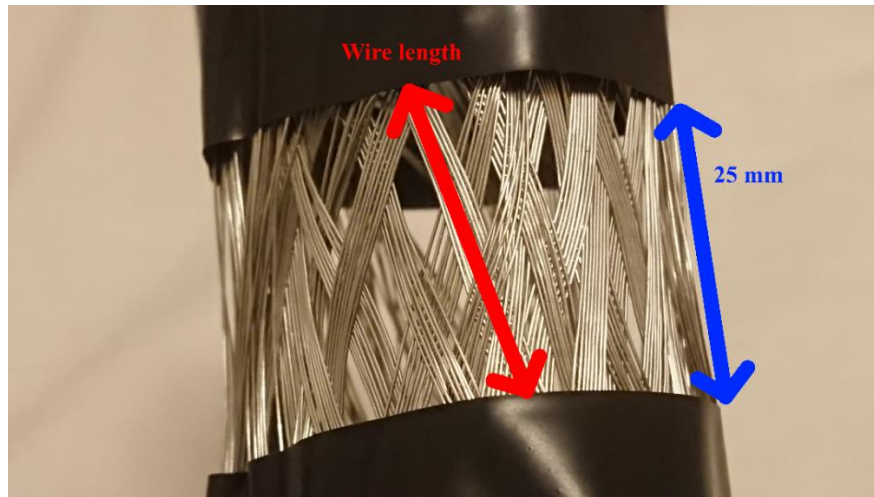
Picture 9.18 Stocking braid parameters

Table 9.17 Measured stocking braid parameters

Parameter	Value	
Diameter of the braid d_{sl}	⌀42 mm	
Required length of the braid L	25 mm	
Wire length δ	**[1;1]**	**[2;1]**
	27 mm	28 mm

9.4.2 Computation results

Table number 9.19 gives the basic parameters published by the manufacturers of stocking braids considered useful for this purpose. The stocking braids are numbered and the numbers in the following tables refer to the numbers in this table.

The stocking braids are numbered for example: [3;1].
- The first number refers to the braid's number.
- The second number refers to the material from which the is braid manufactured.

The numbers of the materials and their specifications are given in Table 9.18.

The measured stocking braids are designated [1;1] and [2;1].

All stocking braids used in the calculations are made of copper, because stocking braids made of aluminium could not be found on the Internet. Manufacturers are probably unlikely to produce them in bulk and it would be necessary to ask specific manufacturers if they would make them to order.

Table 9.18 Table of stocking braid materials

Material number	Material type	Thermal conductivity λ [W·m^{-1}·K^{-1}]	Density ρ [kg·m^{-3}]
1	Cu ETP [21]	390	8900
2	Alu 7075-T73 [3]	155	2810
3	Al 99,5% [23]	235	2700

Table 9.19 Stocking braid manufacturer's parameters

Designation [strip number; material number]	Manufacturer	Nominal area – transversal cross-section S_t [mm^2]	Min. braid diameter [mm]	Max. braid diameter [mm]	Wire diameter d [mm]
1;1	Copper braid products [48]	25	25	120	0,2
2;1	Copper braid products [49]	35	35	120	0,2
3;1	Copper braid products [44]	95	30	120	0,2
4;1	Copper braid products [44]	6	6	40	0,2
5;1	Copper braid products [44]	35	25	120	0,2

Table 9.20 The computed parameters of the stocking braids and the final parameters of the TB

Designation [strip number – material number]	Wire length δ [mm]	Thermal Conductivity of 1 braid C [W·K^{-1}]	Weight of 1 strip m [g]	Braids required for conductivity 1,5 W·K^{-1} n_{TB}	Weight for 1,5 W·K^{-1} M [g]	Total area required for TB S_{TB} [mm^2]
1;1	27	0,361	6,01	5	30,04	159
2;1	28	0,488	8,72	4	34,89	178
3;1	34	1,090	28,75	2	57,50	191
4;1	34	0,069	1,82	22	39,94	168
5;1	34	0,402	10,59	4	42,36	178

Like the sleeving braid, the stocking braid could not be cut to achieve a precise value of thermal conductivity, so the whole braid had to be used in the computation. The values of TB thermal conductivity and weight are given in Figure9.2. The braids marked in yellow were selected in this master's thesis as representatives.
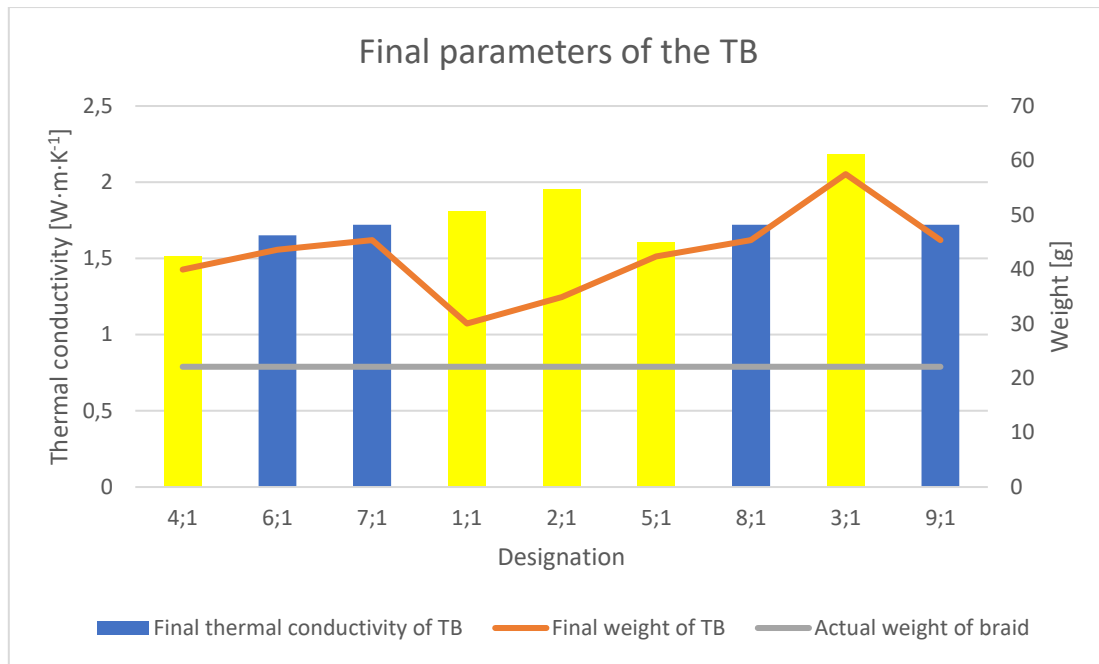
Figure 9.2 Final parameters of the TB
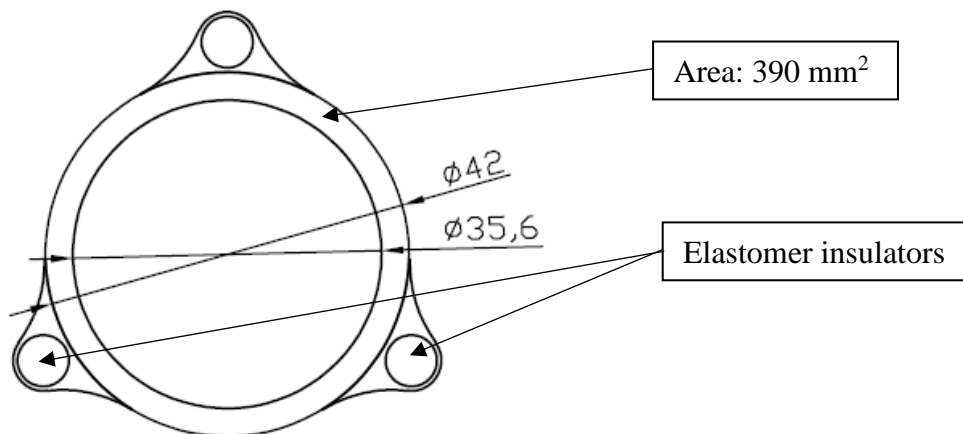
Picture 9.19 Representative usable area

9.4.3 Comparison between requirements and results

Following comparison of selected stocking braids, it seems that they meet dimensional requirements, as the area required for the TB is less than the available area.

As shown in Figure 9.2, stocking braids with the measured wire length are lighter than others, which is due to the reduced length of the wires used in the calculation on the basis of measurements. Longer wires were calculated for other braids, so they do not seem as effective. The results show the influence of wire length and the necessity to get the wires as shorter as possible.

These results also show that the most effective way to achieve the ideal value of thermal conductivity and the lowest possible weight would be to combine several types of stocking braids.

9.5 Carbon fibre structure

The main problem is that carbon fibres with greater thermal conductivity, mostly high-modulus fibres, are not manufactured in braid structures like flat braid, sleeving braid or stocking braid. The only one from a manufacturer that could be found was made from a

conventional fabric similar to that which can be seen in Picture 9.20. This fabric is made of previously mentioned K13C2U fibre [29]. Another possibility is to ask the manufacturer if it would make some sort of braided structure from high conductive carbon fibre to order, which will probably be very expensive.
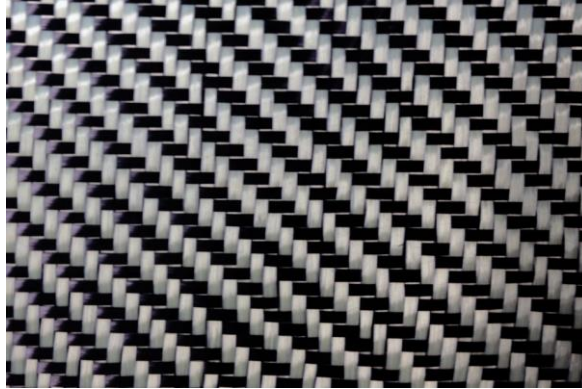
Picture 9.20 Carbon fibre fabric structure [50]

The other possibility is to buy a spool of fibre and try to connect single fibres to both parts of the MHS.

Because these fibres have high thermal conductivity and low density as was mentioned in Chapter 7, it was necessary to calculate at least the estimated parameters for these fibres.

The only possibility of manufacturing of the carbon fibre structure is probably to use previously mentioned C-solder.

9.5.1 Methodology

The methodology for this computation is based on the assumption of the minimum required thermal conductivity of the TB which is 1,5 W·K^{-1}.

The area required for the structure (S_{TB}) was initially computed using Equation (1), where the length of the wires (δ) is 0,04 m, for comparison with other previously mentioned materials.

Volume V is computed using Equation (20), where S_{TB} is the area required for the structure and δ is the length of the wires.

$$V = S_{TB} \cdot \delta \qquad (20)$$

Equation (12) is then used to calculate the weight of all the fibres.

9.5.2 Computation results

Five types of carbon fibres were used for comparison, four of them were pitch-based and one was PAN-based for comparison.

Table 9.21 Carbon fibre structure

Fibre type	Coefficient of thermal conductivity λ [W·m⁻¹·K⁻¹]	Density ρ [kg·m⁻³]	Wire length δ [mm]	Weight for 1,5 W·K⁻¹ M [g]	Total area required for TB S_{TB} [mm²]
T-1000GB PAN-based [25]	12,6	1800	40	342,86	4 762
K13D pitch-based [25]	747	2200	40	7,07	8
K13D pitch-based (CNTs - grafted) [25]	967,1	2200	40	5,46	7
K13C2U [29]	620	2200	40	8,52	10
K13D2U [29]	800	2200	40	6,60	8
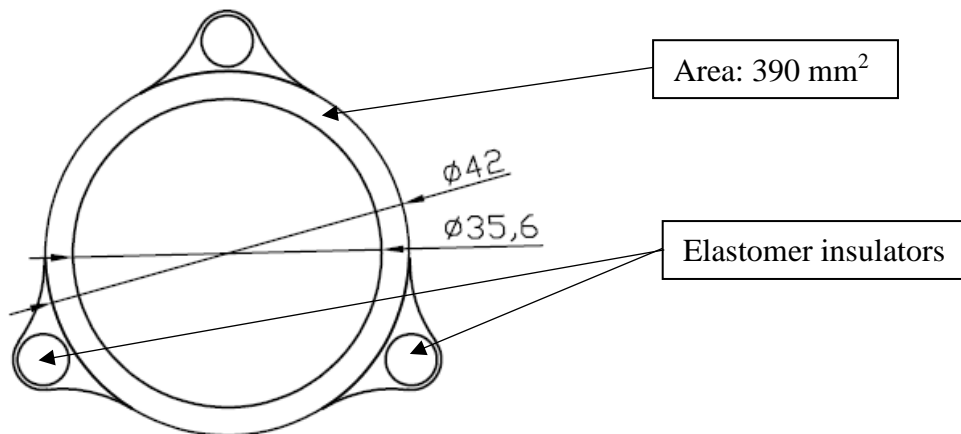
Picture 9.21 Representative usable area

9.5.3 Comparison between requirements and results

As can be seen, all the pitch-based fibres that were calculated have exceptional thermal conductivity, weight and dimensional requirement parameters.

But, as previously mentioned, the biggest problem in relation to this type of concept is in the manufacturing. The solution for connecting this design to the MHS elements has not yet been tested and the soldering method for carbon fibres is probably not yet qualified for space use.

Furthermore, the high modulus can cause complications when used in the form of FOD and is possible less durable than conventional wires. More tests would be required if use of this concept is considered.

9.6 Comparison of braided structures

Five types of braided structures were compared in this chapter, of which the best results are achieved by carbon fibres. But because carbon fibre soldering is a relatively new technology and there is probably no other way to connect this material to small MHS elements, and also because of additional problems with FOD, sleeving braids and stocking braids look like a better solution. When a thermal conductivity of at least 1,5 W·K⁻¹ was required, these structures proved to be the lightest and they could always be inserted into the required space. Furthermore, with regard to the previous concept used in the BB, the wire structure can be connected to the MHS elements. And according to the calculations, there is no need to adjust the dimensions of the MHS for application of these structures.

However, these calculations are only approximate, so tests with real, purchased braids would be necessary.

This chapter possibly also showed why the current design of the BB is unlikely to meet the requirements set out in Chapter 2.

Table 9.22 gives structures selected from the structures mentioned in previous chapters for a final comparison.

Table 9.22 The final selected wire/fibre structures

Designation	Final structure thermal conductivity [W·K⁻¹]	Weight for 1,5 W·K⁻¹ M [g]	Total area required for the TB S_{TB} [mm²]
Flat braid – Heat transfer through transversal direction			
2;1	1,5	55,42	1 189
3;1	1,5	55,52	1 192
Flat braid – Heat transfer through longitudinal direction			
3;1	1,56	56,96	312
8;3	1,52	27,86	516
Sleeving braid			
4;3	1,65	21,85	303
5;3	1,69	22,40	311
Stocking braid			
1;1	1,8	30,04	159
2;1	1,95	34,89	178
Carbon fibre structure			
K13C2U	1,5	8,52	10
K13D2U	1,5	6,60	8

Limit parameters:
- Weight of old braided structure: 22,1 g
- Required area for structure that cannot be cut: 390 mm².
- Required area for structure that can be cut: 1284 mm² or 1383 mm² for heat transfer through transversal direction.
- Thermal conductivity of structure at least 1,5 W·K⁻¹, but not much more.

As can be seen from Table 9.22, the weight of the sleeving braids ranges around the weight of the actual braid used on the BB. but the computed conductivity is significantly higher.

10 Mechanical contact structure

The mechanical contact structure is another type of structure, considered interesting for the MHS project. Heat is transferred through the connection between two solid structures, which moves towards each other. This type of structure allows movement and provides good thermal conductivity.

Each structure of this type must be manufactured on a base, which means that the calculations include not only internal structures such as the braided structure in Chapter 9, but also the contact plate and base plate.

This design could be made of aluminium or copper materials, which are both conventional materials. Some of the mechanical contact structures could be manufactured by machining and consist of just two separate parts after being manufactured.

The mechanical contact structure concepts are designed with the idea that the lower part of the structure and the base plate will be manufactured as a single component.

10.1 Nomenclature

The nomenclature used for the structures is based on what the structure looks like. This terminology is intended to define structure names and key characteristics.

The structures are divided into three different types:

- Cylindrical – The contact surfaces are located at the ends of cylinders that are connected to the base plate and contact plate.
- T-shape - The contact surfaces are T-shaped, or double T-shaped
- Helix – The contact surfaces are helix-shaped

Nomenclature as seen in Picture 10.1 is used in relation to the T-shape structure:

- Ribs: The vertical parts of structure, which connect the contact surfaces to the plates.
- Contact surfaces: The point where mechanical contact is realized
- Contact cores: The collective name for the individual contact surfaces and the ends of the T structure
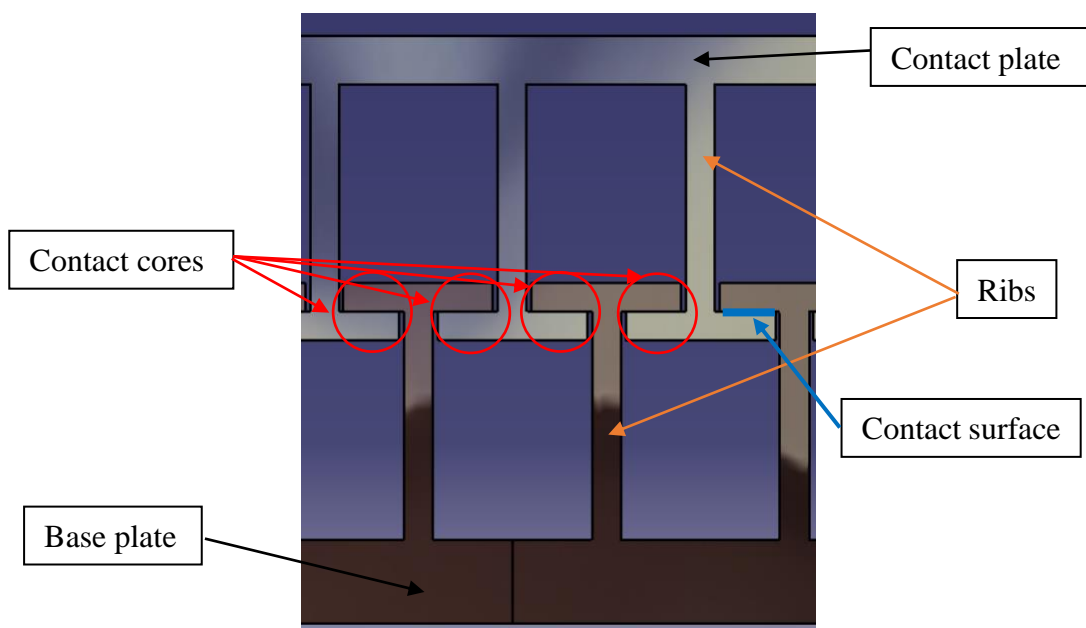
Picture 10.1 T-shape structure nomenclature

Each T-shape structure model is defined by 3 traits defining the basic properties of the design concept, material and geometry:

<div align="center" style="color:red">

(X-Y-Z)

</div>

<div align="center">

X – material (Cu or Al)
Y – general concept geometry
Z – characteristic geometry

</div>

- **Cylindrical** **(e.g.: Al-Ce*3-4.5/1.6 or Cu/Al-Ci2-5.2/1.3)**
    - **X** = 1/2 material used (1 – lower part; 2 – upper part; when equal, only 1 is used)
    - **Y** = C*n (* is a sub-modification defining a moving part: i – internal; e – external; e* - external + inner flat section located directly on the baseplate; n – number of contact surface layers)
    - **Z** = w/t (w – width of contact surface in mm; t – thickness of horizontal plate in mm)

- **T-shape** **(e.g.: Cu-T7-1.2 or Al/Cu-T9/8-1.4/1.2)**
    - **X** = 1/2 material used (1 – lower part; 2 – upper part; when equal, only 1 is used)
    - **Y** = *T** (* is the number of surface contact levels (if 1 then no number); ** is the number of T structures lower/upper; when equal, only 1 number is used)
    - **Z** = v/h (thickness of vertical/horizontal walls in mm – average, mean or the most frequently used value)

- **Helix** **(e.g.: Al-Hi-5/7 or Cu/Al-He*-5/6.3)**
    - **X** = 1/2 material used (1 – lower part; 2 – upper part; when equal, only 1 is used)
    - **Y** = H* (* is a sub-modification defining a moving part: i – internal; e – external; e* - external + helix located directly on the baseplate)
    - **Z** = p/w (p – pitch in mm; w – surface contact width in mm)

The materials used for the structures are Cu OFHC and Aluminium alloy (7075-T73).

10.2 Methodology

The methodology for calculation is identical for all concepts and is therefore described in this subchapter only. The basis is the equation (1) mentioned in Chapter 3. Because these structures are made from a solid piece of material, this affects the equation and parameters.

10.2.1 Input parameters

The input parameters are necessary and were determined in the previous development process.

The input parameters are the mechanical properties of the materials and the pressure that is necessary to maintain the thermal conductivity of the contact. The required pressure in contact was determined in the previous development process as a value of 0,4 MPa. This pressure was determined in relation to contact between the cold plate and the contact plate, but as the contact plate is connected to the inner structure, this pressure must be maintained in contact between all these parts.

The materials used for the calculations are aluminium and copper, but pure aluminium does not have mechanical properties that could withstand these pressures. So an aluminium alloy, specifically Aluminium 7075-T73, had to be used instead of pure aluminium and the copper OFHC. Parameters of these materials are mentioned in Table 10.1.

The parameters of contact surfaces which were determined in computations are mentioned in Table 10.2.

The thermal conductivity of the contact surfaces depending on the materials in contact is given in the Table 10.3.

Table 10.1 Materials for Mechanical contact structure

Material	Density [kg·m⁻³]	Thermal conductivity [W·m⁻¹·K⁻¹]	Ultimate tensile strength [MPa]	Proof stress (0,2%) [MPa]	Microhardness Hc [MPa]
Copper OFHC	8900 [20]	394 [20]	220 – 450 [20]	45 – 320 [20]	882 [3]
Aluminium (7075-T73)	2810 [3]	155 [3]	505 [22]	435 [3]	705 [3]

Table 10.2 Contact surface parameters

Roughness Ra [μm]	Contact pressure p [MPa]
0,8 [3]	0,4

Table 10.3 Contact surface result

Materials in contact	Contact thermal conductivity [W·m⁻²·K⁻¹]
Copper OFHC Copper OFHC	6 374
Copper OFHC Aluminium (7075-T73)	4 756
Aluminium (7075-T73) Aluminium (7075-T73)	3 328

10.2.2 Calculations

The heat conductive structure is divided into several straight sections of a given length and cross-sectional area. The thermal resistance is then calculated separately for these sections using equation (1). Equations (2) and (3) are then used to total up the individual resistance values and the resistance of the entire structure is calculated. The model mentioned in Chapter 3 is used to calculate the heat transfer through thermal contact. As mentioned in that chapter, the thermal conductivity of thermal contact is divided by six, because it better matches previously measured data.

The next important information is the weight of the structure. Weight is computed similarly to thermal conductivity. The heat conductive structure is divided into several geometrical sections in mostly the same way as in the case of thermal conductivity. The volume and weight of these sections is then computed using basic relationships.

The weight is only calculated for parameters like CTB, which means only for the inner thermal conductive structure, contact plate and parts, which are necessary for the function of the structure for example Picture 10.2. The base plate is eliminated from the weight calculations.
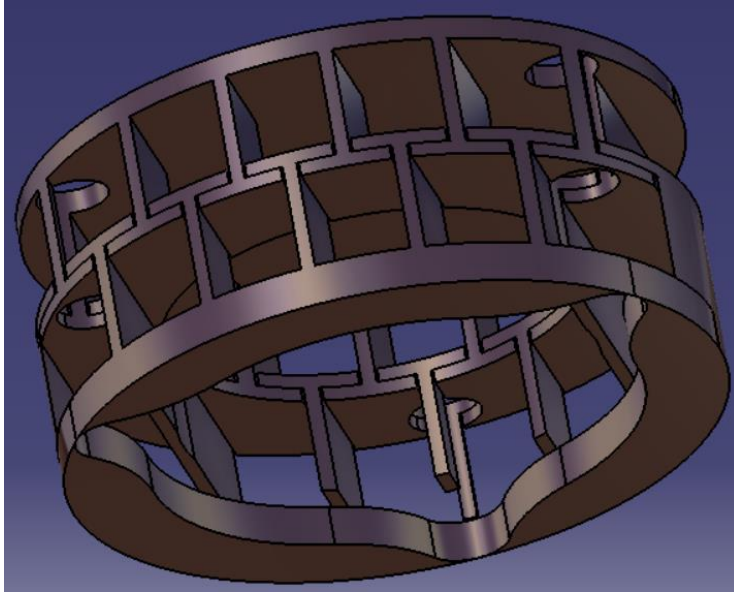
Picture 10.2 Example of structure for weight calculation

In some cases (specifically T-shape structures), the heat conductive path is divided into two different routes according to Picture 10.3, where the heat conductive path through the structure is indicated by arrows.
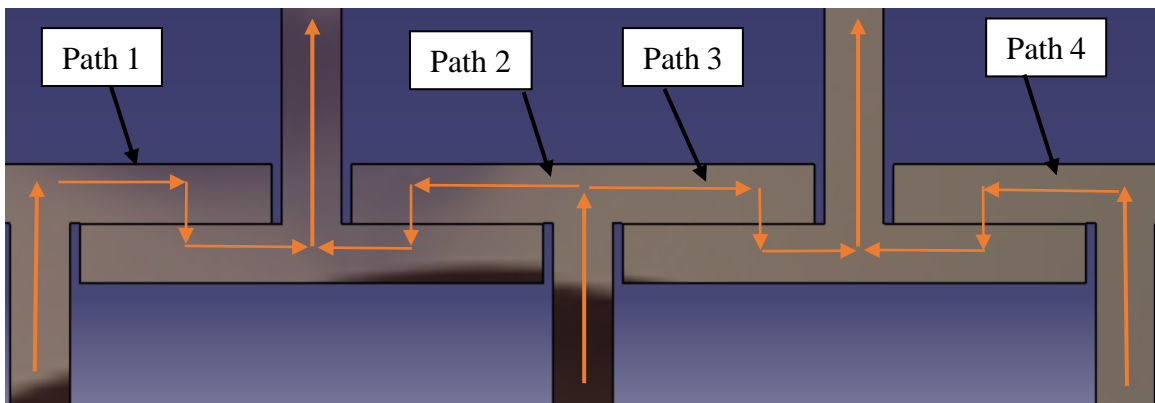
Picture 10.3 Division of the heat conductive path

In the case of this heat conductive structure it was necessary to determine how the heat would behave when divided into two routes. Because the computation is simply analytical using MS Excel, this problem should be solved. In the end, it was decided that the thermal conductivity of the ribs would be divided into two different paths, in proportion to the conductivities of the individual contact cores. The individual paths will then be totalled in parallel.

Calculators were designed for the calculations in MS Excel, where it was possible to change specific parameters and the program itself calculated specific results.

Specific thermal conductivity C_{SP} is used for effective comparison of mechanical contact structures between themselves. It is computed using equation 21.

$$C_{SP} = \frac{C}{M} \cdot 100 \tag{21}$$

In the case of T-shape structures and L-shape structures, the area of contact and cross-sectional characteristics for computation are measured on models created using CATIA software. The parameters were measured and then a database of characteristics based on each model was created. These characteristics were used to create a calculator in MS Excel,

which uses the measured parameters for thermal and weight computations. If the required value is not measured and falls between measured values, linear interpolation is used.

10.3 Structure evolution

The first step in design evolution was computation of the area required for thermal contact. The contact between two surfaces is the key part of this design because it was found on the basis of calculation that for a thermal conductivity of $1{,}5\ \text{W}\cdot\text{K}^{-1}$ through thermal contact itself, an area of roughly $230\ \text{mm}^2$ and a pressure of $0{,}4$ MPa is required in the case of Cu OFHC material.

The mechanical contact structure design was developed in five basic versions. Version 1 was based on L-shape pads enclosing the perimeter as can be seen in Picture 10.4. This version was rejected because it would be difficult to manufacture and would also be impossible to disassemble, which is a key parameter.
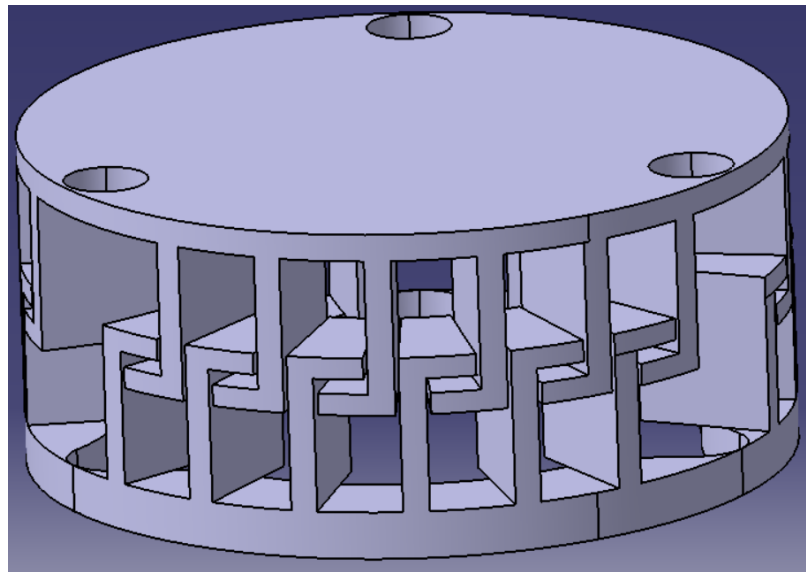
Picture 10.4 L-shape structure surrounding the perimeter (Version 1)

The second step in structure evolution was version 2, which was later redesigned to be detachable. This version was called version 3 and later renamed the cylindrical structure. This version is described in more detail in Chapter 10.4.
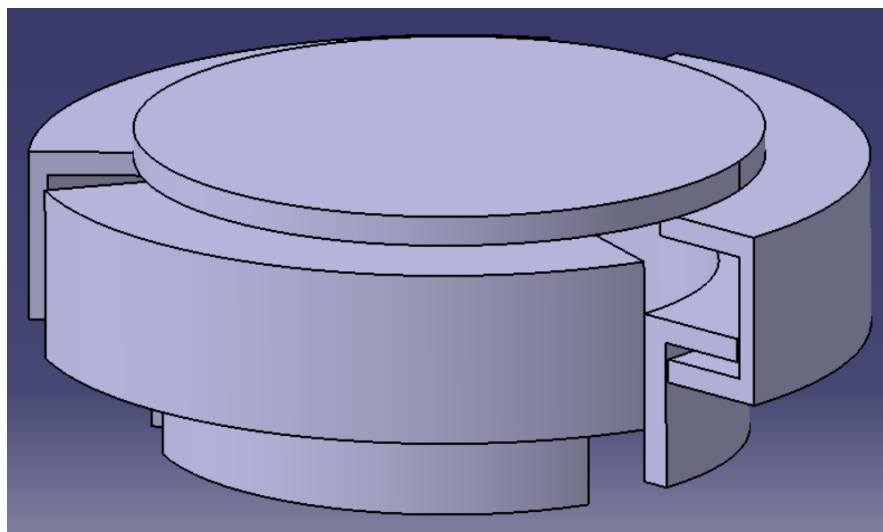
Picture 10.5 Mechanical contact structure Version 2

The third step in mechanical contact structure design was version 4, which consists of L-shape structures as can be seen in Picture 10.6. This version could be manufactured easily by milling and could be easily disassembled. This version was rejected because there were doubts regarding the strength of the structure. Version 4 was redesigned in a T-shape structure, which is mentioned in Chapter 10.5.
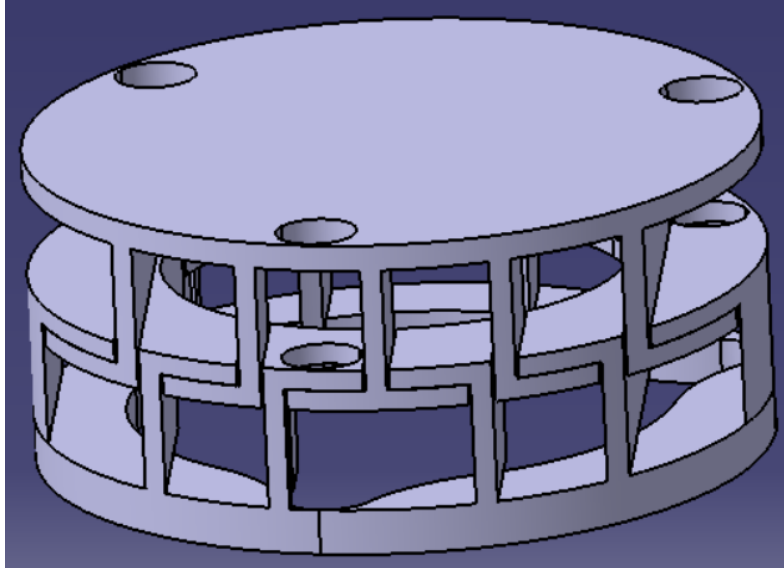
Picture 10.6 Mechanical contact structure Version 4

The last mechanical contact structure design version was version 5, which consists of helix contact areas. This version is described in more detail in Chapter 10.6. This version provides a large contact area, but precise analytical calculations are not possible, so an FEA is necessary.

10.4 Cylindrical structure

The cylindrical contact structure consists of two separate parts where the contact surfaces are in the annulus as can be seen in Picture 10.7. The contact surfaces are on two different planes.

This structure could be manufactured by turning 1 cylindrical semi-finished product.
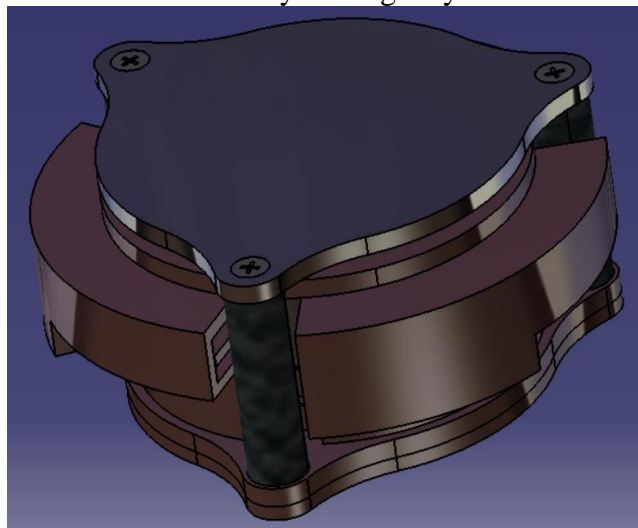
Picture 10.7 MHS with Cylindrical structure in OFF position (isometric view)

10.4.1 Basic geometry definition

The geometry is defined in Picture 10.9. As can be seen in Picture 10.8, the cylindrical contact structure consists of 2 separate parts (lower and upper). Each part has contact surfaces on two planes. The geometrical parameters are the same for both contact planes, but there is a difference in the dimensions. The contact planes basically differ from each other by level distance.
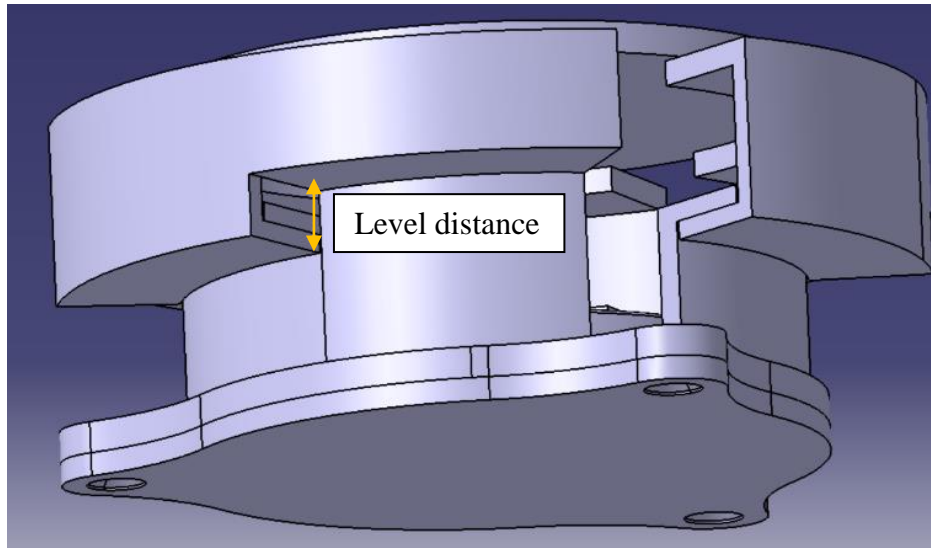
Picture 10.8 Cylindrical contact structure with base plate
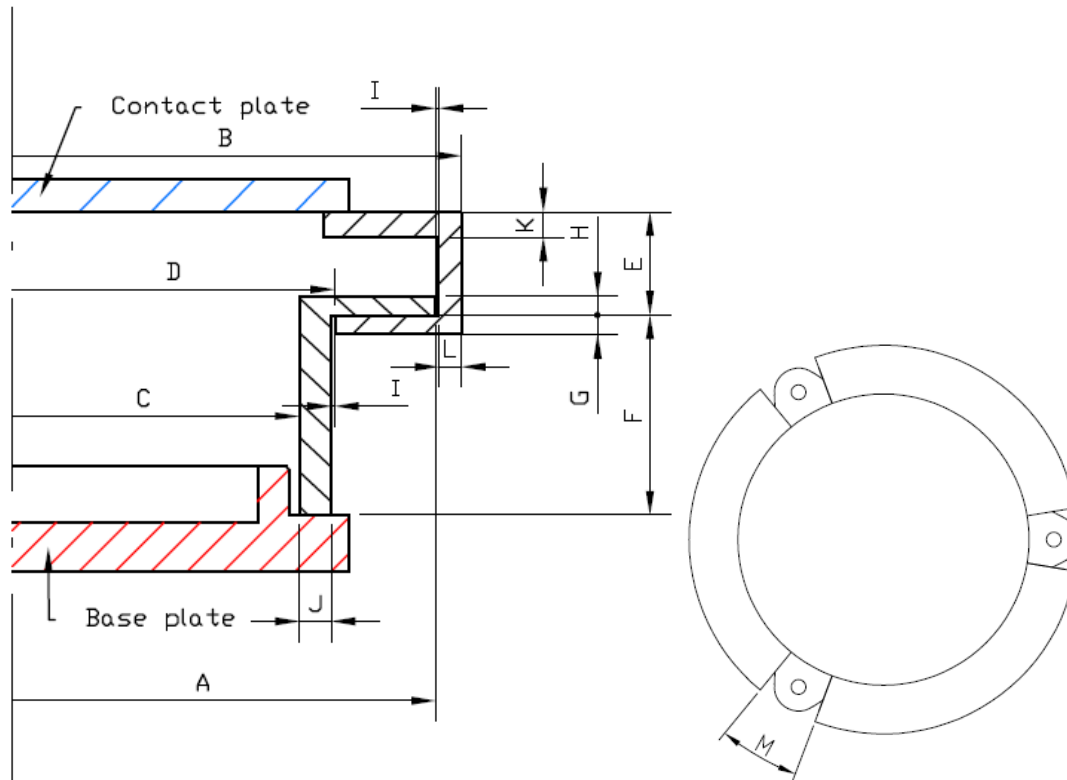
Picture 10.9 Cylindrical contact geometry definition, cross-section through one contact surface plane (left), top view (right)

The geometrical parameters are identified by letter in Picture 10.9:
- A – The outer diameter of the lower part
- B – The outer diameter of the upper part
- C – The inner diameter of the lower part
- D – The inner diameter of the upper part
- E – The distance to the contact surface of the upper part
- F – The distance to the contact surface of the lower part
- G – The flat section thickness of the upper part
- H – The flat section thickness of the lower part
- I – Clearance between the lower and upper parts
- J – Circular section thickness of the lower part
- K – Upper flat section thickness of the upper part
- L – Circular section thickness of the upper part
- M – Dead angle (angle where the elastomer insulator is located). This angle is the same for all structures - 19 °

10.4.2 Thermal model

The thermal model of this structure uses equation (1) for computation of the resistivity of each separate part of the structure, which is numbered in Picture 10.10. The resistivity of the thermal contact surfaces is calculated using the model described in Chapter 3. Picture 10.10 gives also the resistivity diagram for this type of structure for one contact plane. The other contact plane is calculated identically.
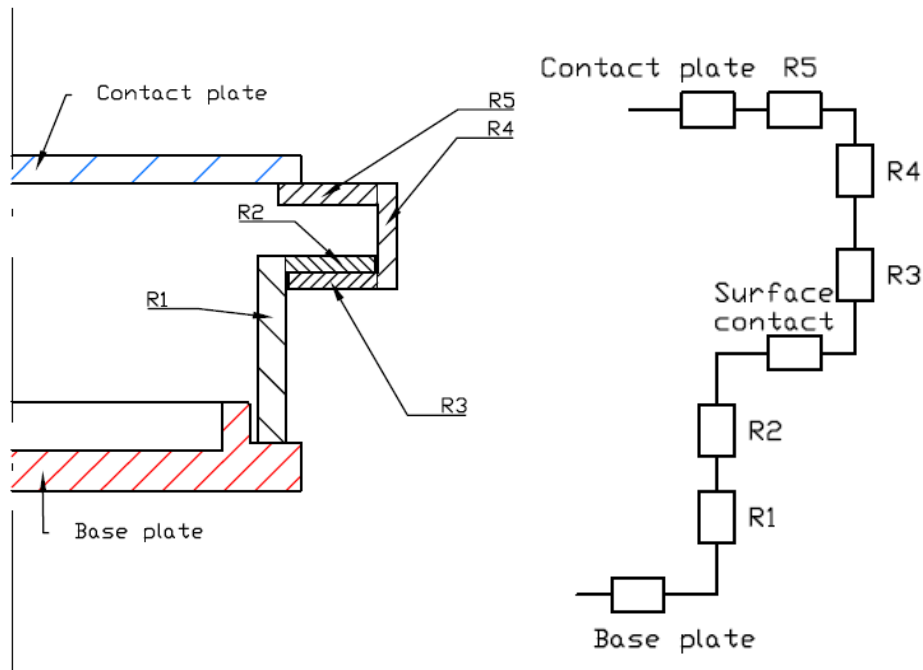
Picture 10.10 Cylindrical contact (left) thermal diagram (right)

The final computations of resistivity use equations (2) and (3).

The resistivity of parts R2 and R3 is only calculated for the dimension of clearance.

10.4.3 Results

The same geometry, which seemed the most effective, was chosen for the test results and the parameters of different materials used on the upper and lower parts of structure were compared.

- The first structure geometry made maximum use of the design space specified in Chapter 5.
- The second structure was designed to achieve the maximum thermal conductivity of the aluminium alloy structure.
- The third structure was designed to achieve the maximum thermal conductivity of the structure with aluminium alloy used on the upper part.
- All structures were designed to meet BB contact plate and base plate parameters.

The letters in the Table 10.4 refer to Picture 10.9. The only difference is between values E and F, which are dependent on the Level distance value. Number 1 refers to plane one and number 2 refers to plane two.

Table 10.4 Structure parameters

Parameter	Structure1	Structure2	Structure3
A	⌀ 40,2 mm	⌀ 42,2 mm	⌀ 41,2 mm
B	⌀ 56 mm		
C	⌀ 35,8 mm		
D	⌀ 52,8 mm	⌀ 49,6 mm	⌀ 51,6 mm
E1	9,45 mm		
F1	9,45 mm		
E2	5,45 mm		
F2	13,45 mm		
G	1,2 mm		
H	1,2 mm		
I	0,2 mm		
J	2 mm	3 mm	2,5 mm
K	1,6 mm	4 mm	5 mm
L	1,4 mm	3 mm	2 mm
Level distance	4 mm		
Contact plate thickness	2 mm		
Base plate thickness	3,5 mm		

Table 10.5 Structures results

Structure	Designation according to nomenclature	Thermal conductivity C [W·K^{-1}]	Total weight M [g]	Specific thermal conductivity C_{SP} [W·K^{-1}·g^{-1}]
1	Cu-Ce2-6,3/1,2	1,78	93	1,93
	Al/Cu-Ce2-6,3/1,2	1,11	71	1,56
	Cu/Al-Ce2-6,3/1,2	1,07	51	2,12
	Al-Ce2-6,3/1,2	0,76	29,19	2,61
2	Al-Ce2-3,7/1,2	0,86	42,22	2,04
3	Cu/Al-Ce2-5,2/1,2	1,36	68,30	1,99

Limit parameters:
- Weight of the CTB structure used on BB: 55,1 g
- Minimum thermal conductivity of the structure of 1,5 W·K^{-1}.
- Maximum diameter of 56 mm.

According to the results given in Table 10.5, it seems that this type of structure is not suitable for the MHS design.

There is initially a problem with lower thermal conductivity, which may be caused by the upper part of the structure being too long.

There is also a problem with the high weight of the structure. Aluminium alloy could be used to solve this problem, but this alloy has lower thermal conductivity and the structure does not then meet thermal conductivity requirements.

The best combination of results can probably be achieved using aluminium alloy on the upper part and Cu OFHC on the lower part of the structure.

Some of the structures seem to be able to be used to further increase weight and therefore the profile of the heat conductive paths, but the problem is that these structures

make the most of the available design space. This means they cannot be used, even after some parameters are increased.

10.5 T-shape structure

The T-shape concept uses individual ribs with contact surfaces at the end. The ribs are located in the middle of the contact surface, so that every rib is symmetrically loaded. Two types of this version were designed, one for copper material, which is heavier and has a high thermal conductivity, and the other for aluminium alloy, which is lighter and has a lower thermal conductivity. Contact is only realised on one plane in the copper alloy type, but in the aluminium alloy type, contact is realised on two planes.

The T-shape structure is designed to use the maximum available space specified in Chapter 5. This T-shape structure on the actual MHS design can be seen in Picture 10.11.

This structure could be manufactured by machining from a cylindrical semi-finished product.
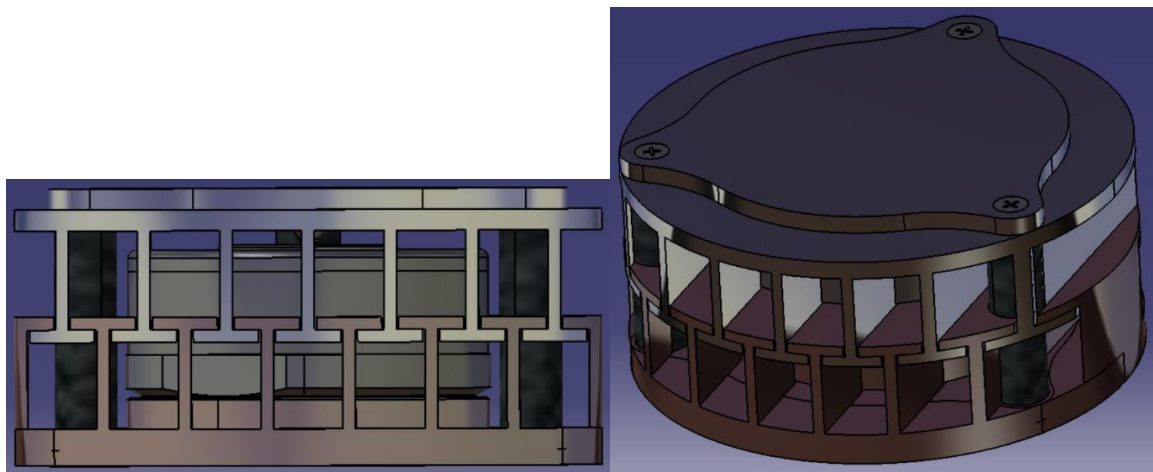
Picture 10.11 T-shape structure on non-modified MHS in ON position front view (left), Isometric view (right)

10.5.1 Modifications

The basic modifications of the T-shape structures are classified according to the material they are intended to be made of. Based on previous calculations, it was found that the basic T-shape structure does not have a sufficient contact area if aluminium alloy is used. A modification was therefore created, which uses a double T. This modification can be seen in picture 10.12. The double T structure provides additional contact surfaces.
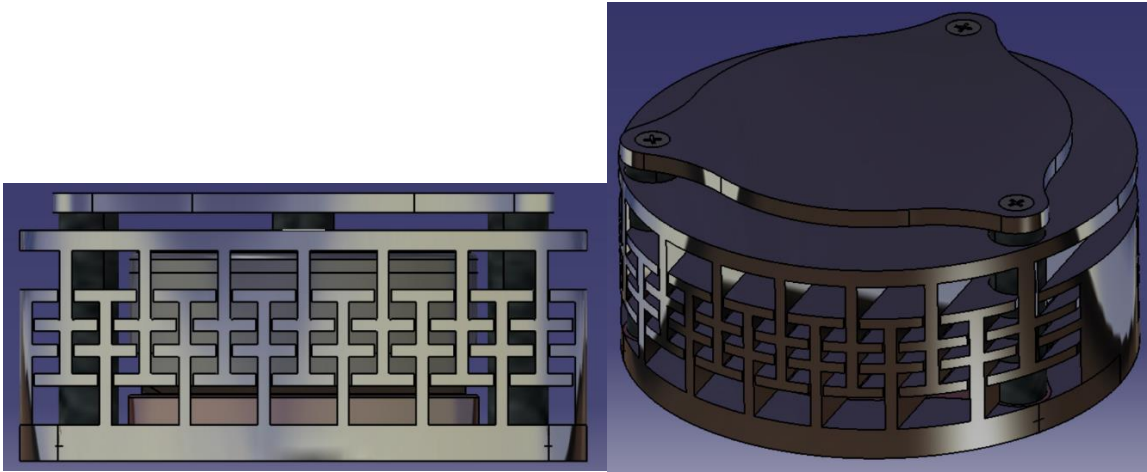
Picture 10.12 Double T-shape structure on non-modified MHS in OFF position front view (left), Isometric view (right)

The second modification of the T-shape structure is the L-shape structure, which can be seen in Picture 10.13. The L-shape structure was initially designed for analytical computations only, to verify if this type of concept has any benefit. The T-shape structure was considered a better solution, because the pressure is evenly distributed, on the contrary to the L-shape structure. There is also potential for better heat redistribution in the structure.
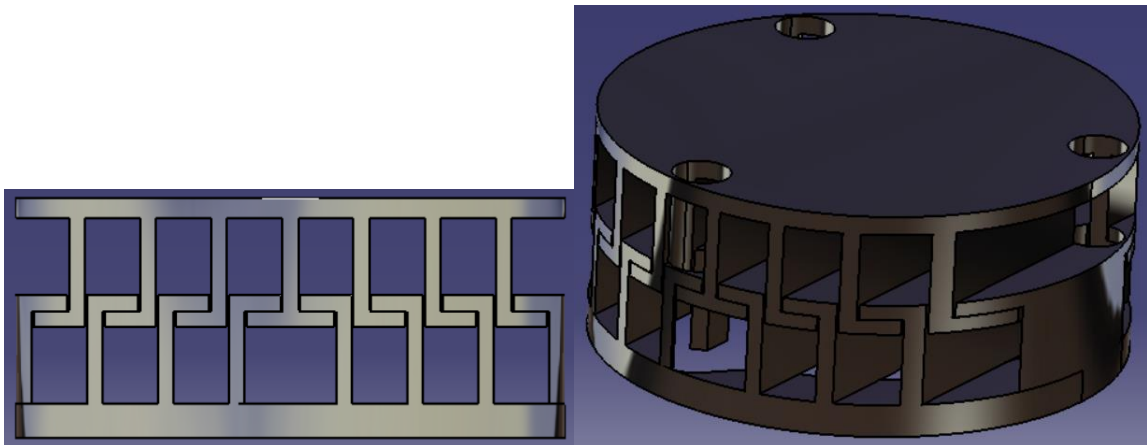
Picture 10.13 L-shape structure in ON position front view (left), Isometric view (right)

10.5.2 Basic geometry definition

The basic geometries are different for the sub-version of the T-shape contact structure. The geometry in Picture 10.14 is used for the T-shape structure. The L-shape structure is similar.
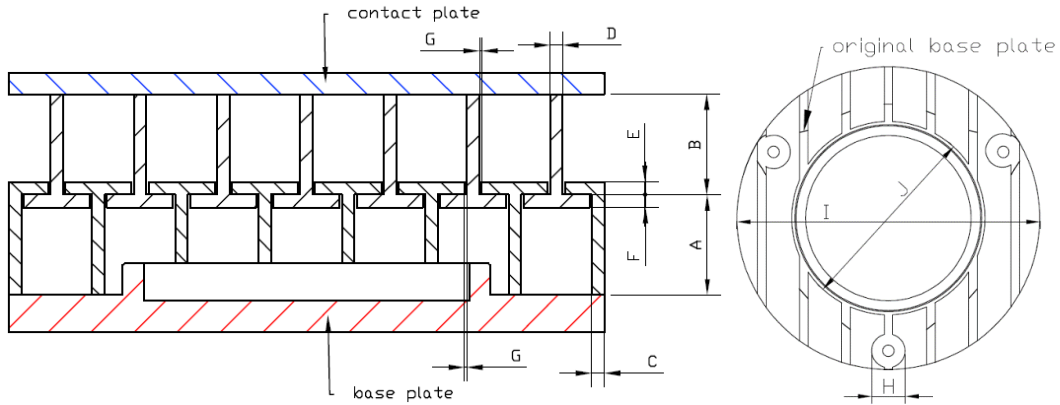
Picture 10.14 T-shape contact geometry definition side view (left), top view on lower part (right)

Picture 10.14 identifies the geometrical parameters by letter:
- A – Distance to the contact surface of the lower part
- B – Distance to the contact surface of the upper part
- C – Lower part rib thickness
- D – Upper part rib thickness
- E – Upper part flat section thickness
- F – Lower part flat section thickness
- G – Clearance between ribs
- H – Space for elastomer insulators
- I – Maximum outer diameter of the MHS (extended base plate)
- J – Minimum inner diameter (Space for actuator)

The basic geometry of the double T-shape structure is given in Picture 10.15.
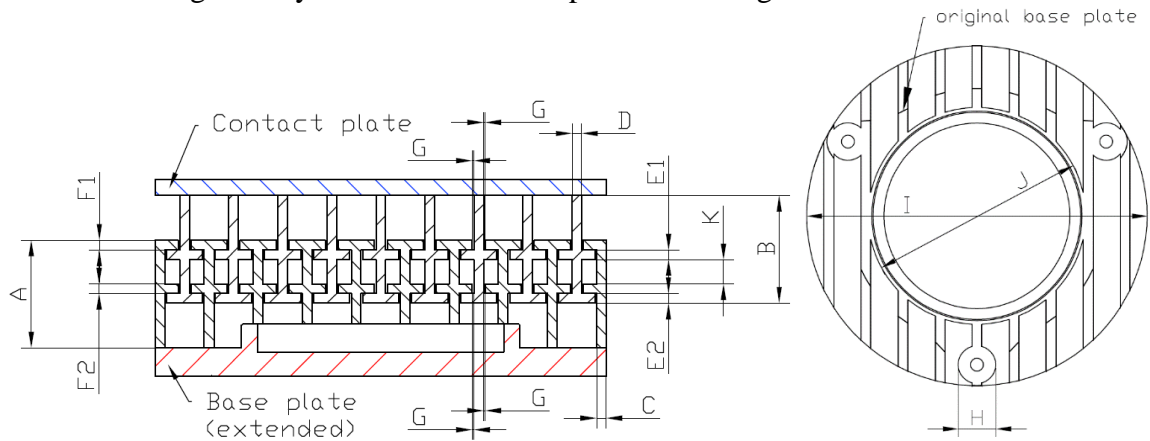
Picture 10.15 Double T-shape contact geometry definition side view (left), top view on lower part (right)

Picture 10.15 identifies the geometrical parameters by letter:
- A – Maximum distance to the contact surface of the lower part
- B – Maximum distance to the contact surface of the upper part
- C – Lower part rib thickness
- D – Upper part rib thickness
- E1, E2 – Upper part flat section thickness (Plane 1 and 2)
- F1, F2 – Lower part flat section thickness (Plane 1 and 2)
- G – Clearance between ribs
- H – Space for elastomer insulators
- I – Maximum outer diameter of the MHS (extended base plate)
- J – Minimum inner diameter (Space for actuator)
- K – Level distance (distance between contact planes)

10.5.3 Thermal models

The thermal model for the T-shape structure uses equation (1) for computation of resistivity of each separate part of the structure, as these are numbered in Picture 10.16. The resistivity of the thermal contact surfaces is calculated using the model described in Chapter 3.

The thermal diagrams, which can be seen in Pictures 10.16 and 10.17, give the contact cores. This value is the sum of the thermal resistances of the individual horizontal surfaces and contact surfaces. The thermal conductivities of the vertical parts (i.e. the ribs) are divided proportionately according to the values of these contact cores.
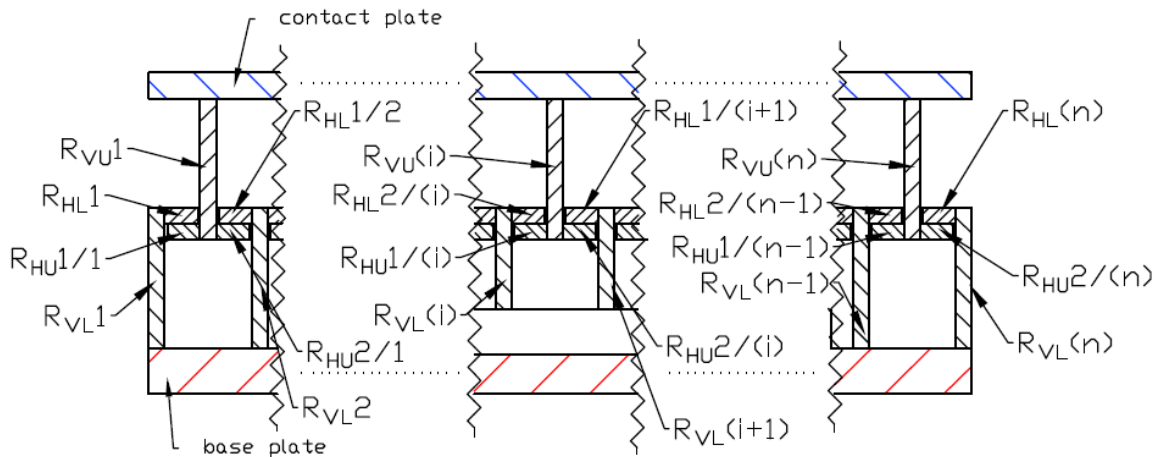
Picture 10.16 T-shape structure thermal resistivity diagram
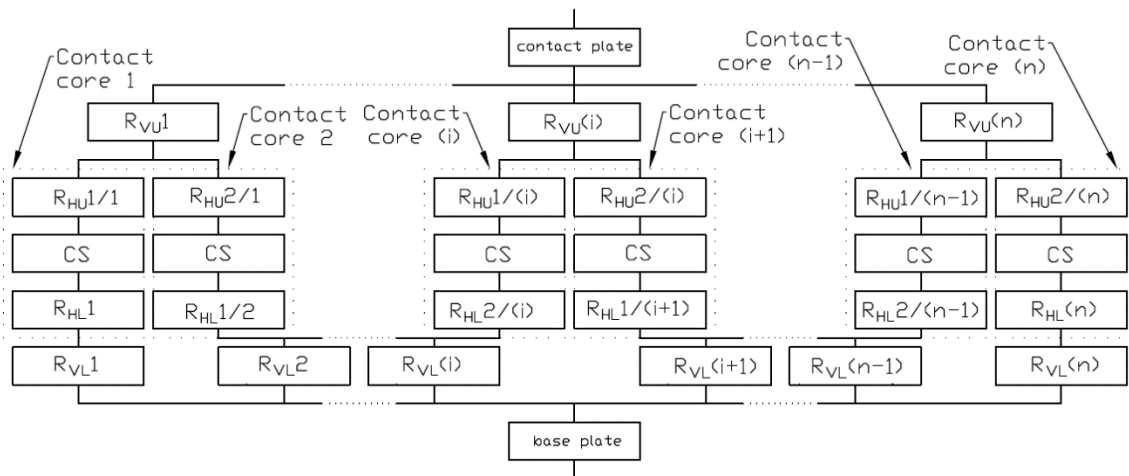
Picture 10.17 T-shape structure thermal resistivity diagram

Explanation of terms in the thermal diagram:
- R – resistivity
- V or H – Vertical/Horizontal element of the structure
- U or L – Upper part/Lower part
- 1/1 or 2/1 – Number of the horizontal element / number of rib
- For example: $R_{HL}1/2$ is the resistivity of horizontal element 1, which belongs to rib 2, which belongs to the lower part of the structure.
- CS – Contact surface

The thermal model of the double T-shape structure uses the same computation method as the basic T-shape structure.
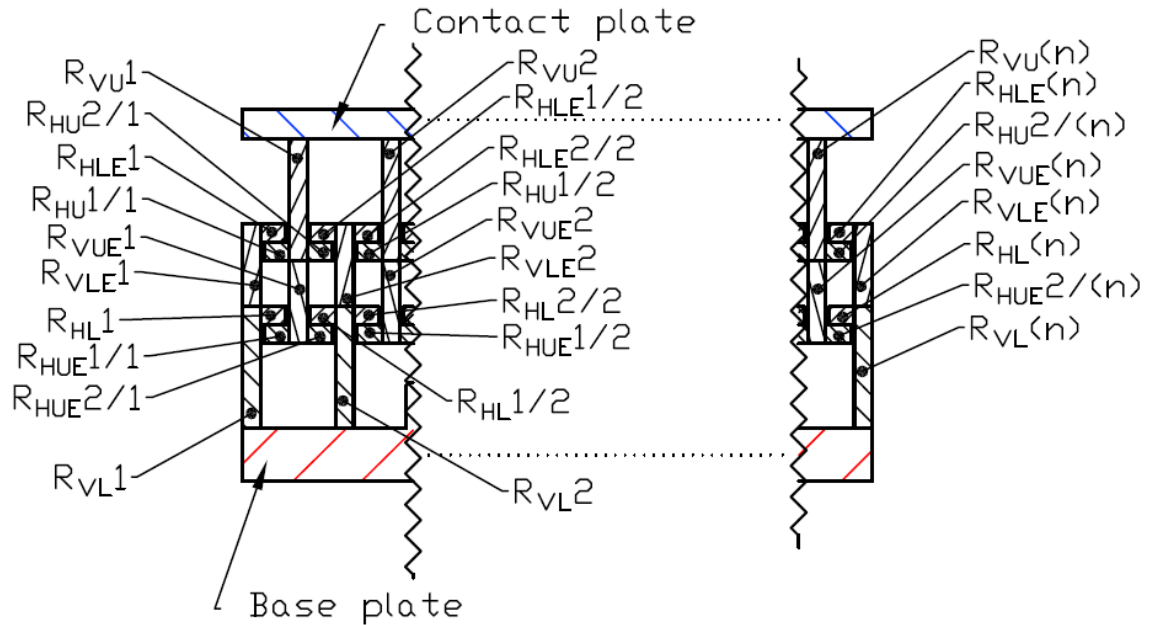
Picture 10.18 Double T-shape structure thermal resistivity diagram
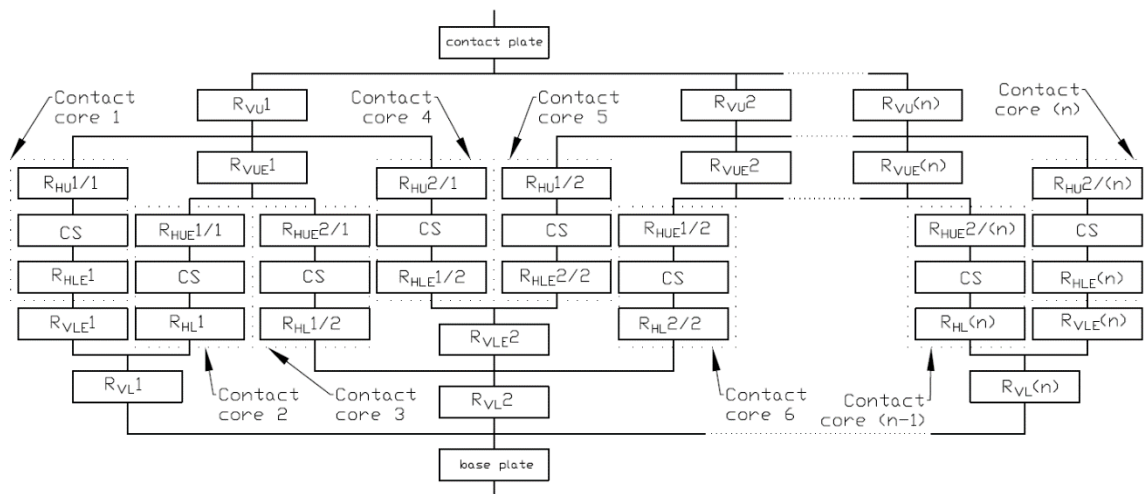
Picture 10.19 Double T-shape structure thermal resistivity diagram

Explanation of terms in the thermal diagram:
- R – resistivity
- V or H – Vertical/Horizontal element of the structure
- U or L – Upper part/Lower part
- E – Extended piece of rib
- 1/1 or 2/1 – Number of horizontal element / number of rib
- For example: $R_{HLE}1/2$ is the resistivity of horizontal element 1, which belongs to the extended piece of rib 2, which belongs to the lower part of the structure.
- CS – Contact surface

10.5.4 Sensitivity analysis

The sensitivity analysis consists of establishing, which parameters change when the properties of the structure change significantly.

The main parameters of the T-shape structures are the number of ribs and rib thicknesses. The other sensitive parameter could be for example the distance to the contact surface and the level distance. The same parameters were tested for both types of structure (T-shape and Double T-shape). The parameters that were tested are:

- Number of ribs
- Ribs thickness in combination with flat section (vertical section) thickness

Individual models were designed for every combination of rib thickness and their numbers, which were subsequently measured and the parameters then calculated.

The dependence of these parameters on the thermal conductivity and weight of the final structure is given in Figures 10.1 and 10.2. The designations of each structure type are similar in nomenclature, but the number of ribs is determined on the x-axis and each structure is represented only by the number of ribs in the lower part.
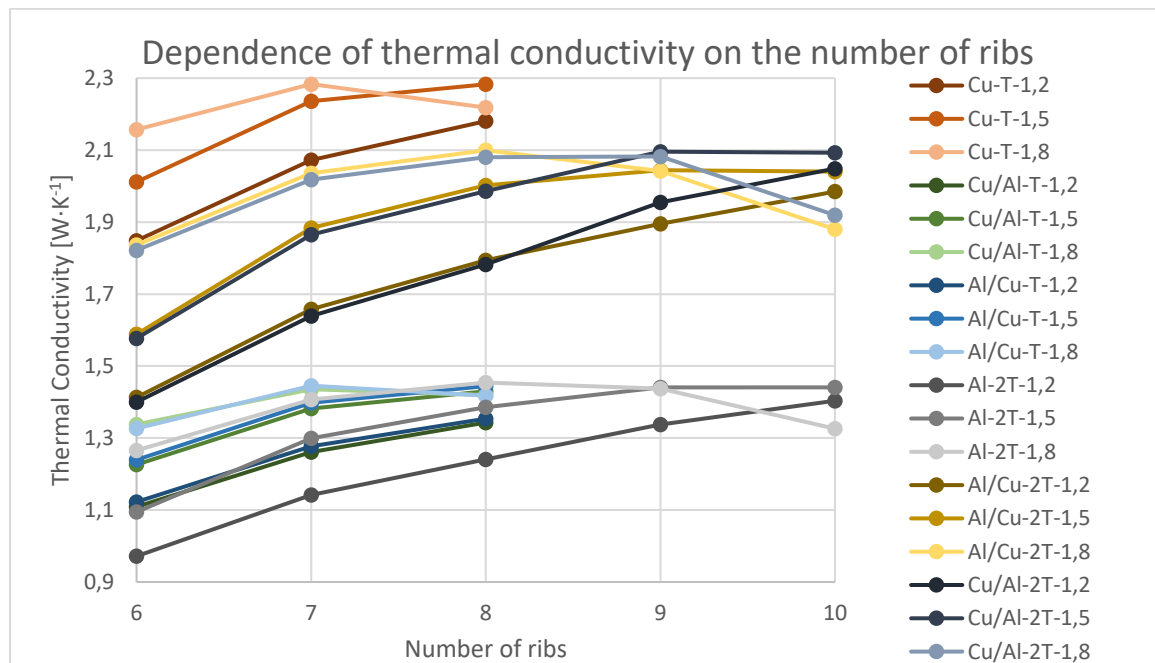
Figure 10.1 Dependence of thermal conductivity on the number of ribs and thicknesses
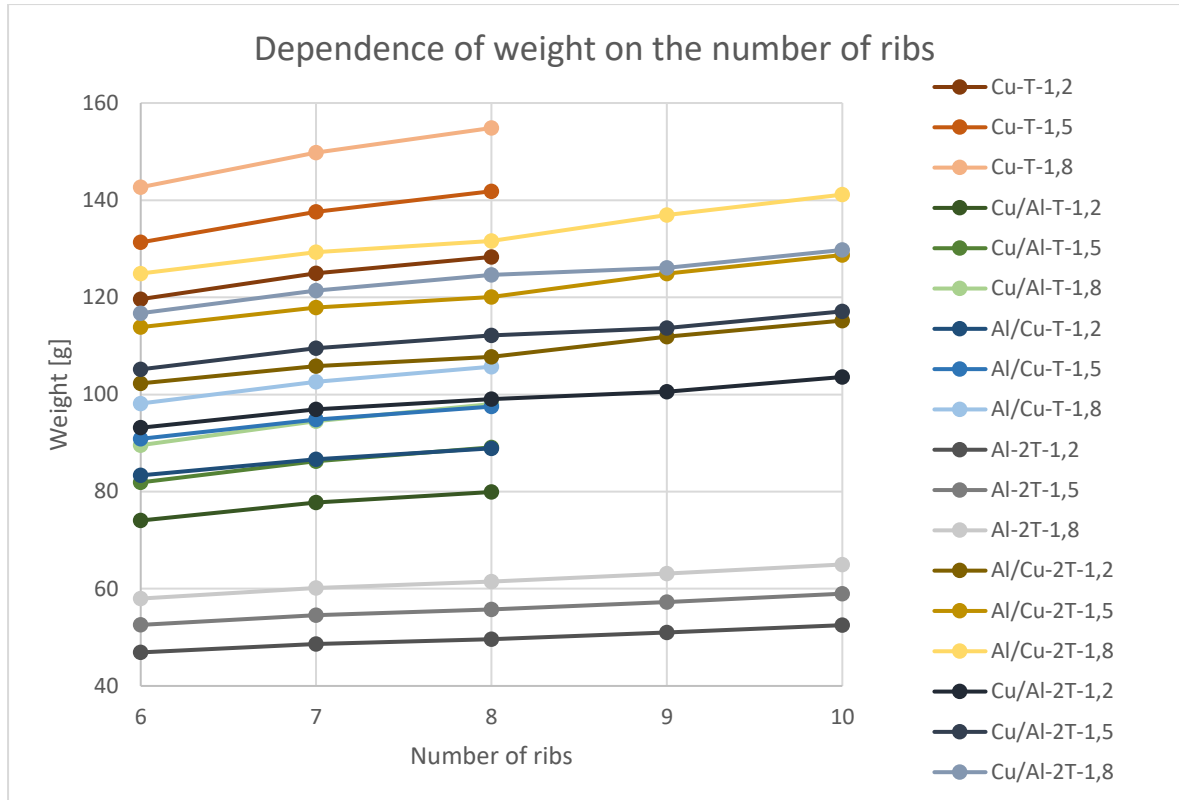
Figure 10.2 Dependence of weight on the number of ribs and thicknesses

10.5.5 Results

The results are based on the sensitivity analysis. The second part of the sensitivity analysis is Figure 10.3, giving specific thermal conductivity. The final decision regarding which structure will be selected as the most advantageous, is based on this figure.
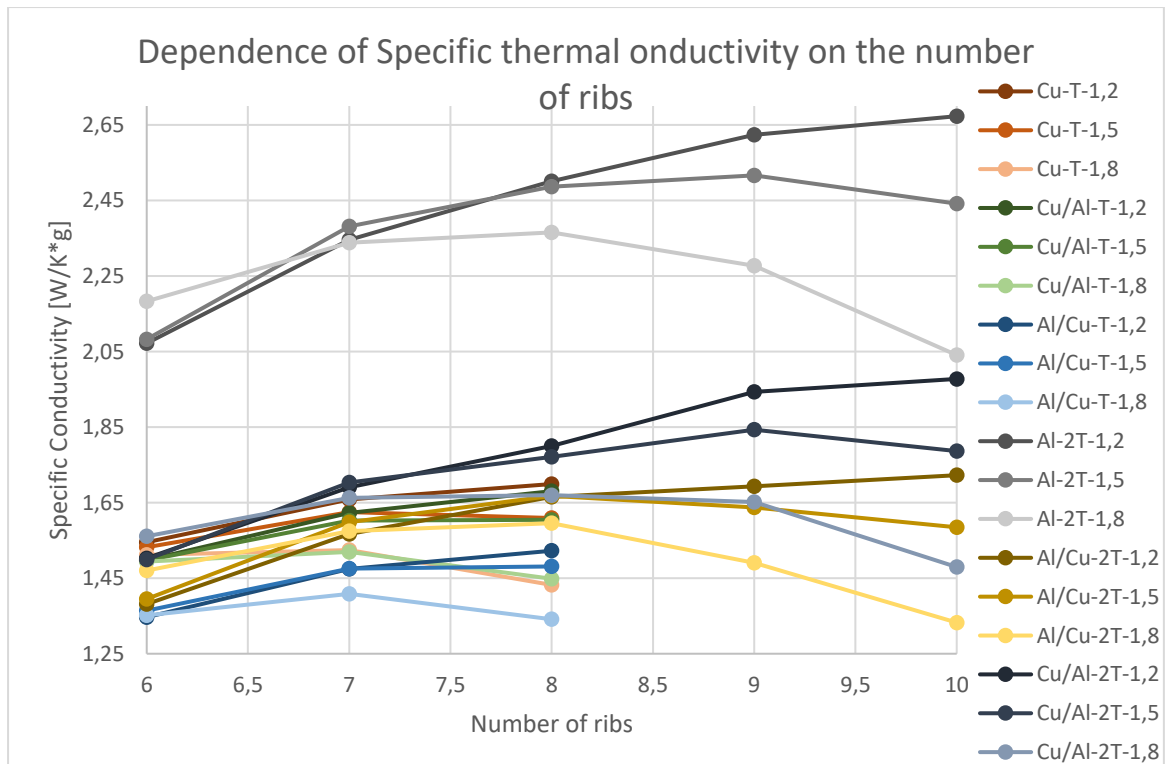
Figure 10.3 Dependence of specific thermal conductivity on the number of ribs

This figure indicates that the highest specific thermal conductivity is achieved using a double T-shape structure manufactured from an aluminium alloy. But when compared to the figure showing thermal conductivity, it is evident that these structures have a thermal conductivity lower than the minimum required value, which is 1.5 W·K⁻¹.

Table 10.6 Structure dimensions

Parameter	Al-2T8/7-1,8	Cu/Al-2T10/9-1,2	Cu/Al-T8/7-1,2
A	12,75 mm	12,15	9,45
B	12,75 mm	12,15	9,45
C			
D			
E1			
E2	1,8 mm	1,2 mm	1,2 mm
F1			
F2			
G	0,2 mm		
H	⌀ 6,2 mm		
I	⌀ 56 mm		
J	⌀ 35,8 mm		
K	3 mm		

Table 10.7 Results of selected structures

Designation	Thermal conductivity C [W·K⁻¹]	Weight M [g]	Specific thermal conductivity C_{SP} [W·K⁻¹·g⁻¹]
Al-2T8/7-1,8	1,45	62	2,37
Cu/Al-2T10/9-1,2	2,05	104	2
Cu/Al-T8/7-1,2	1,34	80	1,68
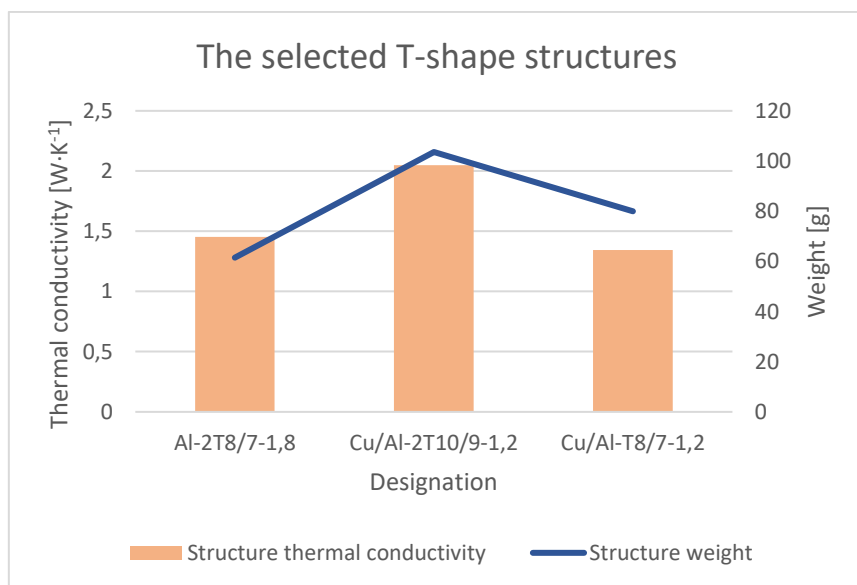
Figure 10.4 The selected T-shape structures

Limit parameters:
- Weight of the CTB structure used on BB: 55,1 g
- Thermal conductivity of structure at least 1,5 W·K^{-1}, but not much more.
- Maximum diameter of 56 mm.

As can be seen in Table 10.7, the thermal conductivity of these structures is slightly below the minimum, but the weight is significantly higher. It seems that these structures are not suitable for the MHS.

Due to the high thermal conductivity of structure Cu/Al-2T10/9-1,2 the dimensions of this structure can be reduced, especially the maximum diameter. It may be possible to slightly reduce the weight after this minor change to structure dimensions.

The best results are achieved by structure Al-2T8/7-1,8, which is the lightest of all the selected structures and also has high thermal conductivity. It falls below the set minimum, but the difference is insignificant, so it may be useful.

The other problem with these thermal structures may be the manufacturing of different levels of contact surfaces.

The other advantage, except thermal conductivity, of the structure is that it can be easily assembled and disassembled.

10.6 Helix structure

The helix structure is the last type of mechanical contact structure to be designed. This type of structure is based on the contact of helix contact surfaces between two cylindrical parts.

Picture 10.20 shows this structure connected to the MHS and a cross-section through the structure and MHS where contact of the two helix parts can be seen.

The helix structure can be manufactured by turning from a cylindrical semi-finished product or by a combination of machining and turning.
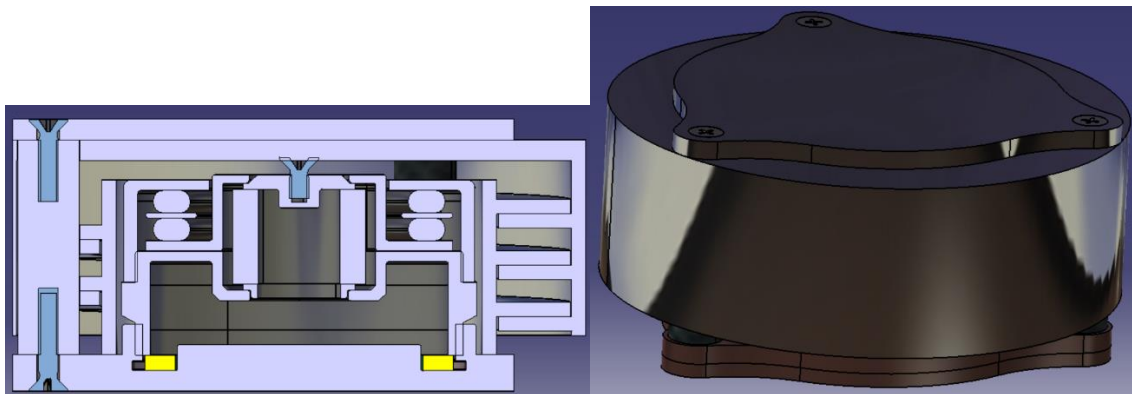
Picture 10.20 Helix structure mounted on non-modified MHS in the ON position cut (left), isometric view (right)

Switching between ON and OFF positions is based on vertical movement (without rotation) of the parts. This means that the main parameter of this structure is the pitch of the helix. The difference between the ON and OFF position can be seen in picture 10.21.
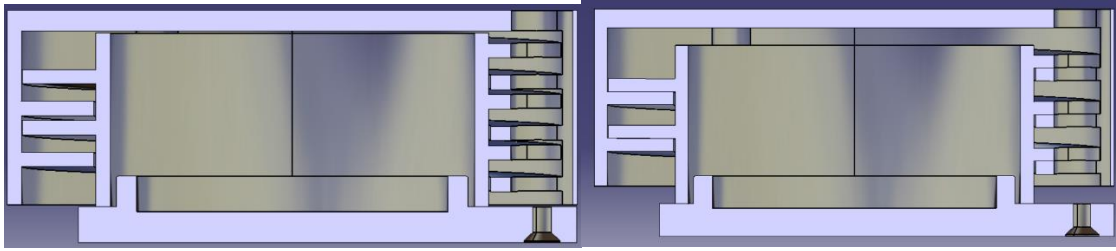
Picture 10.21 The helix structure in the OFF position (left) and in the ON position (right)

The helix as such is used primarily for two reasons. The first is a large contact area and the second is disassembly of the structure itself. It can be easily unscrewed after separation of the elastomer insulators.

10.6.1 Modifications

Two possible modifications to this structure have been proposed, based on whether the outer or inner part of the structure moves.

The first modification can be seen in Picture 10.22 and is based on the movement of the outer helix.
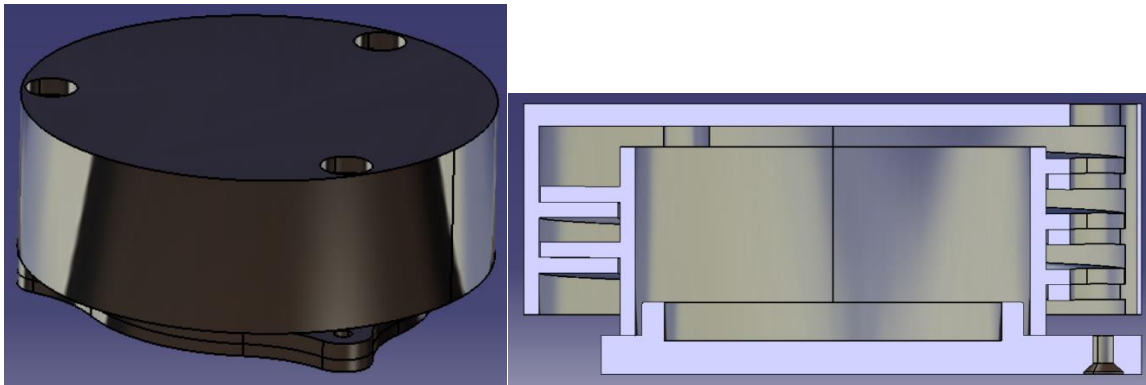
Picture 10.22 First modification in the ON position isometric view (left), cross-section (right)

The second modification can be seen in the Picture 10.23 and is based on movement of the inner helix.
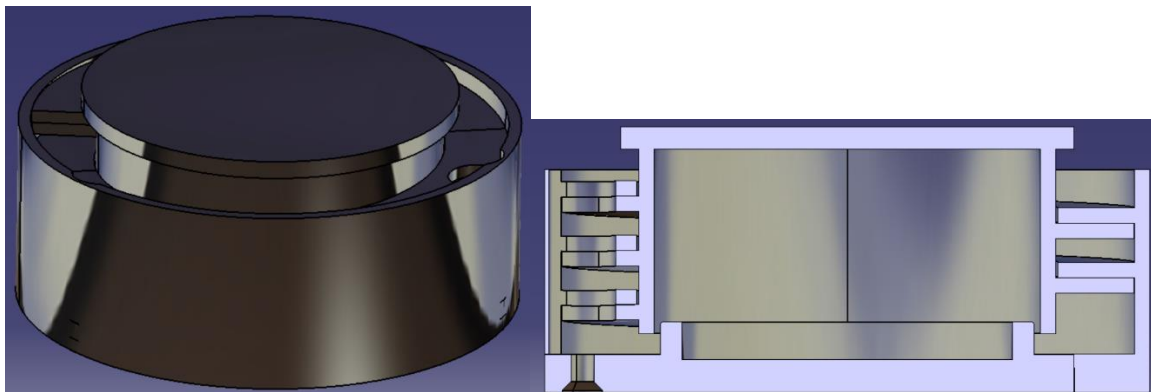
Picture 10.23 Second modification in the ON position isometric view (left), cross-section (right)

10.6.2 Basic geometry definition

The basic geometry of both modifications is similar, so only one type is described here.

The key part of this concept is the pitch of the helix.
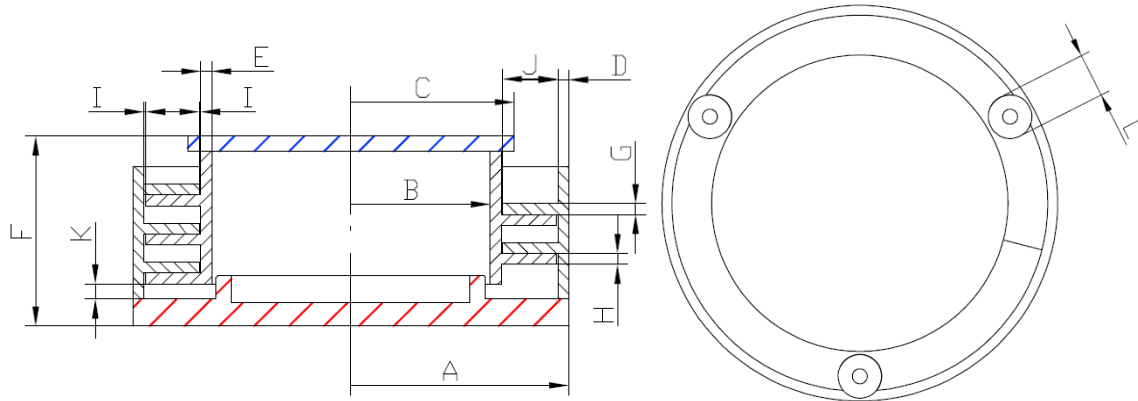
Picture 10.24 Helix contact geometry definition side view (left), top view (right)

Picture 10.24 gives the geometrical parameters identified by letter:
- A – Maximum outer diameter of the MHS design space
- B – Maximum inner diameter of the MHS design space
- C – Contact plate diameter
- D – Outer part wall thickness
- E – Inner part wall thickness
- F – Maximum height of the structure
- G – Lower part helix thickness
- H – Upper part helix thickness
- I – Clearance between the lower and upper parts
- J – Width of helix
- K – Clearance in ON/OFF position (this value is of primary importance in the OFF position, it is the space required for movement of the structure)
- L – Space needed for elastomer insulator (usually ⌀6,2 mm)

10.6.3 Results

Because the contact surface of this structure is a helix, which rises around the circumference of both cylinders, it is practically impossible to perform a usable analytical calculation of thermal conductivity in this case. The only calculation that could be performed was the weight of the structure, based on the volume measured in relation to the model created in CATIA. These models must be subjected to finite element analysis for thermal conductivity calculations.

The weights calculated on the basis of knowledge of the volume of the models can be found in Table 10.9. The first helix types, which were calculated, are given in Table 10.8.

Table 10.8 Dimensions of helix structure

Parameter	Al-He-5/7 Cu-He-5/7	Al-Hi-5/7 Cu-Hi-5/7
A	⌀56 mm	
B	⌀35,8 mm	
C	⌀56 mm	⌀42 mm
D	1,4 mm	
E	1,4 mm	
F	24,4 mm	
G	1,4 mm	
H	1,4 mm	
I	0,2 mm	
J	7,2 mm	
K	In the ON position: 1,9 mm In the OFF position: 0,2 mm	
L	⌀6,2 mm	
Base plate type	Standard base plate of MHS	Extended base plate (on maximum diameter 56 mm)

Table 10.9 Final parameters of helix structure

Designation of structure	Weight of the structure [g]
Al-He-5/7	51
Cu-He-5/7	161
Al-Hi-5/7	54
Cu-Hi-5/7	171

Limit parameters:
- Weight of the CTB structure used on BB: 55,1 g
- Thermal conductivity of structure at least $1,5 \ W \cdot K^{-1}$, but not much more.
- Maximum diameter of 56 mm.

The main problem of the helix structure would probably be its manufacture. The helix must be very precisely manufactured which can be very expensive.

The results shows that a design based on a base plate extension is heavier in comparison to a structure design requiring a larger contact plate.

10.7 Comparison

The comparison of mechanical contact structures processes the results mentioned in previous chapters and compares mechanical contact structures on the basis of thermal conductivity, weight and specific thermal conductivity.

Representatives with the best parameters were selected from each type of structure and can be found in Table 10.10.

Table 10.10 Structures selected for comparison

Designation	Thermal conductivity C [W·K⁻¹]	Weight [g]	Specific thermal conductivity C_{SP} [W·K⁻¹·g⁻¹]
Cu/Al-Ce2-6,3/1,2	1,07	51	2,12
Cu/Al-Ce2-5,2/1,2	1,36	68,30	1,99
Al-2T8/7-1,8	1,45	62	2,37
Cu/Al-2T10/9-1,2	2,05	104	2
Al-He-5/7	-	51	-

Limit parameters:
- Weight of the CTB structure used on BB: 55,1 g
- Thermal conductivity of structure at least 1,5 W·K⁻¹, but not much more.
- Maximum diameter of 56 mm.
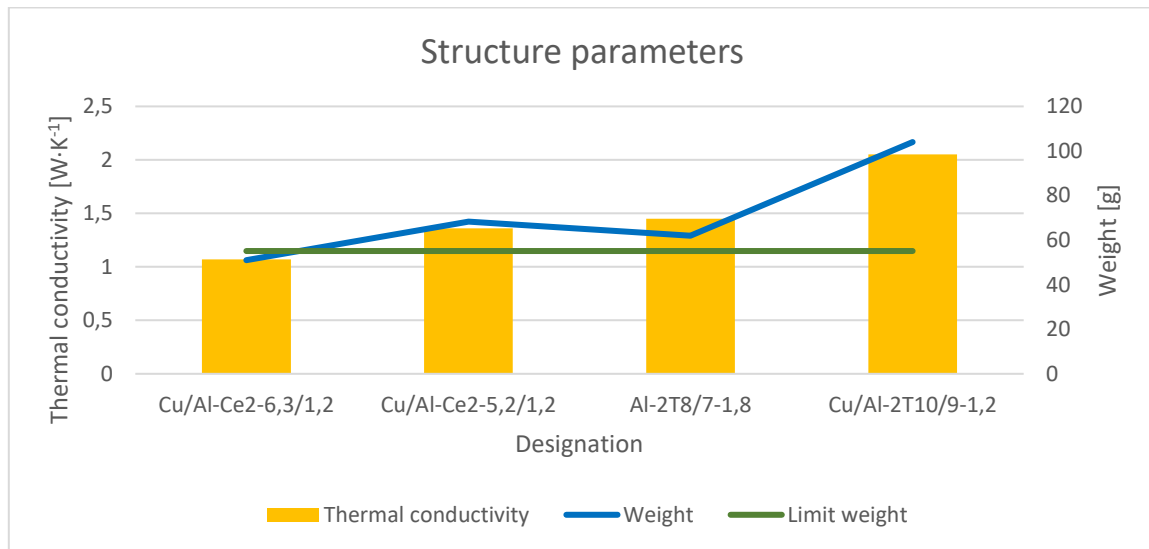
Figure 10.5 Structure parameters

There are no structures that meet all the specified requirements for the heat conductive structure. Each of the concepts always fails to meet the requirements of at least one parameter. In the case of the helix structure, the thermal conductivity parameters are unknown and have not yet been tested.

The best combination of parameters, which is confirmed by the specific conductivity, is achieved in the case of structure Al-2T8/7-1,8. Although this structure does not meet either of the parameters, in comparison to other structures, it is close to the limit values for both key parameters.

A probable problem in relation to the Al-2T8/7-1,8 structure is its manufacture. This type of structure can probably be manufactured, but the 2 planes of contact require high accuracy.

The other interesting type of structure is Cu/Al-2T10/9-1,2. This type of structure is very heavy, but the weight can probably be reduced somewhat by lowering the thermal conductivity, which is considerably higher than the required value.

11 Foil structure

The foil structure is often used in thermal straps that are used in the cryogenic, aerospace and space industry for heat conduction [12]. Thermal foil straps can be made of materials such as copper, aluminium or graphene [12].
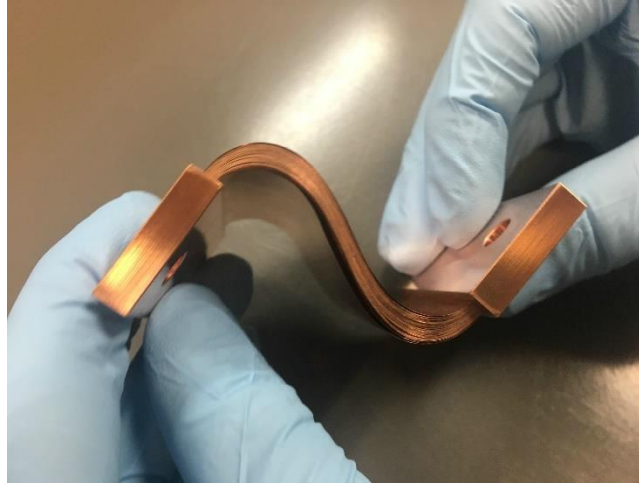
Picture 11.1 Copper foil thermal strap [51]

The concept of a heat conductive structure based on foils is designed similarly to the thermal straps itself. It consists of many thin films, which allow some flexibility. The difference between the foil strap and the braided strap is that the braided strap provides flexibility through 3 axes [51].

The foil structure provides good flexibility and very good thermal conductivity, and it can also be used in a limited volume [12]. The foil structure can probably provide greater thermal conductivity than the actual wire braid structure.

One possibility with great potential is the graphene foil structure, because graphene thermal straps have already been qualified for use in space [52].

Thanks to a wide selection of different copper and aluminium foil thicknesses it could be possible to design a high flexibility structure with the required thermal conductivity.

The manufacturing of this type of structure could be the biggest problem, because the MHS has a round shape, which may cause problems when the foils are bent. The other manufacturing issue could be the technology. Welding could probably be used in the case of metal foils and soldering in the case of carbon materials.

11.1 Methodology

The approximate length of the foil strips that could be used instead of the TB structure initially had to be established. A small experiment using ordinary aluminium kitchen foil and pieces of cardboard was carried out to establish this.

A dimensional model of the MHS was made out of cardboard, to which 10 pieces of foil of various lengths were subsequently attached. Three lengths of foil were used in these experiments and it was determined how they would bend.
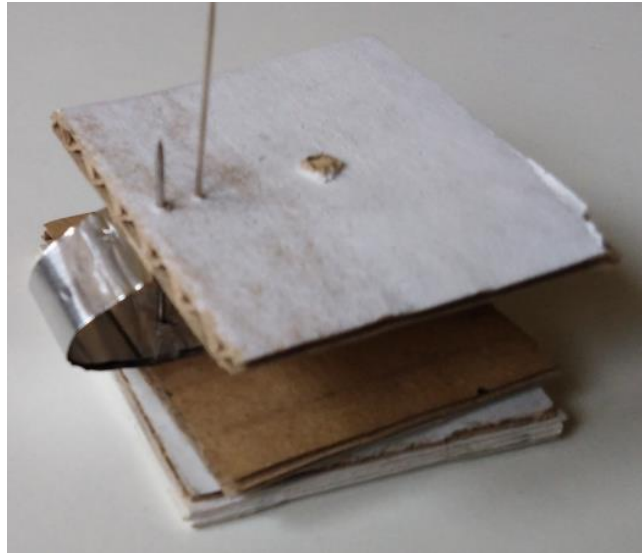
Picture 11.2 Model with attached foil structure

Table 11.1 Experimental foil length

Parameter	Value
First model foil length	18 mm
Second model foil length	21 mm
Third model foil length	24 mm

Picture 11.3 Foil length 18 mm

Picture 11.4 Foil length 21 mm
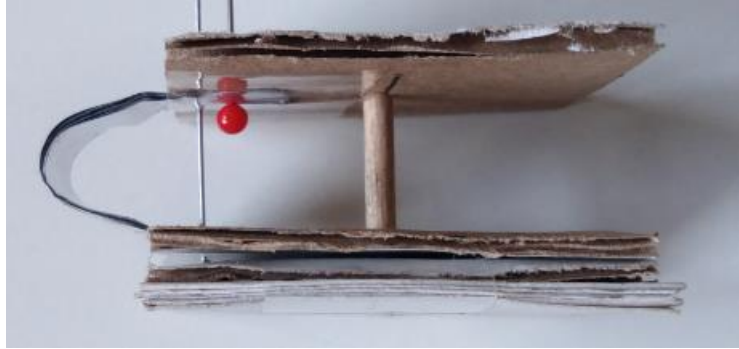
Picture 11.5 Foil length 24 mm

The result of these tests was that the useful length could be 18 mm. This length is sufficient for the movement of the contact plate and it simultaneously requires a smaller amount of material for the required thermal conductivity.

The next step was to determine the area of the thermal structure (S_{TB}). The Equation (1) where the thermal conductivity of the structure (C) was based on the thermal conductivity requirement for structures as given in the previous chapters, which is 1.5 W·K^{-1} was used for this purpose. The length of the thermal structure (δ) was previously given as 18 mm and the thermal conductivity coefficient (λ) of the required material was used.

Volume V is computed using equation (20). where S_{TB} is the area required for the structure and δ is the length of the structure.

Equation (12) is then used to calculate the weight of the entire structure.

11.2 Computation results

These results contain a selection of several foils of different thicknesses and different materials and the parameters of the resulting structure calculated on the basis of input data from the manufacturer or determined experimentally.

Because the density of graphene is not mentioned by the manufacturer. this value was obtained from another source.

Table 11.2 Foil parameters

Foil Number	Manufacturer	Material	Foil thickness e [mm]	Thermal conductivity λ [W·m^{-1}·K^{-1}]	Density ρ [kg·m^{-3}]
1	Advent research materials [53]	Cu OFHC [20]	0,05	394	8900
2	Advent research materials [54]	Cu OFHC [20]	0,25	394	8900
3	Advent research materials [55]	Al 99,5% [23]	0,05	235	2700
4	Advent research materials [56]	Al 99,5% [23]	0,25	235	2700
5	Topsen [31]	Graphene [31]	0,05	1700	2267 [57]
6	Pro graphite shop [58]	Graphite [58]	0,017	1500	2000

Table 11.3 Foil structure parameters

Foil Number	Foil length δ [mm]	Weight for 1,5 W·K⁻¹ M [g]	Total area required for TB S_{TB} [mm²]
1	18	11	69
2	18	11	69
3	18	6	115
4	18	6	115
5	18	0,7	16
6	18	0,7	18
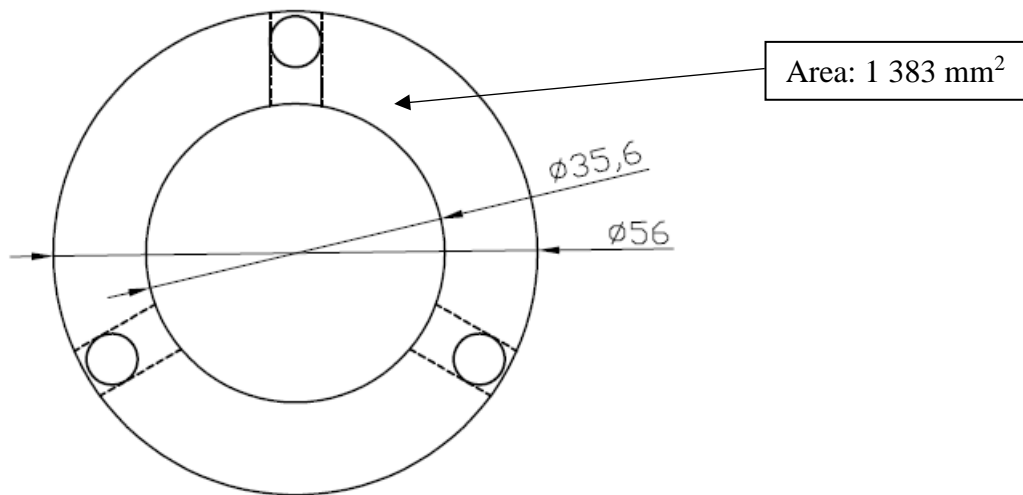
Picture 11.6 Representative usable area

11.3 Comparison with requirements and results

The results were compared with the available area and it seems that, after applying the parameters given above, this structure will also fit into the standard MHS design.

The comparison between several materials shows, that carbon materials such as graphene or graphite foil have excellent thermal conductivity and the possibility of soldering, there is also the option to manufacture the structure of this material.

However the manufacturing process of these samples showed that it is very difficult to arrange all the foils manually. and foils of different dimensions would be necessary on one strap when layering a greater number of foils, to ensure flexibility.

12 Comparison of structures and selection of the most beneficial solution

This chapter focuses on final comparison of all the types of structures and compares their benefits according to the limitations. The most beneficial structure will be selected at the end of the chapter.

In order to compare all the structures, it is important to take into account that the weight and thermal conductivity of the mechanical structures was calculated differently to that of foils and TB.

In the case of foils and TB, only their values were calculated, not the summary values of any connecting structures and base plates or contact plates. Given that the thermal conductivity of the base plate and contact plate is significantly higher than the thermal conductivity of the structures themselves, their impact on this parameter can be omitted. In their case, the weight is also compared to the actual weight of TB used on BB, which is measured.

In the case of mechanical contact structures calculations also include the contact plate, base plate and, in some cases where this is required, the extended part of the base plate.

A numerical score from 1 to 7 was used for the comparison.

This method of evaluation consists of assigning numbers to specific values of the measured parameters. A score of 1 means that the parameter is completely unsatisfactory and, on the contrary, a score of 7 means that the parameter has a completely satisfactory value (better than the one it is compared to). A score of 4 is allocated to parameters that are close to the ideal parameters.

And finally, the number of points allocated to the structures is calculated

The parameters that will be monitored are:
- Thermal conductivity (according to structure type)
- Weight (according to structure type)
  - Due to the unknown weight of the required soldering material, the score is reduced by several points.in case of the TB and foil structures.
- Required space
  - In some cases the area required for the thermal contact is not as big a problem as the space that the structure requires around the switch itself. Due to this problem the score value is reduced by several points in case of foil structures and TB structures for heat transfer in longitudinal direction.
- Manufacturability and technology verification

The values of parameters, which are ideal:
- Thermal conductivity: 1,5 $W \cdot K^{-1}$
- Weight: Mechanical contact structures: 55,1 g, TB and foils: 22,1 g.
- Required space: Mechanical contact structure: 1 539 mm^2, TB and foils 390 mm^2

Table 12.1 Structures comparison

Designation	Thermal conductivity [W·K⁻¹]		Weight [g]		Required space [mm²]		Manu-facturability	Result
	Value	Score	Value	Score	Value	Score	Score	
Mechanical contact structure								
Cu-Ce2-6,3/1,2	1,78	6	93	2	1 539	2	3	13
Al/Cu-Ce2-6,3/1,2	1,11	2	71	3	1 539	2	3	10
Cu/Al-Ce2-6,3/1,2	1,07	1	51	4	1 539	2	3	10
Al-Ce2-6,3/1,2	0,76	0	29,19	7	1 539	2	3	0
Al-Ce2-3,7/1,2	0,86	0	42,22	6	1 539	2	3	0
Cu/Al-Ce2-5,2/1,2	1,36	3	68,30	3	1 539	2	3	11
Al-2T8/7-1,8	1,45	4	62	3	2 430	2	4	13
Cu/Al-2T10/9-1,2	2,05	7	104	2	2 430	2	4	15
Cu/Al-T8/7-1,2	1,34	3	80	2	2 430	2	4	11
Al-He-5/7	-	-	51	4	1 539	2	3	9[***]
Cu-He-5/7	-	-	161	1	1 539	2	3	6[***]
Al-Hi-5/7	-	-	54	4	2 430	2	3	9[***]
Cu-Hi-5/7	-	-	171	1	2 430	2	3	6[***]
Flat braid – Heat transfer in the transversal direction								
1;1	1,5	4	55,45[*]	2	1 190	2	2	10
2;1	1,5	4	55,42[*]	2	1 189	2	2	10
3;1	1,5	4	55,52[*]	2	1 192	2	2	10
Flat braid – Heat transfer in the longitudinal direction								
1;1	1,5	4	55,54[*]	2	312[**]	3	2	11
6;2	1,5	4	43,84[*]	2	780[**]	3	2	11
7;3	1,5	4	28,08[*]	3	585[**]	3	2	12
8;3	1,5	4	27,86[*]	3	516[**]	3	2	12
Sleeving braid structure								
2;1	2,093	7	34,82[*]	3	185[**]	5	2	17
3;1	1,638	5	43,21[*]	2	182[**]	5	2	14
4;3	1,645	5	21,85[*]	3	303[**]	4	2	14
5;3	1,69	6	22,40[*]	3	311[**]	4	2	15
Stocking braid structure								
1;1	1,8	6	30,04[*]	3	159[**]	5	2	16
2;1	1,95	7	34,89[*]	3	178[**]	5	2	17
4;1	1,52	4	39,94[*]	2	168[**]	5	2	13
Carbon fibre structure								
K13D pitch-based [25]	1,5	4	7,07[*]	4	8[**]	3	1	12
K13D pitch-based (CNTs - grafted) [25]	1,5	4	5,46[*]	4	7[**]	3	1	12
K13C2U [29]	1,5	4	8,52[*]	4	10[**]	3	1	12
Foil structure								
2	1,5	4	11[*]	4	69[**]	3	3	14

[*] TB and foil structure maximum weight of 22,1 g
[**] TB and foil structure maximum area of 390 mm²
[***] The value of thermal conductivity is unknown

Designation	Thermal conductivity [W·K⁻¹]		Weight [g]		Required space [mm²]		Manu-facturability	Result
	Value	Score	Value	Score	Value	Score		
Foil structure								
3	1,5	4	6*	4	115**	3	3	14
5	1,5	4	0,7*	6	16**	3	1	14
6	1,5	4	0,7*	6	18**	3	1	14

According to the Table 12.1, the structures for mechanical contact are not so good. The primary problem is their weight, when the structure is made of copper. Structures made of aluminium have lower thermal conductivity in some cases, they are essentially unusable. However two of these structures seem to be a second best option. The best of mechanical structures are those where the upper part is made of aluminium alloy and the lower part is made of copper. The best results of mechanical contact structures are achieved by Cu/Al-2T10/9-1,2, which combines the copper lower part and aluminium alloy upper part. This structure is very heavy, but the weight can be lowered by adjusting the dimensions. The helix structures are also good choice according to the results, nevertheless the FEA analysis of thermal conductivity is required, until then the value is unknown. Another problem of mechanical contact structures could be stress concentrators (sharp edges), especially if high fatigue resistance is required. The manufacturing method can be turning or machining of cylindrical semi-finished product.

The carbon materials, both foils and fibres, achieved good properties of thermal conductivity and weight. Although these materials are space proven, their use in this project would probably be unique. At the same time the connection using a new type of solder requires additional tests. Another problem could be how to fold the fibres correctly and easily so they can be soldered or how to work properly with the graphene foil. The use of these materials for the MHS project would probably mean more demanding certification, despite their undeniable advantages. Because of that, the manufacturability score is so low in case of these structures. It would be necessary to produce test specimens on which the behaviour of these materials and the actual thermal conductivity parameters would be tested.

According to the Table 12.1, the foil structures are the third best concept. This type of structure has not been examined in as much detail as in mechanical contact structures and TB concepts. The foil structure concept have good thermal and weight properties, but there is problem with the design space. The contact area is small enough, but the additional space for bended foil must be provided. The manufacturing of conventional foil materials, such as aluminium and copper, can be made by soldering. The weight score is lowered as the solder material is additional weight for the structure. Another alternative of fixing these parts together can be, for example, electron beam welding or laser welding (other type of laser beam than red).

The best results in all structures are achieved in the case of wire structures, but not those that were used on BB, but wire structures composed of the sleeving braid and stocking braid. These structures have the great advantage in combination of low required area and high thermal conductivity. The weight can be lowered by using of different braids combinations. Those structures have also high advantage in the required space. It doesn't require additional space for expansion like for example foil structures. The manufacturing with use of electron beam welding will be very expensive and other manufacturing processes which were tried in previous design are not so suitable. Also there can be problems with verification of technologies for use in space. For further data, it would be necessary to use the purchased pieces of these textiles and create experimental samples, which would then be subjected to tests for thermal conductivity and possibly cyclic loads. Also it is necessary to try the electron beam welding technology for these structures.

Thus, the final comparison is based on the fact that the best structures are probably sleeving braid or stocking braid structures and further tests should be taken in this direction, at least to determine other possible advantages and disadvantages of this structure and manufacturability. The second best structure is type of double T-shape mechanical contact structure which must be tested by the finite elements analysis.

13 Discussion and conclusions

The main goal of my diploma thesis was final theoretical proposal of heat conductive structure for the MHS project, in accordance with demands of ESA. This proposal is based on the BB design developed by Arescosmo approximately two years ago. This original switch was developed well in dimensions, used materials and other parameters, but haven't fill the requirements for thermal conductivity, including all conditions connected to that and weight requirement. These problems were recognised in details on institute of aerospace engineering BUT, by CT scans, computations and other tests. On the base of this development we started to look for the solution of these problems.

As the solution for the previous concept development we decided to use three different types of structure concepts, braided structure, mechanical contact structure, foil structure, each of them is working in different ways. For every of these structures we decided to concentrate on 8 sub-structures together, what together included 49 of selected representatives, from which 34 are mentioned in the Table 12.1.

For the thermal computations was used equation for thermal conductivity in material and for the computations of thermal conductivity in contact of surfaces was used Yovanovich's model. For the computation of final thermal conductivity of single parts were used equations for parallel and serial connection. For the computations of weight were used basic equations for calculating of the volume.

According to the calculations the most beneficial structures seem to be sleeving braids and stocking braids structures made of copper and aluminium, from which the copper materials structures are the best, as they have thermal conductivity roughly 2 W·K^{-1}, which is higher than the required value of $1,5 \text{ W·K}^{-1}$, weight of 35 grams and they require roughly 180 mm^2 for the contact realisation. The weight of these braids is also higher than the value required. Nevertheless combination of different types of these braids can possibly lower the weight and the thermal conductivity. Another advantage is that these structures do not need additional space for their movement and this space is roughly equal to the area required to connect them. We decided to prioritise the copper braids because the aluminium braids require more area for contact. The problem of this structure can be in manufacturing. The soldering is not much suitable as the previous design of CTB showed, the only possibility is electron beam welding. This technology is very expensive and there can be problems with verification.

The other problem of MHS was insufficient welding quality of original CTB structure, where kind of laser welding was used, which results in bad connections of wires and CTB parts. By studying of welding possibilities in the literature it looks like the best solution for future using of electron beam welding.

Due to the coronavirus crisis, theoretically computed results were not confirmed by practical tests yet. Also we haven't practically tested the proposed electron beam welding technology and other technologies for verifying of manufacturability, which were theoretically prepared.

The Miniaturised Heat Switch project should be solved up to the end of 2021, just now is finished theoretical part of the heat conductive structure with the proposal of the most beneficial structure. In next month will be necessary to confirm theoretical results by practical tests of all three structures (mechanical contact structure, braided structure, foil structure) and verify sufficient welding technology. After selection of the best structure according to practical tests and finite element analysis in case of mechanical contact structures, will be needed:

- Assembly of developed structures with other MHS parts
- Cyclic loads tests
- Environmental tests of MHS

14 Bibliography

[1] 2012_ESA SOW Heat Switch - General requirements: Appendix 1 to ITT 1-6801/11/NL*/NA*. Netherlands, 2011.

[2] MAŠEK, Jakub a Robert POPELA. Heat Switch Design Overview & Advanced MHS definition: LU-01-2018-ADA.TS. Brno, 2018.

[3] BONZANO, Giuseppe a Massimo CONTE, ed., Marco ADAMI. Miniaturized Thermal Switch Breadboard Tests and Design Selection *Report: TN* 05 301609A. Rev. A. Aprilia, 2017.

[4] MAŠEK, Jakub, Marek HORÁK *a* Pavel ZIKMUND. Miniaturized Thermal Switch Report on BB Testing: LU33-2017-MHS.PR. Brno, 2018.

[5] *PAVELEK, Milan. Termomechanika. První. Brno: Akademické* nakladatelství CERM, 2011. ISBN 978-80-214-4300-6.

[6] *HALLIDAY, David, Robert RESNICK a Jearl WALKER,* Petr DUB. Fyzika. Svazek 2. **Druhé**. Brno: VUTIUM, 2013. ISBN 978-80-214-4123-1.

[7] *YOVANOVICH, M.M, J.R. CULHAM a* P. TEERTSTRA. Calculating interface resistance. **Electronics** cooling [online]. [cit. 2020-04-10]. Available: http://www.mhtlab.uwaterloo.ca/pdf_papers/mhtl97-4.pdf

[8] *MATEÁŠIK, Timko. THERMAL CONTACT RESISTANCE OF PLANAR* SURFACES [online]. Brno, 2019 [cit**.** 2020-04-10]. Available: https://www.vutbr.cz/studenti/zav-prace/detail/117064. Bakalářská práce. Vysoké učení technické v Brně, Fakulta strojního inženýrství. Vedoucí práce Ing. Jakub Mašek.

[9] *MAŠEK, Jakub. Tomography of Copper Textile Braid:* LU-XX-20XX-000.TS. Brno, 2017.

[10] *Braided copper strips and twisted cables. Kabel Leitungen* Isoliermaterial [online]. Mülheim an der **Ruhr**: Gerhard Hesselmann oHG, 2020 [cit. 2020-03-22]. Available: https://www.hesselmann.de/data-download/produktinfo/geflecht.pdf

[11] *European Cooperation for Space Standardization [online]. Netherlands*: European Space Agency, 2020 [cit. 2020-04-12]. Available: https://ecss.nl

[12] *Thermal Straps. TAI Technology applications [online].* Boulder, 2019 [cit. 2019-09-27]. Available: https://www.techapps.com/thermal-straps

[13] *Document Tree | European Cooperation for Space Standardization.* European Cooperation for Space Standardization [online]**.** Netherlands: ESA-ESTEC ECSS Secretariat, 2020 [cit. 2020-05-19]. Available: https://ecss.nl/standards/ecss-document-tree-and-status/

[14] *ECSS-E-ST-32C. Space engineering: Structural general requirements. Netherlands*: ESA-ESTEC Requirements & Standards Division, 2008**.**

[15] *ECSS-E-ST-32-10C REV.2 CORRIGENDUM 1. Space engineering:* Structural factors of safety for spaceflight hardware. Rev.2. Netherlands: ESA-ESTEC Requirements & Standards Division, 2019.

[16] *ECSS-Q-ST-70C REV.2. Space product assurance: Materials,* mechanical parts and processes. Rev.2. Netherlands: ESA-ESTEC Requirements & Standards Division, 2019.

[17] *ECSS-Q-ST-70-04C. Space product assurance: Thermal testing for* the evaluation of space materials, processes, **mechanical** parts and assemblies. Netherlands: ESA-ESTEC Requirements & Standards Division, 2008.

[18] *ECSS-E-ST-32-03C. Space engineering: Structural finite element models.* Netherlands: ECSS Secretariat ESA-ESTEC Requirements & **Standards** Division, 2008.

[19] *Metal Properties Table. Tibtech [online]. France,* 2018 [cit. 2019-09-27]. Available: https://www.tibtech.com/conductivite.php?lang=en_US

[20] *ECSS-Q-70-71A REV. 1. Space product assurance: Data* for selection of space materials and processes**.** Rev.1. Netherlands: ESA-ESTEC Requirements & Standards Division, 2004.

[21] *Material Datasheet Cu-ETP. Aurubis Stolberg [online].* Stolberg [cit. 2020-06-01]. Available: https://www.aurubis-stolberg.com/wdb/band/eng/Copper/Cu-ETP-PNA%20211_EN.pdf

[22] *ASM Material Data Sheet: Aluminum 7075-T73; 7075-T735x.* ASM Aerospace Specification Metals, Inc. | Florida Aerospace Metal Distributor [online]. Florida Webmaster | Website Design | Small Business Internet Marketing | Search Engine Optimization, 2020 [cit. 2020-05-28]. Available: http://asm.matweb.com/search/SpecificMaterial.asp?bassnum=MA7075T73

[23] *Conductor materials: Aluminium – LEONI. Wire Products* & Solutions – LEONI [online]. [cit. 2020-06-01]. Available: https://www.leoni-wire-products-solutions.com/en/materials/conductor-materials/aluminium/

[24] *C-Solder. Supplier of materials for research and development* - Goodfellow [online]. United Kingdom: Goodfellow Cambridge, c2008-2020 [cit. 2020-03-06]. Available: http://www.goodfellow.com/news-article/c-solder/

[25] *NAITO, Kimiyoshi, Jenn-ming YANG, Yibin XU a* Yutaka KAGAWA. Enhancing the thermal conductivity **of** polyacrylonitrile- and pitch-based carbon fibers by grafting carbon nanotubes on them. Carbon [online]. Elsevier Ltd, 2010, 48(6), 1849-1857 [cit. 2019-10-02]. DOI: 10.1016/j.carbon.2010.01.031. ISSN 0008-6223. Available: https://www.sciencedirect.com/science/article/pii/S0008622310000540

[26] *HEREMANS, J., I. RAHIM a M.* DRESSELHAUS. Thermal conductivity and Raman spectra **of** carbon fibers. Physical Review B [online]. 1985, 32(10), 6742-6747 [cit. 2020-03-06]. DOI: 10.1103/PhysRevB.32.6742. ISSN 0163-1829. Available: https://link.aps.org/doi/10.1103/PhysRevB.32.6742

[27] *Graphite Fiber Thermal Straps. Thermal Space [online].* Boulder: Success by design, c2015-2016 **[**cit. 2020-03-01]. Available: https://thermal-space.com/graphite-fiber-thermal-straps-obsolete-1/

[28] *USINGER, R., P. DELOUARD a G.* MILLER. European Space Agency, (Special **Publication**) ESA SP [online]. 691. Zürich: European Space Agency, 2012, [cit. 2020-03-04]. ISBN 9789290922551. ISSN 03796566. Available: https://ui.adsabs.harvard.edu/abs/2012ESASP.691E...7U/metrics

[29] *Pitch Fiber - Mitsubishi Chemical Carbon Fiber Composites.* Home - MCCFC - Mitsubishi Chemical Carbon Fiber and Composites [online]. Mitsubishi Chemical Carbon Fiber and Composites, 2020 [cit. 2020-05-27]. Available: http://mccfc.*com/*pitch-fiber/

[30] *X-Series® Thermal Straps - PGS & Graphene* Foil. Technology Applications, Inc. (TAI) - Thermal Straps/Links [online]. Boulder: Technology Applications, 2020 [cit. 2020-05-28]. Available: https://www.techapps.*com/*graphene-pgs-thermal-straps

[31] *Graphene Thermal Conducting Film for Electronic Devices Manufacturers* and Suppliers - Factory Price - TOPSEN **TECHNOLOGY**. Anti-Corrosion Primer, Graphene Absorbing Material, Air Filtering Material, Thermal Conducting Film,

Battery Cathode Material Manufacturers and Suppliers - Factory Price - *TOPSEN TECHNOLOGY* [online]. [cit. 2020-05-30]. Available: http://www.topsentech.net/thermal-conducting-film/graphene-thermal-conducting-film-and.html

[32] *The top 5 benefits of Laser welding. Industrial* Laser Solutions Manufacturer | SPI Fiber Laser Products [online]. United Kingdom: SPI Lasers, 2020 [cit. 2020-03-16]. Available: https://www.spilasers.com/application-welding/the-top-5-benefits-of-laser-welding/

[33] *CW and Pulsed Laser Welding | EB Industries.* Electron Beam Welding | Laser Welding | EB Industries [online]. New York: EB Insdustries, 2020 [cit. 2020-03-16]. Available: https://www.ebindustries.com/cw-and-pulsed-laser-welding/?cn-reloaded=1

[34] *LASCAMCZ, . Lasery pro svařování - LASCAM systems*. LASCAM systems - průmyslové laserové a **kamerové** systémy [online]. Praha: LASCAM Systems, 2019c [cit. 2020-03-17]. Available: https://www.lascam.cz/lasery-pro-svarovani/

[35] *TruDisk se zelenou vlnovou délkou | TRUMPF. TRUMPF* GmbH + Co. KG | TRUMPF **[**online]. Praha: TRUMPF, 2020 [cit. 2020-03-17]. Available: https://www.trumpf.com/cs_CZ/produkty/laser/diskovy-laser/trudisk-se-zelenou-vlnovou-delkou/

[36] *WęGLOWSKI, M.St, S BłACHA a A* PHILLIPS. Electron beam welding – Techniques and trends – Review. Vacuum [online]. Elsevier Ltd, 2016, 130, 72-92 [cit. 2020-03-19]. DOI: 10.1016/j.vacuum.2016.05.004. ISSN 0042-207X. Available: https://www-sciencedirect-com.ezproxy.lib.vutbr.cz/science/article/pii/S0042207X16301245

[37] *Machining Introduction. EFunda: The Ultimate Online Reference* for Engineers [online]. Sunnyvale: eFunda, c1999-2020 [cit. 2020-03-21]. Available: http://www.efunda.com/processes/machining/machin_intro.cfm

[38] *VIČAR, David. Moderní dokončovací metody obrábění a* jejich využití [online]. Brno, 2011 **[**cit. 2020-03-21]. Available: https://www.vutbr.cz/studenti/zav-prace/detail/38533. Bakalářská práce. Vysoké učení technické v Brně, Fakulta strojního inženýrství. Vedoucí práce Prof. Ing. Miroslav Píška, CSc.

[39] *KOCMAN, Karel a Jaroslav PROKOP. Technologie obrábění.* Vyd. 2. Brno: Akademické nakladatelství **CERM**, 2005, 270 s. : il., tabulky, grafy, schémata. ISBN 80-214-3068-0.

[40] *Copper braid products. In: Tranect [online].* Liverpool, 2016 [cit. 2019-09-27]. **Available:** https://www.tranect.co.uk/wp-content/uploads/2017/03/Copper-Braid-Products.pdf

[41] *Flat copper braid. Copper Braid Products [online].* United Kingdom, 2019 [cit. 2019-09-27**]**. Available: https://www.copperbraid.co.uk/flat-braid/

[42] *Copper Thermal Straps. Thermal Space [online].* Boulder: Success by design, c2015-2016 [cit**.** 2019-09-27]. Available: https://thermal-space.com/copper-thermal-straps/

[43] *Flat and Round Braid. In: Heat Shrink* Tubing and Cable Protection | Hilltop Products **Ltd** [online]. Warrington: Hilltop, 2019 [cit. 2020-03-22]. Available: https://www.hilltop-products.co.uk/media/Flat%20and%20Round%20Braid.pdf

[44] *Tubular Shielding Braids. Copper Braid Products [online].* United Kingdom, 2019 [cit. 2019-09-27**]**. Available: https://www.copperbraid.co.uk/tubular-shielding-braids/

[45] *Copper braid. Techflex, Flexible sleeving - cable* and wire management [online]. Netherlands: **techflex**, 2020 [cit. 2020-06-01]. Available: https://www.techflex.nl/metalshielding-copper-braid-c-146_158.html?language=EN

[46] *Braids: Shielding braids – LEONI. Wire Products* & Solutions – LEONI [online]. [cit. 2020-06-01]. Available: https://www.leoni-wire-products-solutions.com/en/products-solutions/braids/shielding-braids/

[47] *EFX-EMC měděný ochranný CU oplet kabelu pro EMC* stínění. REVELET - průmyslové konektory , ochranné hadice kovové, hliníkové krabice [online]. [*cit. 2020-06-01]. Available: http://www.revelet.cz*/detail/oplety_kabelu/oplet_EFX-EMC.html

[48] *Copper Stocking Braid 25 mm2 Tinned (25* mm minimum dia, 120 mm max diameter) – Copper Braid Products. Copper Braid Products – Supply of products made from copper braid [online]. United Kingdom, 2020 [cit. 2020-06-01]. Available: https://www.copperbraid.co.uk/product/copper-stocking-braid-25-mm2/?attribute_pa_length=1-metre

[49] *Copper Stocking Braid 35 mm2 Tinned (35* mm minimum dia, 120 mm max diameter) – Copper Braid Products. Copper *Braid* Products – Supply of products made from copper braid [online]. United Kingdom, 2020 [cit. 2020-06-01]. Available: https://www.copperbraid.co.uk/product/copper-stocking-braid-35-mm2/?attribute_pa_length=1-metre

[50] *19.75 oz Carbon Fiber Fabric 2x2 Twill* | Woven Carbon | ACP Composites. Custom Composite Solutions & Stock Products | ACP *Composites* [online]. Livermore, 2020 [cit. 2020-06-04]. Available: https://store.acpsales.com/products/8778/19-75-oz-carbon-fiber-fabric-2x2-twill

[51] *OFHC Copper Foil Thermal Straps. In: Technology* Applications, Inc. (TAI) - Thermal **Straps**/Links [online]. Boulder: Technology Applications, 2020 [cit. 2020-06-01]. Available: https://www.techapps.com/copper-foil-straps

[52] *Thermal LyNX graphene thermal straps have superior thermal* efficiency and flexibilityThermal Space. Thermal Space [**online**]. Boulder: Success by design, c2015-2016 [cit. 2020-06-05]. Available: https://thermal-space.com/thermal-lynx/

[53] *CU1260 Copper Foil - Advent Research Materials. Supplying* high purity metals, alloys and polymers **-** Advent Research Materials [online]. [cit. 2020-06-07]. Available: https://www.advent-rm.com/en-GB/Products/Pure-Metals/Copper/Form/Foil/Line/CU1260

[54] *CU1346 Copper Foil - Advent Research Materials. Supplying* high purity metals, alloys and polymers **-** Advent Research Materials [online]. [cit. 2020-06-07]. Available: https://www.advent-rm.com/en-GB/Products/Pure-Metals/Copper/Form/Foil/Line/CU1346

[55] *AL1052 Aluminium Foil - Advent Research Materials. Supplying* high purity metals, alloys and polymers **-** Advent Research Materials [online]. [cit. 2020-06-07]. Available: https://www.advent-rm.com/en-GB/Products/Pure-Metals/Aluminium/Form/Foil/Line/AL1052

[56] *AL1051 Aluminium Foil - Advent Research Materials. Supplying* high purity metals, alloys and polymers **-** Advent Research Materials [online]. [cit. 2020-06-07]. Available: https://www.advent-rm.com/en-GB/Products/Pure-Metals/Aluminium/Form/Foil/Line/AL1051

[57] *Graphene | AMERICAN ELEMENTS ®. AMERICAN ELEMENTS® |* The Advanced Materials Manufacturer [online]. Loas Angeles: American Elements, ©

1998-2020 [cit. 2020-06-07]. Available:
https://www.americanelements.com/graphene-1034343-98-0

[58] *Thermal Conductive Graphite Foil - Heat Spreader - 17 micron thickness, 200 x 300 mm | Graphite Shop – Graphite Powder, Graphite Foils, Nanoplateletes, Expandable graphite etc. Graphite-shop.com | Graphite Shop – Graphite Powder, Graphite Foils, Nanoplateletes, Expandable graphite etc.* [online]. Gambio, 2019 [cit. 2020-06-07]. Available: https://www.graphite-shop.com/en/foil-200x300-mm-17my-PG1510-106.html

15 List of Tables

91

16 List of Pictures

17 List of Figures

18 List of abbreviations and symbols

Abbreviation	Meaning
BB	Breadboard
BUT	Brno University of Technology
CATIA	Computer-aided three-dimensional interactive application
CC	Cemented Carbide
CEITEC	Central European Institute of Technology Brno | Czech Republic
CNT	Carbon nanotubes
CT	Computed Tomography
CTB	Copper Textile Braid
DIA	Diamond
DML	Declared Materials List
DMPL	Declared Mechanical Parts List
DPL	Declared Processes List
DR	Design Requirement
ECSS	The European Cooperation for Space Standardization
ESA	European Space Agency
ETP	Electrolytic Tough Pitch
FEA	Finite Elements Analysis
FOD	Foreign object debris
FOS	Factors of Safety
FOSU	Ultimate design factors of safety
FOSY	Yield design factors of safety
FPR	Functional and performance requirement
ISO	International Organisation for Standardization
MHS	Miniaturised Heat Switch
MS	Microsoft
NASA	National Aeronautics and Space Administration
OFHC	Oxygen-Free High Conductivity
PRR	Operational requirement
RMS	Root Mean Squared
TB	Textile Braid

Variable	Name	Unit
a	height of strip	[m]
b	length of the longest wire projected in longitudinal cross-section	[m]
c	length of the longest wire	[m]
C	thermal conductivity	[W·K^{-1}]
C_{SP}	Specific thermal conductivity	[W·K^{-1}·g^{-1}]
d	diameter of wires	[m]
d_{sl}	Diameter of the sleeving braid	[m]
d_{st}	Diameter of stocking braid	[m]
e	thickness of one strip	[m]
l	length of the used strip	[m]
l_m	Middle Length	[m]
L	required length	[m]
m	weight of the strip of Middle Length	[kg]
M	weight of TB	[kg]
n_{TB}	number of single strips/braids	[-]
n_l	number of wires in longitudinal cross-section	[-]
n_t	number of wires in transversal cross-section	[-]
p	Contact pressure	[MPa]
R	thermal resistivity	[K·W^{-1}]
Ra	roughness	[μm]
S	cross-section area	[m^2]
S_{TB}	Total area required for TB	[m^2]
S_l	nominal area of longitudinal cross-section	[m^2]
S_t	transversal nominal area	[m^2]
V	volume	[m^3]
α	angle	[°]
δ	Thickness / lenght of the wires	[m]
λ	coefficient of thermal conductivity.	[W·m^{-1}·K^{-1}]
ρ	density of wire material	[kg·m^{-3}]

Attachment A

1.1. Functional and Performance requirements [1]

Specification reference	Description
FPR1	The Heat Switch shall have a peak conductance value greater than $1W \cdot K^{-1}$.
FPR2	The Heat Switch shall have an ON/OFF ratio greater than 100.
FPR3	The Heat Switch Shall operate in vacuum and in 10mbar of CO_2.
FPR4	The variable conductivity of the Heat Switch shall be between 15°C to 25°C of the hot interface.
FPR5	The Heat Switch shall be designed to transport 1W to 10W in closed/ON mode with a maximum delta temperature of 10K.
FPR6	The Heat Switch shall have a temperature stability of +/- 1°C with a constant power input and constant sink Temperature.
FPR7	In a redundant configuration, it shall be possible to mount two separate and identical Heat Switches in parallel between the radiator and the heat source without any individual performance degradation.

1.2. Interface Requirements [1]

Specification reference	Description
IR1	The Heat Switch shall have a flat mechanical interface on the Hot and Cold side for mounting onto the dissipating component and to temperature sink
IR2	The Heat Switch shall have a hot mounting surface area of roughly 16 cm^2 (TBC)
IR3	The Heat Switch shall meet the requirements with cold interface temperatures between -125°C and 50°C and with hot interface temperatures between -55°C and 60°C

1.3.   Environmental Requirements [1]

Specification reference	Description
ER1	The qualification temperatures for the Heat Switch are the temperature listed in IR3 with margin of 10K
ER2	The Heat Switch (at the evaporator level) shall sustain the following mechanical environment in each of the 3 orthogonal axes : - Sinus (from AD4): | Freq [Hz]	Level
5 – 21	11mm
21 – 60	20g
60 – 100	6g
Sweep rate	2 octaves/minute, 1 sweep up | - Random (from AD4): | Freq [Hz]	Level
20 – 100	+3dB/oct.
100 – 300	$0{,}94g^2$/Hz
300 – 2000	-5dB/oct.
Composite	23,3 g rms	
ER3	The Heat Switch shall not be affected by a radiation environment of 30kRad accumulated over its life. Note: In order to cover a larger range of applications, the Heat Switch should be insensitive to the radiation environment since possible future missions could be subject to 30kRad/day.
ER4	The Heat Switch shall be able to work in every position with respect to gravity acceleration and in 0g.

1.4.   Physical and Resource Requirements [1]

Specification reference	Description
PRR1	The Heat Switch shall have a mass lower than 60 grams.

1.5.   Operational Requirements [1]

Specification reference	Description
PRR1	The Heat Switch shall have an operational life greater than 7 years

1.6. Product Assurance Requirements [1]

Specification reference	Description
PA1	The Heat Switch shall comply with product safety requirements stated in ECSS-Q-ST-40 C
PR2	The materials and processes shall comply to the requirements of
PR3	The contractor shall be compliant with ECSS-Q-ST-20C chapter 5.6

1.7. Design Requirements [1]

Specification reference	Description
DR1	The heat switch design should allow the set-point to be changed
DR2	Fatigue life demonstration shall be performed in conformance with ECSS-E-ST-32C Rev.1
DR3	The prevention and control effects of the corrosion shall be in accordance with ECSS-E-ST-32C Rev.1
DR4	The requirements on material section, material design allowable and characterisation shall be in conformance with ECSS-E-ST-32C Rev.1
DR5	The Heat Switch shall fail open, meaning that in all failure cases the heat switch shall remain OFF.
DR6	The Heat Switch design shall be capable to be sterilized with Dry Heat Microbial Reduction process at +125°C for 30 hours
DR7	The Heat Switch shall be designed to sustain 100000 open and close cycles (TBC)

1.8. Verification and Testing Requirements [1]

Specification reference	Description
VTR1	The Heat Switch shall be subject to 8 thermal cycles over the temperature range specified in IR3 with a hold-time of 1hour at each temperature extreme.
VTR2	The Heat Switch shall be subject to sinusoidal tests for all axes with 1 sweep-up at 2 octaves per minute.
VTR3	The Heat Switch shall be subject to random vibration for the duration of 2.5 minutes per axis.
VTR4	The thermal performance of the Heat Switch shall be Measured.
VTR5	The simulation of large heat load variations shall be performed (i.e. by increasing and decreasing the applied heat load).

Bibliography

[1] *2012_ESA SOW Heat Switch - General requirements: Appendix 1 to ITT 1-6801/11/NL/NA*. Netherlands, 2011.